DOT/FAA/AR-96/111

Office of Aviation Research
Washington, D.C. 20591

Advanced Certification Methodology for Composite Structures

NAWCADPAX--96-262-TR

Naval Air Warfare Center—Aircraft Division
Department of the Navy
Patuxent River, MD 20670-5304

April 1997

Final Report

Naval Air Warfare Center
Department of the Navy

U.S. Department of Transportation
Federal Aviation Administration

NOTICE

This document is disseminated under the sponsorship of the U.S. Department of Transportation in the interest of information exchange. The United States Government assumes no liability for the contents or use thereof. The United States Government does not endorse products or manufacturers. Trade or manufacturer's names appear herein solely because they are considered essential to the objective of this report.

Technical Report Documentation Page

1. Report No.	2. Government Accession No.	3. Recipient's Catalog No.
DOT/FAA/AR-96/111		

4. Title and Subtitle	5. Report Date
ADVANCED CERTIFICATION METHODOLOGY FOR COMPOSITE STRUCTURES	April 1997
	6. Performing Organization Code

7. Author(s)	8. Performing Organization Report No.
Kan, H.P., Cordero, R., and Whitehead, R.S.	

9. Performing Organization Name and Address	10. Work Unit No. (TRAIS)
Northrop Corporation Aircraft Division One Northrop Avenue Hawthorne, CA 90250-3277	11. Contract or Grant No.

12. Sponsoring Agency Name and Address	13. Type of Report and Period Covered
U.S. Department of Transportation Federal Aviation Administration Office of Aviation Research Washington, DC 20591	Final Report
	14. Sponsoring Agency Code AAR-431

15. Supplementary Notes

The Federal Aviation Administration technical manager is Don Oplinger, AAR-431.

16. Abstract

An improved certification methodology for composite structures was developed. The methodology permits certification of bonded and cocured composite structures with the same level of confidence as bolted structures. This methodology also ensures that the threat of in-service low-velocity impact is adequately addressed.

The methodology was demonstrated on actual composite aircraft structures to evaluate the damage tolerance capability of these structures. The F/A-18A upper wing skin was used for methodology demonstration. Sensitivity studies were conducted to determine the influence of impact damage threat scenarios and damage tolerance design requirements on the reliability of composite structures.

17. Key Words	18. Distribution Statement
Composite structures Composite materials Damage tolerance Graphite/epoxy Aircraft certification	Document is available to the public through the National Technical Information Service, Springfield, Virginia 22161

19. Security Classif. (of this report)	20. Security Classif. (of this page)	21. No. of Pages	22. Price
Unclassified	Unclassified	166	

Form DOT F1700.7 (8-72) Reproduction of completed page authorized

PREFACE

This report was prepared by the Northrop Corporation, Aircraft Division, Hawthorne, California, covering work performed under U.S. Navy Contract N6226987-C-0259 between September 1987 and September 1989. The contract was administered by the Naval Air Development Center, Warminster, Pennsylvania. Mr. Ed Kautz was the Navy Project Engineer. Partial funding of this effort was provided by the Federal Aviation Administration William H. Hughes Technical Center, Atlantic City International Airport, New Jersey. Mr. L. M. Neri acted as the FAA Technical Manager.

The work was performed in Northrop's Strength and Life Assurance Research Department under the overall supervision of Dr. R. S. Whitehead and Dr. R. B. Deo. The following Northrop personnel were the major contributors to the program.

Program Manager	Dr. R. S. Whitehead
Principal Investigator	Dr. H. P. Kan
Data Analysis	R. Cordero
Documentation	R. Urias
	R. Cordero

TABLE OF CONTENTS

LIST OF ILLUSTRATIONS

LIST OF TABLES

EXECUTIVE SUMMARY

The application of fiber reinforced composites to primary aircraft structures requires proven certification procedures for verification of structural integrity. The present report, which addresses this subject, describes the results of a follow-on to an earlier effort reported in DOT/FAA/CT-86/39 (Navy Report Number NADC-87042-60), "Certification Testing Methodology for Composite Structure," which, as in the present case, was supported jointly by the Naval Air Development Center and the FAA William J. Hughes Technical Center.

In the earlier effort, the broader issues involved in certification of composite structure were addressed. The key feature in that effort was the development of a Weibull statistics methodology for interpretation of the effects of scatter in static strength and fatigue life of composite laminates and bolted joints on requirements for full-scale structural testing and other aspects of the certification process.

In the present effort, the methodology has been extended to allow for assessment of the effects of impact damage on damage tolerance certification approaches as well as for the effects of strength scatter on structural integrity validation of bonded and cocured joints under static and fatigue loading.

In the discussion of impact damage and damage tolerance requirements, the report provides a review of typical service experience for military aircraft subjected to impact induced by operations (runway debris, hail, etc.) as well as maintenance induced damage (dropped tools etc.), from which probabilistic models describing typical levels of impact are provided. A procedure for probabilistic modeling of distributions of impact energy in terms of the Weibull distribution is given. Hypothetical distributions are established for use in subsequent studies of structural reliability of damaged aircraft and compared with experimental data obtained from IRAD programs. Discussion is also provided on observed relationships between impact energy and dent depth measurements.

A methodology for predicting the effect of impact-induced damage on the strength of compressively loaded structure for both simple laminates as well as built-up structure such as stiffened panels is presented, based on which a damage tolerance methodology is outlined and demonstrated for a typical composite wing component. Various aspects of the impact damage problem, including the level of threat and the risk of structural failure for a given level of impact damage are treated on a probabilistic basis so that structural reliability estimates for damage tolerance assessment can be provided. The

results of the present as well as the earlier effort covered in DOT/FAA/CT-86/39 are incorporated into a combined certification methodology which is proposed for dealing with static and fatigue loading in unnotched composite structure as well as in bolted and bonded joints and in structure subjected to the effects of impact damage.

FORTRAN listings for computer programs Post Impact Structural Reliability version 1 (PISTRE1) and Post Impact Structural Reliability version 2 (PISTRE2) which provide for (1) failure predictions for stiffened panels subjected to selected distributions of impact damage and (2) structural reliability predictions for impact damaged panels are given. A listing for an additional routine Damage Area Based Structural Reliability (DABSR) which predicts structural reliability for stiffened panels containing impact damage characterized by C-scan assessed area of impact damage is also given.

SECTION 1

INTRODUCTION

The application of composite materials to primary aircraft structures requires proven certification procedures to demonstrate their structural integrity. The crux of a certification methodology is to demonstrate, with a high degree of confidence, adequate static strength, fatigue life and damage tolerance capability by test and analysis. For metal structures, a successful structural certification methodology that provides this confidence has evolved over the years. Because of the inherent differences between composites and metals, direct application of the metallics certification methodology to composites is limited. Consequently, the Navy funded two programs (References 1 and 2) to address the issue of certifying composite structures. In these programs, various approaches to static strength and fatigue life certification were evaluated to determine their capability to certify composite structures. Based on the results of these evaluations, a certification methodology for composite aircraft structures has been formulated.

The objective of this program was to expand the previously developed certification procedures for composite structures (References 1 and 2) to include adhesively bonded and cocured composite structures and to address the effects of in-service impact damage on the static strength and fatigue life of composite structures. Specifically, the objective is to establish guidelines for the use of bonded and cocured structure data scatter and define realistic impact damage requirements for structural certification. These elements were then integrated into an improved certification methodology for composite structures. This improved methodology permits certification of bonded and cocured composite structures with the same level of confidence as bolted structures. It also ensures that the threat of in-service low-velocity impact is adequately addressed. Analyses and testing requirements for the certification of future composite aircraft structures were defined by the methodology developed.

The program was composed of five tasks:

- o TASK I - SCATTER ANALYSIS
- o TASK II - IMPACT DAMAGE REQUIREMENTS
- o TASK III - IMPACT DAMAGE ANALYSIS
- o TASK IV - DAMAGE TOLERANCE METHODOLOGY
- o TASK V - CERTIFICATION METHODOLOGY DEVELOPMENT

During Task I, a literature survey was conducted to obtain static strength and fatigue life data on adhesively bonded and cocured composite structures. These data were statistically analyzed to determine and quantify the scatter in static strength and fatigue life. The influence of different test parameters was also statistically determined. The scatter for these types of composite structures was then compared with that observed in unnotched, unloaded hole and bolted structure data (References 1 and 2). The results of this scatter analysis are given in Appendix A.

In Task II, sources of in-service low-velocity impact threats, the structure affected, and the parameters that influence the severity of resulting structural damage were identified. A statistical distribution was used to describe the frequency of occurrence of the impact threat. Based on this distribution, realistic impact damage requirements for structural certification were defined. These requirements are discussed in Section 2.

In Task III, state-of-the-art analysis methods for predicting the influence of impact damage on structural integrity were evaluated. This evaluation included mathematical analyses, such as quasi-static or dynamic plate analyses, and simplified engineering approaches. Strength prediction methods for impact-damaged composite structures were also evaluated in this task. The capability of the existing methods, such as the Northrop developed delamination and stiffness reduction models, were verified by comparing analysis results with experimental data from the literature. Section 3 describes the details of the applicable analysis methods.

The impact damage requirements defined in Task II and the analysis methods selected in Task III were used in Task IV to develop a damage tolerance evaluation methodology. The methodology has the capability to assess the reliability of an impact-damaged composite structure at a given applied load. A methodology demonstration was conducted using an F/A-18A composite full-scale structure. The methodology is presented in Section 4 and results of the methodology demonstration are given in Section 5.

An improved certification methodology for composite structures was developed in Task V. In this task, the results of the previous tasks were integrated into the certification methodology developed by Northrop in Reference 1. The improved methodology permits certification of bonded and cocured composite structures with the same level of confidence as bolted structures. This methodology also ensures that the threat of in-service low-velocity impact is adequately addressed. Section 6 summarizes the key elements of this improved methodology. Summary and conclusions are given in Section 7.

SECTION 2

IMPACT DAMAGE REQUIREMENTS

The objective of this task is to define realistic impact damage requirements for composite structural certification. To accomplish this objective the sources of in-service impact damage and the structures affected must be identified, and the influence of the impact parameters on the severity of resulting structural damage must be evaluated. Statistical methods of analysis must also be developed to define the distribution of impact threats. Details of these requirements are discussed in the following paragraphs.

2.1 Sources of In-Service Impact Damage

Sources of in-service impact damage to composite structures can be divided into two categories: (1) damage induced during aircraft operations, and (2) damage induced during maintenance. Damage induced during operations is basically that due to foreign object impact. Foreign object impact includes impacts from runway stones or tire blowout debris. Impactor velocity for this type of impact generally relates to the landing speed of the aircraft, and can exceed 200 feet per second in some instances if tire spin-up contributes to the relative velocity of impact. Maintenance-induced damage results from ground handling of the aircraft such as dropped tools, dropped equipment, or foot traffic. The impactor velocity in this case is generally lower and below 20 feet per second. The impact energies for both types of impact are approximately the same and in the range of 4 to 100 foot-pounds. In addition to these two types of impact damage, external surfaces of an aircraft are also susceptible to hailstone impact. The velocity for hail impact is normally below 90 feet per second and the energy level is in the range of one to four foot-pounds.

Several government-sponsored studies have been conducted in the past to identify the frequency and extent of impact damage and its correlation with the above sources. Some of the results of these studies are reported in References 3 through 10. Reference 3 documents a survey of actual damage which occurred to aircraft in service. Three basic types of impact were identified. These are (1) surface impact, (2) edge or corner impact, and (3)

surface indentation due to walking. In addition, the results of the survey indicated that a significant portion of the damage resulted from major impacts, such as a truck or forklift backing into an aircraft or a maintenance stand deeply gouging a component. The general conclusions from the survey conducted in Reference 3 are (1) The frequency of damage depends on location and structural configuration, and (2) the extent of damage can vary widely.

Reference 5 presents the anticipated in-service impact damage scenario for the N333-15 aircraft, with the wing structure zoned for variable energy level threat. The impact energy level for the wing upper skin was estimated between 4 to 50 ft-lb and from 4 to 16 ft-lb for the lower wing skin. Reference 10 identifies eleven types of impacts for military helicopter structures. The impact energy level considered in Reference 10 ranged from 1 to 40 ft-lb and an estimate of the frequency of occurrence for each type of impact is also presented.

Results reported in References 3 through 10 have indicated that the frequency of impact damage depends on the location of the structural component on the aircraft and the structural configuration. In general, parts which are high on the aircraft or have vertical surfaces receive less damage than lower, more horizontal parts. Although bottom horizontal surfaces are not immune to impact damage, they tend to be damaged less than top surfaces, where walkways exist and equipment drops are more likely.

Surface damage occurs in high-traffic areas during fueling, armament loading, access door removal, etc. Landing gear strut doors and parts near wheels (such as lower surfaces of flaps) are more vulnerable to pieces of blown tires. Extremities of projections, such as wing tips, ends of tail surfaces, and trailing edge panels are vulnerable to being bumped by vehicles or equipment. Top surfaces or near-horizontal surfaces are most susceptible to dropped objects. Edge and corner type of impacts are most likely to occur in high-traffic areas at exposed edges. These areas are most likely to be impacted by maintenance stands or other movable equipment. Removable aircraft parts tend to be dropped or otherwise impacted on edges or corners. Walking on top surfaces of nearly horizontal surfaces is a relatively common cause of damage. Heel pressure, or stepping on a tool, bolt, or other dropped object, frequently causes local indentations and internal laminate damage.

2.2 Impact Parameters

The parameters that influence the severity of resulting structural damage have been extensively investigated by Northrop in References 11 and 12. The most important parameters that influence the damage area and post-impact strength include impact energy, impactor velocity and size, laminate thickness and orientation, laminate material type, structural configuration, and impact location.

Test results reported in Reference 11 indicate that the impact energy required to cause a 0.1 inch deep indentation depends on the impactor diameter, the laminate thickness, and the impact location. Test data were generated in Reference 11 for a 0.25 inch thick (42/50/8) laminate. The test data showed that the energy required to cause a 0.1 inch indentation increases with impactor diameter at all impact locations. For smaller diameter impactor, $I_D \leq 0.5$ inch, the energy required is independent of the impact location. For a larger diameter impactor, the required energy increases as the impact location moves from the corner of the spar/rib towards midbay. This trend is also true for thicker laminates.

The influence of impactor diameter, skin thickness, and impact energy on the C-scan damage size was also investigated in Reference 11. The results showed that the damage area increases with impact energy. In most cases, the damage size reaches a peak value and begins to decrease as the energy approaches the through penetration level. The results also showed that for the 0.25 inch thick laminate, both the damage area and the through penetration energy level increase with impactor diameter. The damage area caused by the different impactors is approximately the same for 0.5 inch thick laminates. However, the penetration energy for the 0.5 inch diameter impactor is significantly higher than that of a 0.125 inch diameter impactor.

The influence of laminate layup on post-impact compression strength is shown schematically in Figure 1. The curves shown in the figure are generated based on the observed trend of experimental data. Experimental data have shown that the loss of strength after impact increases as the percentage of zero degree plies (along the loading direction) increases.

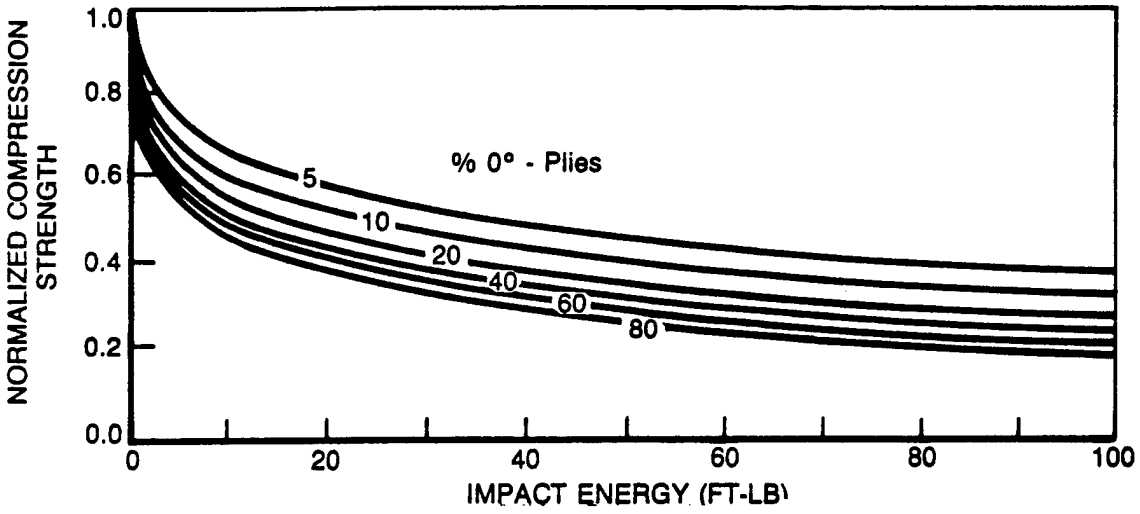

Figure 1. Influence of Ply Orientation on Post-Impact Strength – AS4/3501-6.

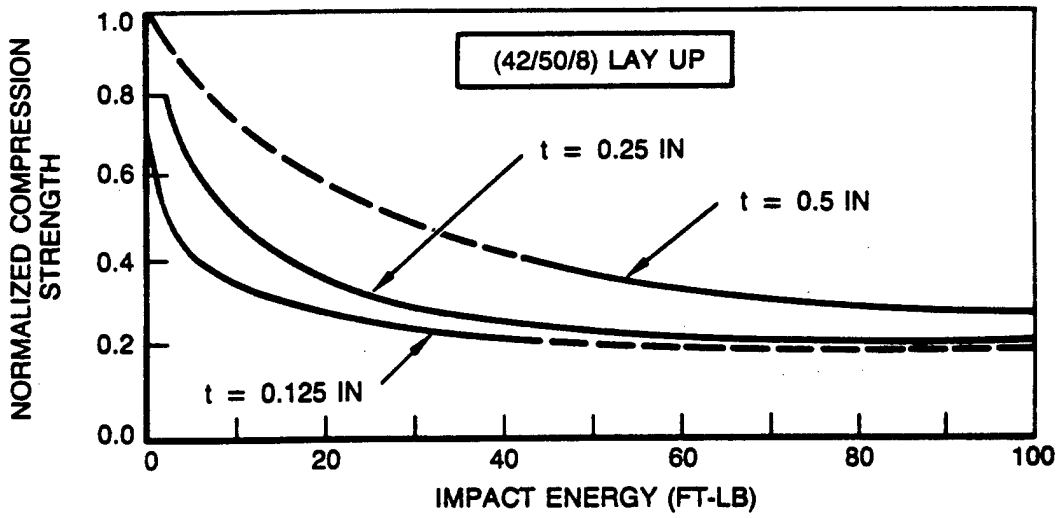

Figure 2. Thickness Effect on Post-Impact Compression Strength – AS4/3501-6.

Figure 2 shows the experimentally observed influence of thickness on normalized post-impact compression strength. The figure shows experimental data for AS4/3501-6 laminates with the same orientations (42/50/8). The laminate thicknesses were 0.125, 0.25, and 0.5 inch. The impactor diameter was 1.0 inch. The solid lines in the figure indicate the trend of the measured average strength and the dotted lines are extrapolated from average data. The figure shows that the percent of strength reduction is larger for thinner laminates for a constant impact energy.

The post-impact strength of composites is strongly influenced by the amount of internal damage (matrix cracks and delaminations) produced by the impact. The amount of damage produced by a given impact depends on the material's capability to resist creation of new surfaces in the material. This capability is characterized by the fracture toughness of the resin material in the composite system (G_{IC}). Figure 3 shows the influence of material toughness on the post-impact compression strength. The figure shows the post-impact compression strength of four material systems: AS4/F650, AS4/3501-6, CE12000/5245C, and AS4/APC2. The values of G_{IC} for these materials are approximately 0.5, 0.75, 2.4 and 6.5 in-lb/in^2, respectively. As can be seen from this figure, the post-impact strength increases with the resin material Mode I fracture toughness, G_{IC}. The figure also indicates that there is a coupling effect of impact energy and G_{IC} on the post-impact strength. The influenced of G_{IC} is larger at lower impact levels.

The influence of impact location and support condition on the post-impact strength is determined by the amount of energy actually available to produce internal damage in the laminate. This is because, during low velocity impact event, the total energy is divided into two parts. The first part of the energy, which causes elastic deformation of the laminate, is stored in the laminate as strain energy. This portion of the energy is recoverable through elastic deformation of the plate. The other part of the energy is consumed by the laminate to create damage. This portion of the energy is irrecoverable. The ratio between the recoverable and irrecoverable energy is strongly influenced by the boundary condition of the plate. Experimental data also indicate that the post-impact strength is significantly influenced by the support condition. This influence is shown in Figure 4. The figure shows the

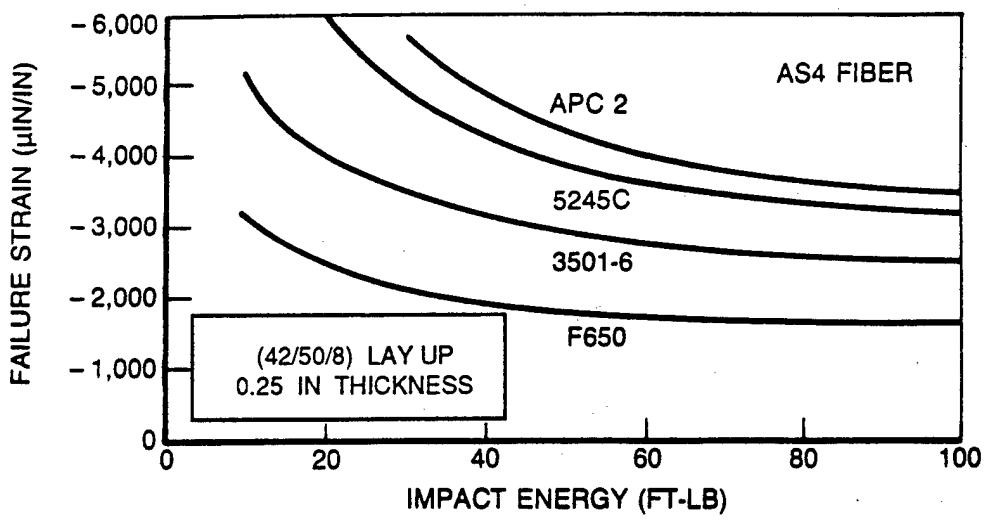

Figure 3. Influence of Material on Post-Impact Strength.

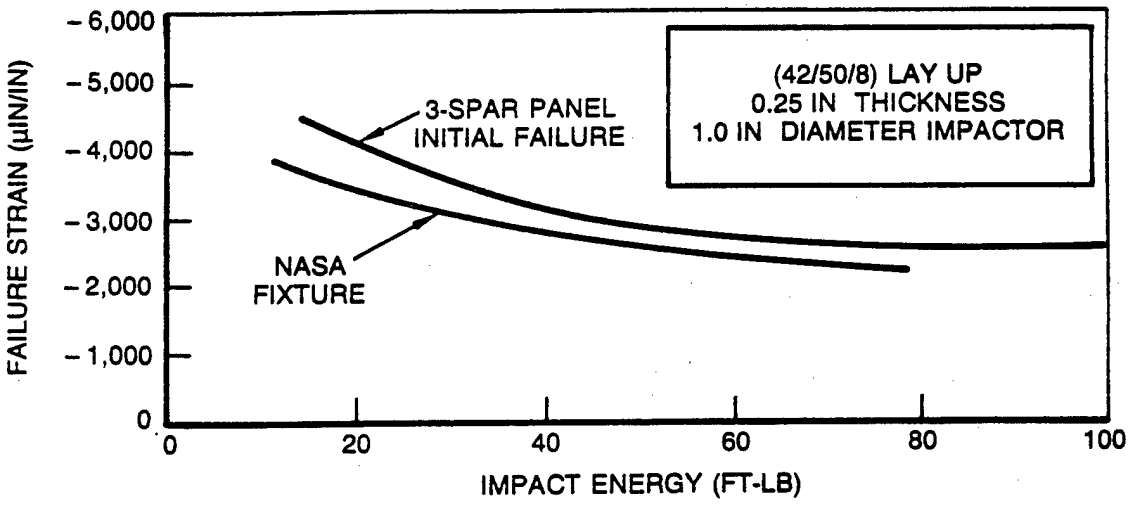

Figure 4. Influence of Support Conditions on Post-Impact Strength – AS4/3501-6.

post-impact compression strength for the same laminate tested under two different procedures. The curve designated by the NASA fixture is the average data obtained from 5 by 10 inch coupons impacted according to the NASA procedure (Reference 13). The 3-spar panel initial failure curve represents the average initial failure strain of the 3-spar panels tested in Reference 12.

For a built-up structure, the overall post-impact strength is significantly influenced by the structural configuration. It was observed, during the static tests of the impact-damaged 3-spar panels (Reference 12), that failure in most of the specimens was in two stages. At the initial failure, the damage propagated to the spar fastener lines. The damage propagation was arrested by the spars, with final failure taking place at a higher applied load. The failure strain shown in Figure 4 is the strain at initial failure of the panel.

The damage propagation arrestment mechanism is provided by the stiffeners through (1) increased local stiffness due to the presence of the stiffeners and (2) the clamping force of the fastener that prevents out-of-plane delamination displacement. After the initial failure, further increase of the applied load will cause load redistribution within the structure. With the damage zone acting as a stress concentrator, severe stress concentration builds up near the spars, and the final failure mode is compression failure outside the damaged bay. The failure load is controlled by the severity of the stress concentration, similar to the failure of specimens with an open hole.

2.3 Impact Threat Distribution

From the discussion of the in-service impact sources (Subsection 2.1), it is clear that the impact threat depends on the location of the structure and its structural configuration. In order to establish realistic impact damage requirements, a structural zoning procedure should be used to categorize the structure. Based on the available data, the impact threat is tentatively divided into three levels - high, medium and low. The probabilistic distributions of these impact threats are discussed below.

To quantify the different levels of impact threat, the probability that a structure is exposed to a given impact is assumed to be described by a two-parameter Weibull distribution in terms of the impact energy. Instead of expressing the distribution by the usual scale (β) and shape (α) parameters, the threat is characterized by two impact energy levels. These are (1) the modal impact energy (X_m), and (2) the energy level associated with a low probability of occurrence (X_p). The relationships between the energy parameters and the Weibull scale and shape parameters are expressed by the two equations given below.

$$X_m = \left(\frac{\alpha-1}{\alpha}\right)^{1/\alpha} \beta \tag{1}$$

and

$$\beta = \frac{X_p}{[-\ln(p)]^{1/\alpha}} \tag{2}$$

where p is the probability of occurrence of the impact energy X_p.

Combining equations (1) and (2), one obtains

$$\frac{X_m}{X_p} = \left[\frac{\alpha-1}{-\alpha\ln(p)}\right]^{1/\alpha} \tag{3}$$

Equation (3) can be solved for α by iteration and β is then obtained from Equation (2). The Weibull distribution for the impact threat on a structure is then defined from the values of α and β obtained.

The three scenarios of impact threats, denoted as high, medium and low, are defined in Table 1. The table also shows the computed Weibull parameters corresponding to these threats. The high threat distribution has a modal energy of 15 ft-lb with the probability of occurrence for a 100 ft-lb or higher energy impact of 0.1. This is a very conservative estimate of the impact threat imposed on a structural area that requires frequent maintenance with relatively heavy tools. The probability of an impact with energy of 15 ft-lb or higher for this threat is 0.81.

TABLE 1. IMPACT THREAT SCENARIOS.

	HIGH THREAT	MEDIUM THREAT	LOW THREAT
MODAL ENERGY X_m (ft-lb)	15	6	4
PROBABILITY AT 100 ft-lb p (100)	0.1	0.01	0.0001
α	1.264	1.192	1.221
β (ft-lb)	51.7	27.8	16.2

The medium threat has a modal energy of 6 ft-lb. The probability of an impact event with energy exceeding 6 ft-lb is 0.85. The impact energy of 100 ft-lb or higher is likely but small (p=0.01) for this threat. This class of threat is a conservative estimate of impact received by a structural area exposed to both operational and maintenance induced impact damage. The low threat is a more realistic estimate of the impact damage threat for primary composite structures. The low threat has a modal energy of 4 ft-lb. The likelihood of a 100 ft-lb impact is remote (p=0.0001).

The probabilistic distribution of the three classes of threats are shown in Figure 5. These impact distributions will be used in conjunction with the stiffness reduction residual strength prediction model to establish the damage tolerance requirements. This methodology is discussed in Section 4.

Under a Northrop/MCAir collaborate IRAD program MCAir conducted a field survey of low-velocity impact damage to quantify impact threat to composite aircraft structures. In this survey, impact data from four different in-service aircraft types (F-4, F-111, A-10, and F-18) were collected. These data were expressed in terms of dent depth and presented as an exceedance curve, as shown in Figure 6. As shown in the figure, the dent depths measured for all the aircraft types are below 0.10 inch. The majority of the dents, approximately 90%, have depth measured less than 0.02 inch. The shape of the dent depth distribution for each aircraft is similar to the curve shown in Figure 6.

The dent depth data for the four aircraft types surveyed are for metallic aircraft structures. In order to apply this information to composite structures, an impact threat expressed in terms of impact energy is needed. This was accomplished by using an experimentally established impact energy versus dent depth relationship. The energy-dent depth correlation shown in Figure 7 was obtained by MCAir, under a Northrop/MCAir joint IRAD program, from an F-15 wing skin impact test. This experimentally established relation was used to transfer the exceedance curve in Figure 6 to an impact energy based exceedance curve, shown in Figure 8. The figure shows that the upper limit impact energy for the aircraft surveyed is approximately 35 ft-lb. Figure 8 also indicated that more than 90% of the impacts are below the energy level of 15 ft-lb. These results seem to agree with the discussion in Subsection 2.1.

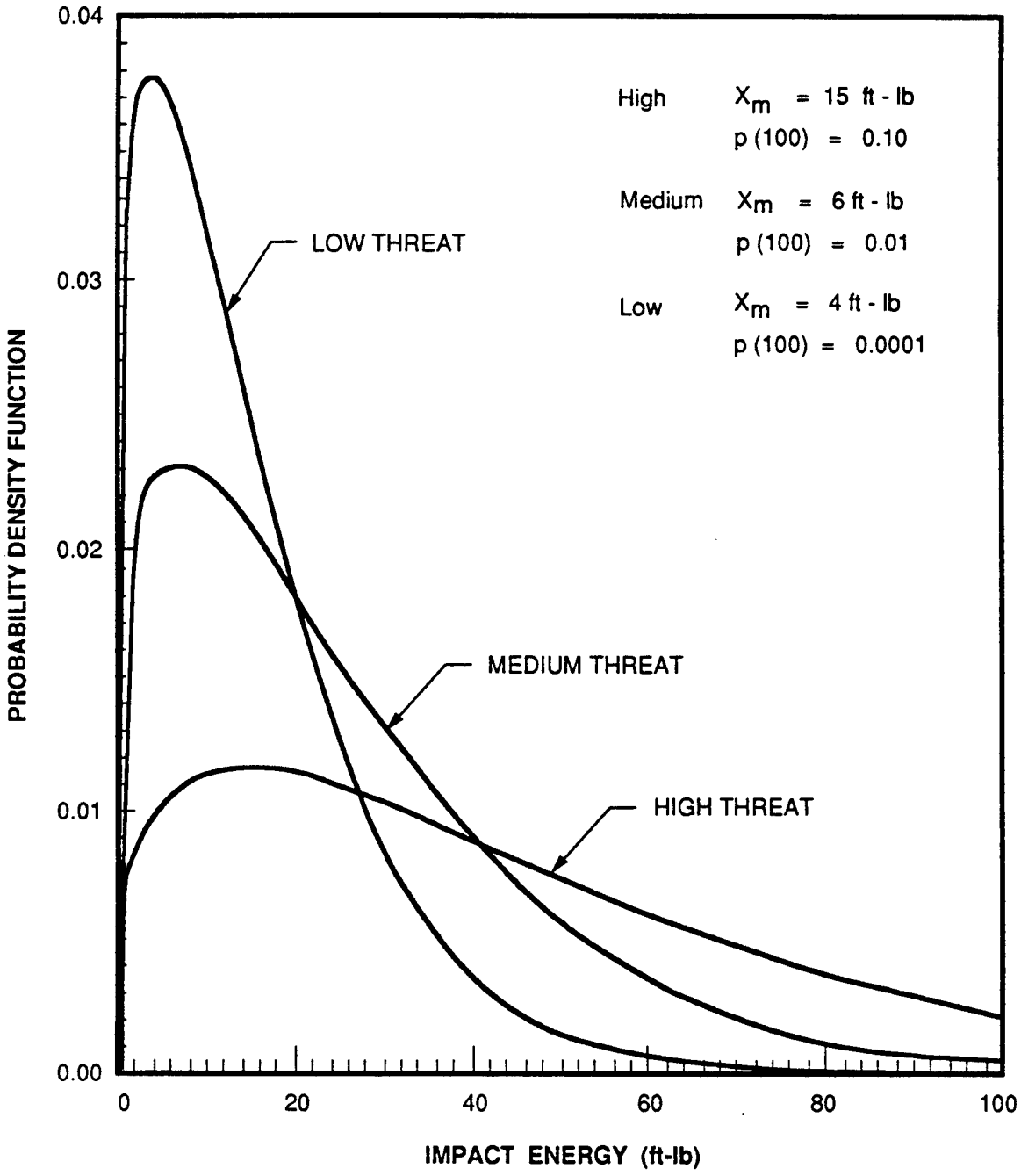

Figure 5. Probability Distribution of Impact Threats.

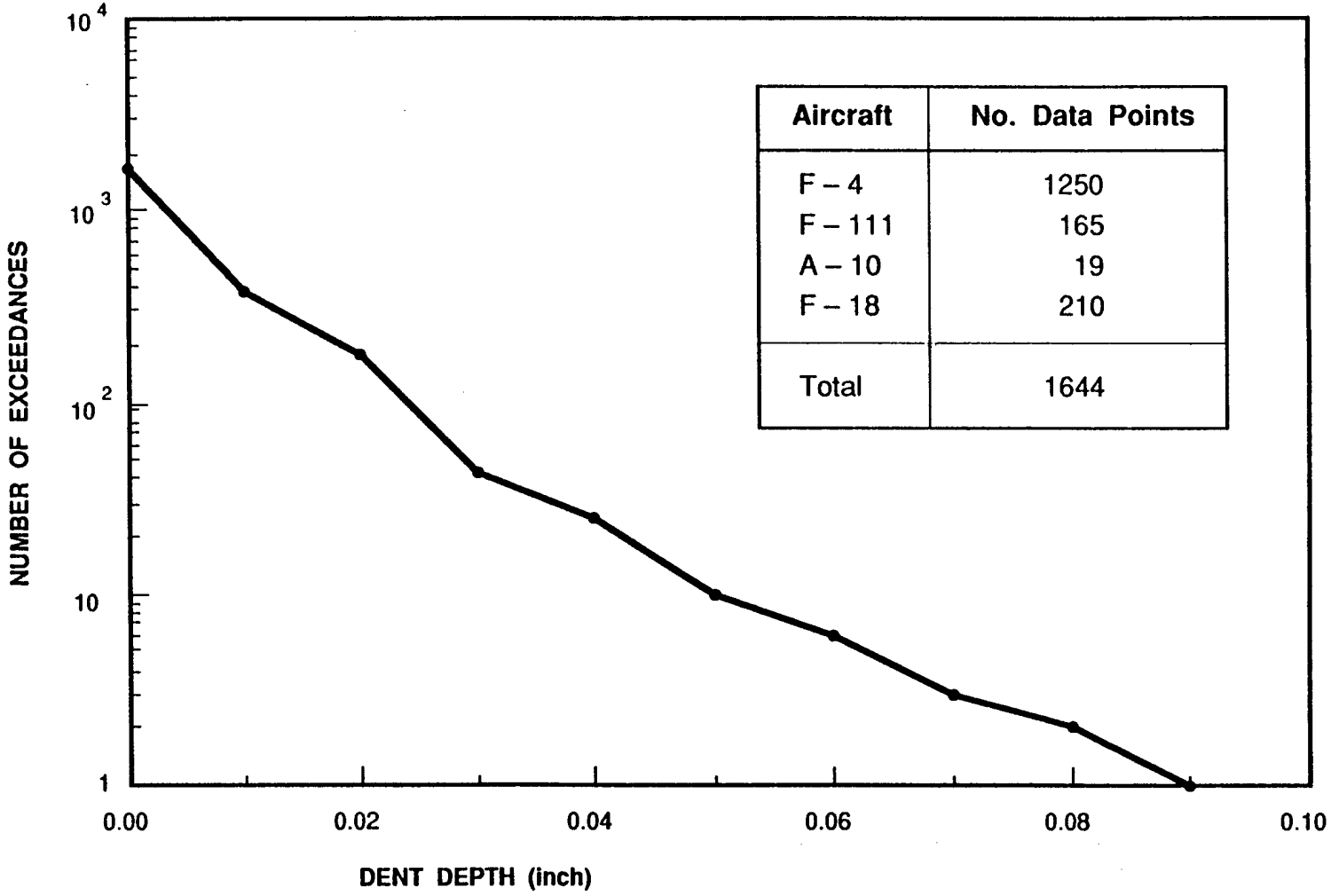

Figure 6. Dent Depth Distribution of In-Service Fighter Aircraft.

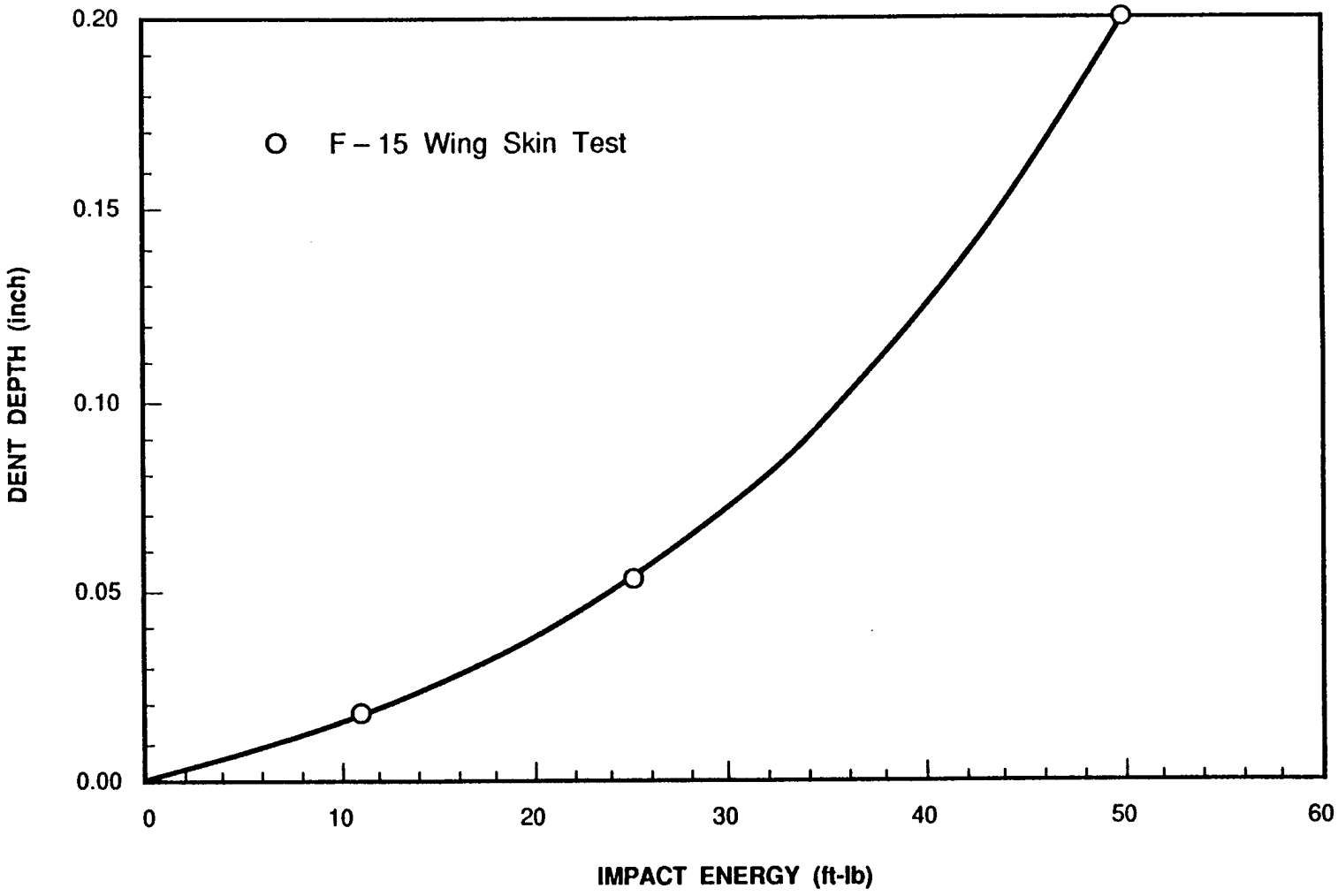

Figure 7. Baseline Impact Energy and Dent Depth Correlation for Metallic Structures.

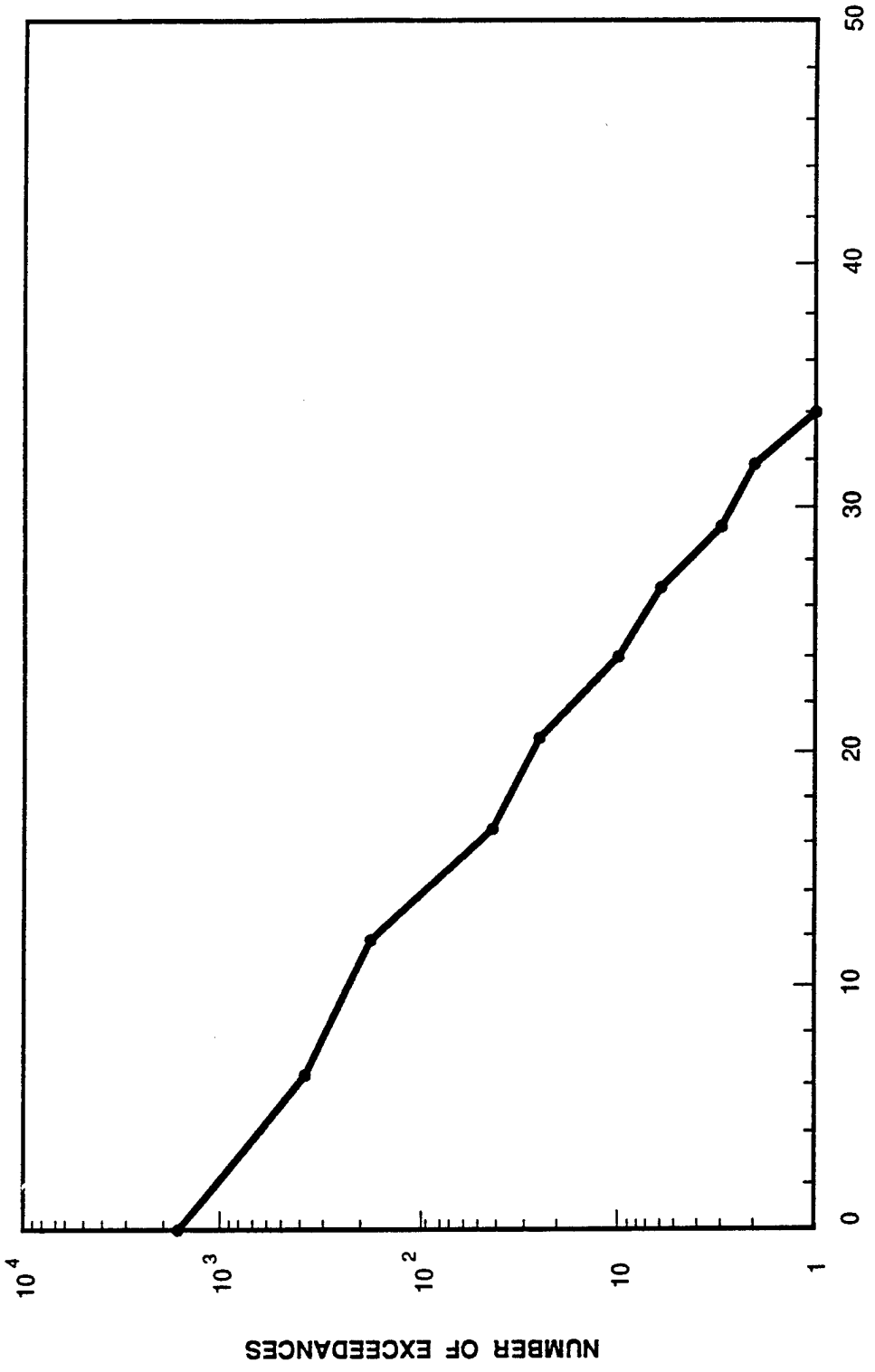

Figure 8. Impact Energy Excedances for the In-Service Fighter Aircraft Surveyed.

The impact energy based exceedances shown in Figure 8 was converted into a probability distribution and compared with the three threats defined earlier. This comparison is shown in Figure 9. This figure shows that the three threats are very conservative compared to in-service survey results. The in-service survey data were fitted into the Weibull modal given by Equations (1) and (2). The fitted curve is also shown in Figure 9. The parameters used for the fitted curve were : X_m = 1 ft-lb., X_p = 35 ft-lb with p = 0.0005. The resulting Weibull shape and scale parameters were 1.147 and 5.98, respectively.

The influence of different impact threats on the damage tolerance of a composite structure will be discussed in Section 5, when the methodology developed in this program is demonstrated on an aircraft structure.

2.4 Barely Visible Impact Damage

Composite laminates exposed to low-velocity impact may sustain extensive internal damage without visual signs of damage on the impacted surface. This internal damage can cause significant reduction in the strength of the laminate. Concerned about the strength degradation caused by the nonvisible impact damage, the Navy established a barely visible impact damage (BVID) criterion for damage tolerance design of composite structures. This criterion requires that composite aircraft structures containing BVID shall not fail under the design ultimate load (DUL). In this subsection, a practical BVID limit is recommended and the impact energy associated with the BVID is established based on experimental data. The influence of the BVID criterion on the structural strength will be discussed in Section 5.

A practical criterion for visible damage is the measurement of dent depth resulting from low-velocity impact. In Reference 12, a 0.1 inch dent depth is used as a visible damage criterion. Based on this criterion, the energy required to produce a visible impact damage (0.1 inch dent) would be significantly higher than the impact threat experienced by in-service aircraft. The Navy recently conducted a series of impact tests on the F/A-18A upper wing skin (Reference 14). The test data were analyzed to define a visible impact damage criterion. From the results of this analysis a combined dent depth and impact energy criterion was established. This criterion is considered more consistent with the impact threat scenarios of in-service aircraft discussed earlier. The criterion defines visible impact damage as

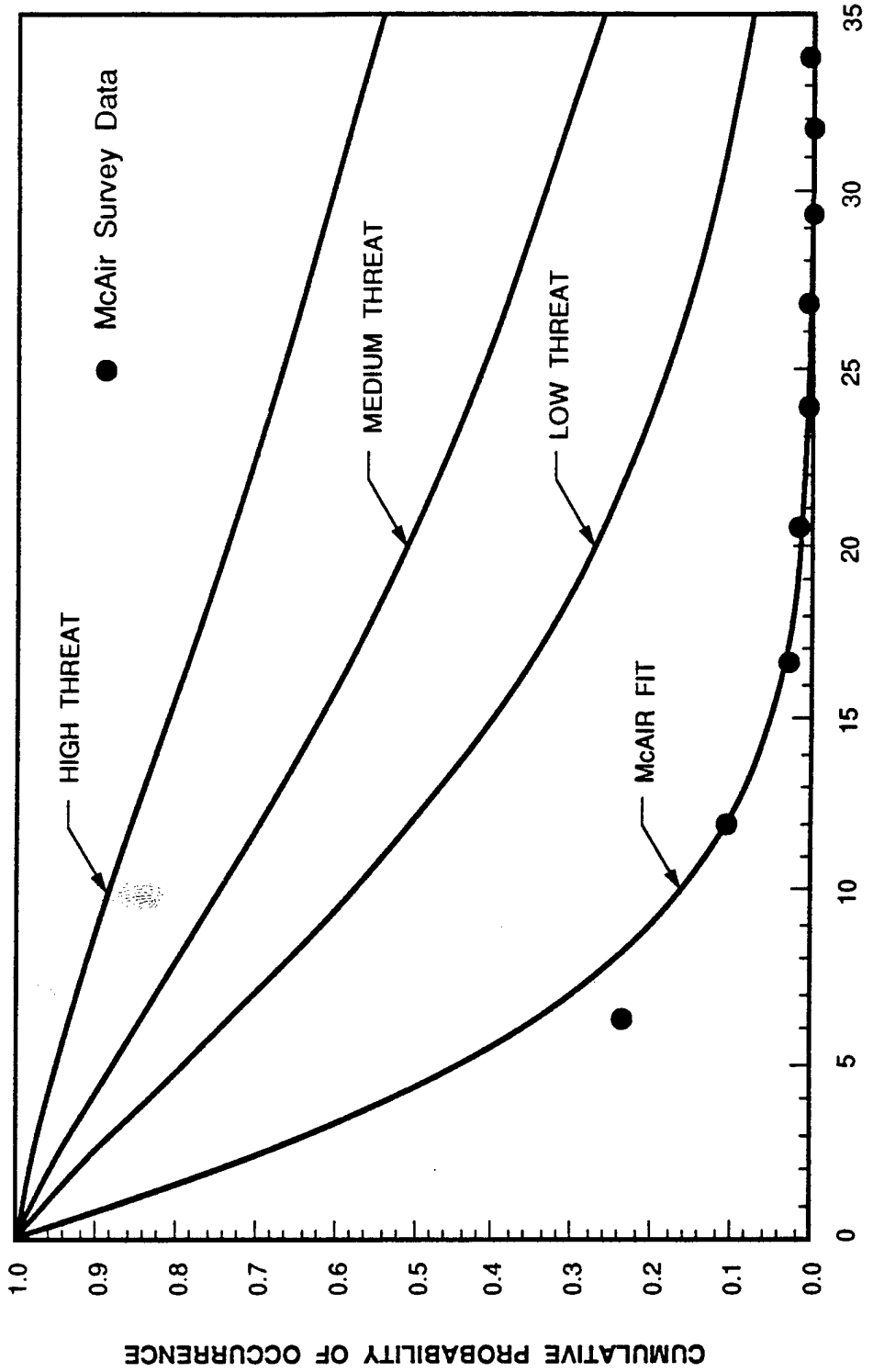

Figure 9. Comparison of Impact Threat Distributions.

damage with 0.05 inch or deeper dent for thin laminates and damage produced by 100 ft-lb impact for thick laminates. This criterion was established for the F/A-18A wing skin material, based on the Navy test data. However, based on data comparison with data generated by Northrop and the results of McAir's field survey, the criterion is believed to be applicable for other composite materials. The Navy test data and the data analysis are discussed below.

The F/A-18A drop test data were divided into three groups based on skin thickness. Tables 2, 3, and 4 show the skin thickness, impact location, impact energy, C-scan damage area and the dent depth for each impact event. Table 2 gives test data for impacts on 0.15 to 0.20 inch thick skin. The relationship between impact energy and dent depth is shown in Figure 10. The figure shows that the dent depth increases with impact energy and can be fitted by a fourth-degree polynomial. The dent depth reaches 0.05 inch at 40 ft-lb of impact energy. Table 2 also shows the measured C-scan damage area for each impact event. However, a relationship between dent depth and C-scan damage area could not be established because of large scatter.

Table 3 shows the impact test data for skin thickness between 0.20 and 0.25 inch. The dent depth data are plotted in terms of impact energy in Figure 11. The figure shows a similar relationship between dent depth and impact energy as that for skin thickness between 0.15 and 0.20 (Figure 10). The impact energy required to produce a 0.05 inch deep dent is 50 ft-lb.

Impact data obtained from skin thickness of greater than 0.25 inch are listed in Table 4. The dent depth data are plotted against impact energy in Figure 12. In this figure, the data are further separated into three subgroups ($0.25 < t < 0.40$; $0.40 < t < 0.60$; and $0.60 < t < 0.686$). Because of the large range in skin thickness in this data group, Figure 12 shows large scatter in the dent depth. A simple polynomial fit for these data is difficult. Figure 12 shows a fitted curve for dent depth data obtained from skin thickness approximately equal to 0.525 inch. The figure shows that for this thickness the energy required to produce a dent of 0.05 inch deep would be significantly higher than 100 ft-lb. Because a 100 ft-lb impact is considered as a very remote impact event for an in-service aircraft, this energy level is used as a cut-off energy for BVID.

TABLE 2. NAVY F/A-18A DROP TEST DATA – GROUP A
$t = 0.175 \pm 0.025$ inch.

DROP No.	THICKNESS (in)	DROP LOCATION *	ENERGY (ft-lb)	C-SCAN AREA (in^2)	DENT DEPTH (in)
45	0.193	MB	18.8	3.16	0.006
49	0.192	MB	19.3	3.61	0.008
44	0.187	MB	19.7	2.94	0.008
47	0.187	MB	24.7	4.23	0.010
48	0.187	MB	26.7	5.66	0.006
28	0.198	NR	30.8	3.31	0.023
29	0.187	MB	33.7	6.09	0.020
32	0.190	NS	34.8	3.28	0.036
30	0.187	MB	39.6	3.80	0.043
31	0.187	MB	39.6	4.69	0.051

* DROP LOCATION

MB Mid-Bay
NS Near Spar
NR Near Rib

TABLE 3. NAVY F/A-18A DROP TEST DATA – GROUP B
$t = 0.225 \pm 0.025$ inch.

DROP No.	THICKNESS (in)	DROP LOCATION *	ENERGY (ft-lb)	C-SCAN AREA (in^2)	DENT DEPTH (in)
33	0.230	MB	19.3	1.86	0.008
43	0.208	MB	19.3	3.61	0.008
37	0.208	MB	22.3	2.81	0.012
40	0.224	MB	26.7	4.20	0.009
39	0.250	MB	27.5	4.66	0.008
34	0.208	MB	29.9	3.52	0.013
46	0.239	MB	30.8	6.94	0.014
36	0.208	MB/NR	33.7	6.19	0.022
35	0.208	MB	34.8	4.62	0.014
26	0.208	MB	35.9	4.58	0.014
25A	0.229	MB	38.3	6.31	0.014
25	0.250	MB	38.5	4.17	0.010
27	0.203	NS	39.6	3.73	0.032
52	0.250	NR	45.4	7.52	0.032
41	0.223	MB	47.1	5.36	0.048

* DROP LOCATION

MB Mid-Bay
NS Near Spar
NR Near Rib

TABLE 4. NAVY F/A-18A DROP TEST DATA - GROUP C
$t \geq 0.25$ inch.

DROP No.	THICKNESS (in)	DROP LOCATION *	ENERGY (ft-lb)	C-SCAN AREA (in^2)	DENT DEPTH (in)
38	0.343	MB	19.7	0.20	–
50	0.276	MB	20.2	6.38	0.006
51	0.255	MB/NR	32.7	4.97	0.011
55	0.307	MB	33.7	5.08	0.010
1	0.504	MB	45.3	2.12	–
20	0.582	NS	47.1	10.44	0.008
21	0.504	MB	48.2	14.53	0.010
2	0.504	MB	48.8	0.84	–
22	0.639	MB	49.4	7.53	0.006
23	0.520	NS	50.0	8.27	0.012
18	0.608	MB	50.3	25.8	0.006
53	0.364	MB	50.7	4.00	0.010
54	0.328	MB	52.7	8.03	0.010
16	0.442	MB	69.0	19.22	0.012
19	0.608	NS/NR	69.4	9.00	0.007
24	0.442	MB	70.5	11.36	0.014
6	0.504	MB	71.5	6.97	0.010
11	0.541	NS	71.8	17.44	0.012
8	0.504	NS	72.0	6.03	–
9	0.686	NS/NR	73.1	3.77	–
5	0.504	MB	73.6	9.33	0.011
10	0.608	MB	74.8	17.89	0.010
7	0.614	NS	75.0	7.84	0.012
56	0.328	NS	77.0	6.11	0.005
14	0.634	MB	92.7	17.34	0.012
17	0.504	NS	93.8	11.00	0.016
12	0.666	NS/NR	94.6	7.00	0.011
15	0.608	NS	94.6	16.84	0.014
4	0.499	MB	94.6	15.86	0.016
3	0.504	MB	96.2	8.64	0.015
13	0.499	NS	98.6	6.25	0.012

* DROP LOCATION

MB Mid-Bay
NS Near Spar
NR Near Rib

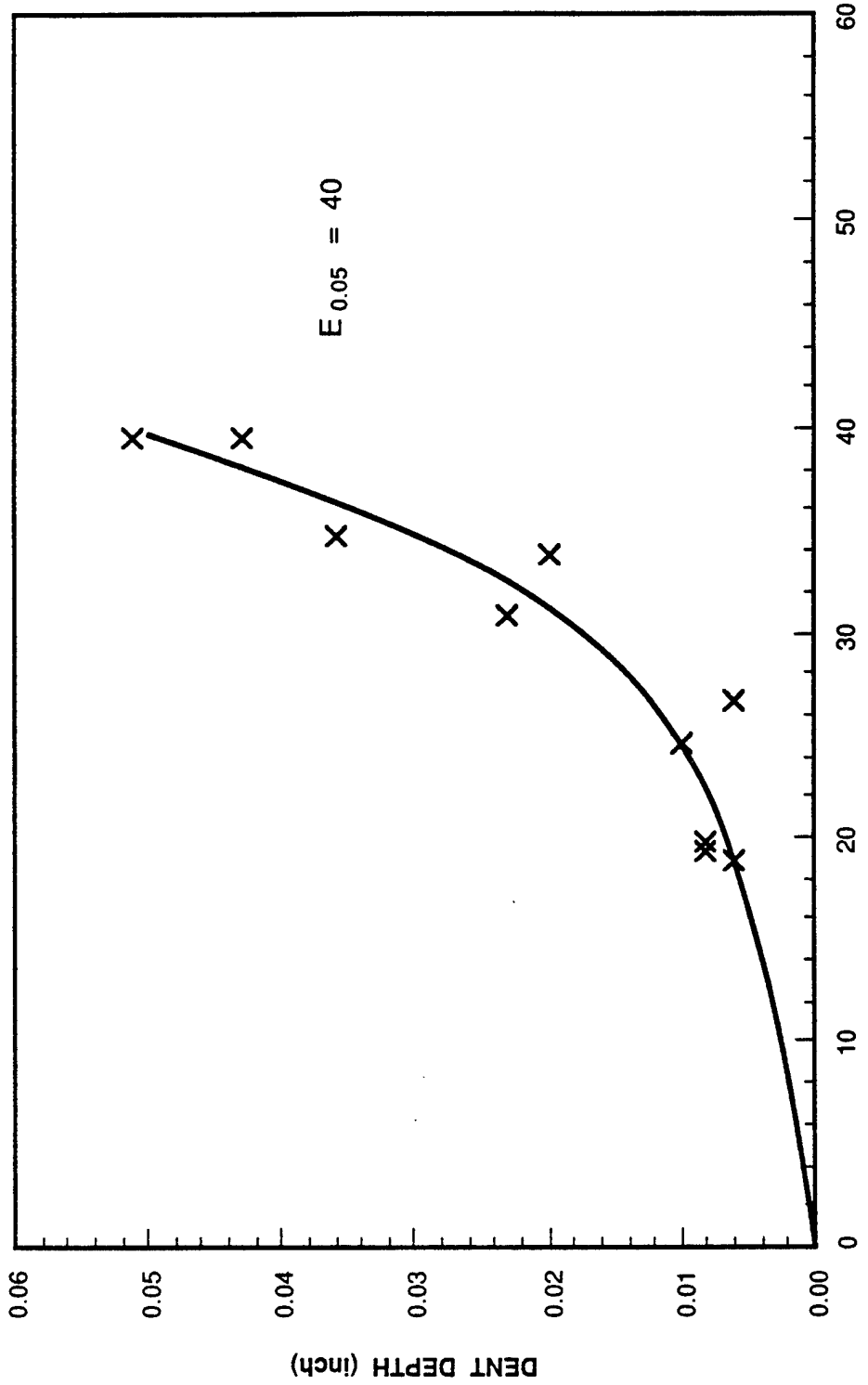

Figure 10. Relationship Between Dent Depth and Impact Energy for $0.15 < t < 0.20$ in.

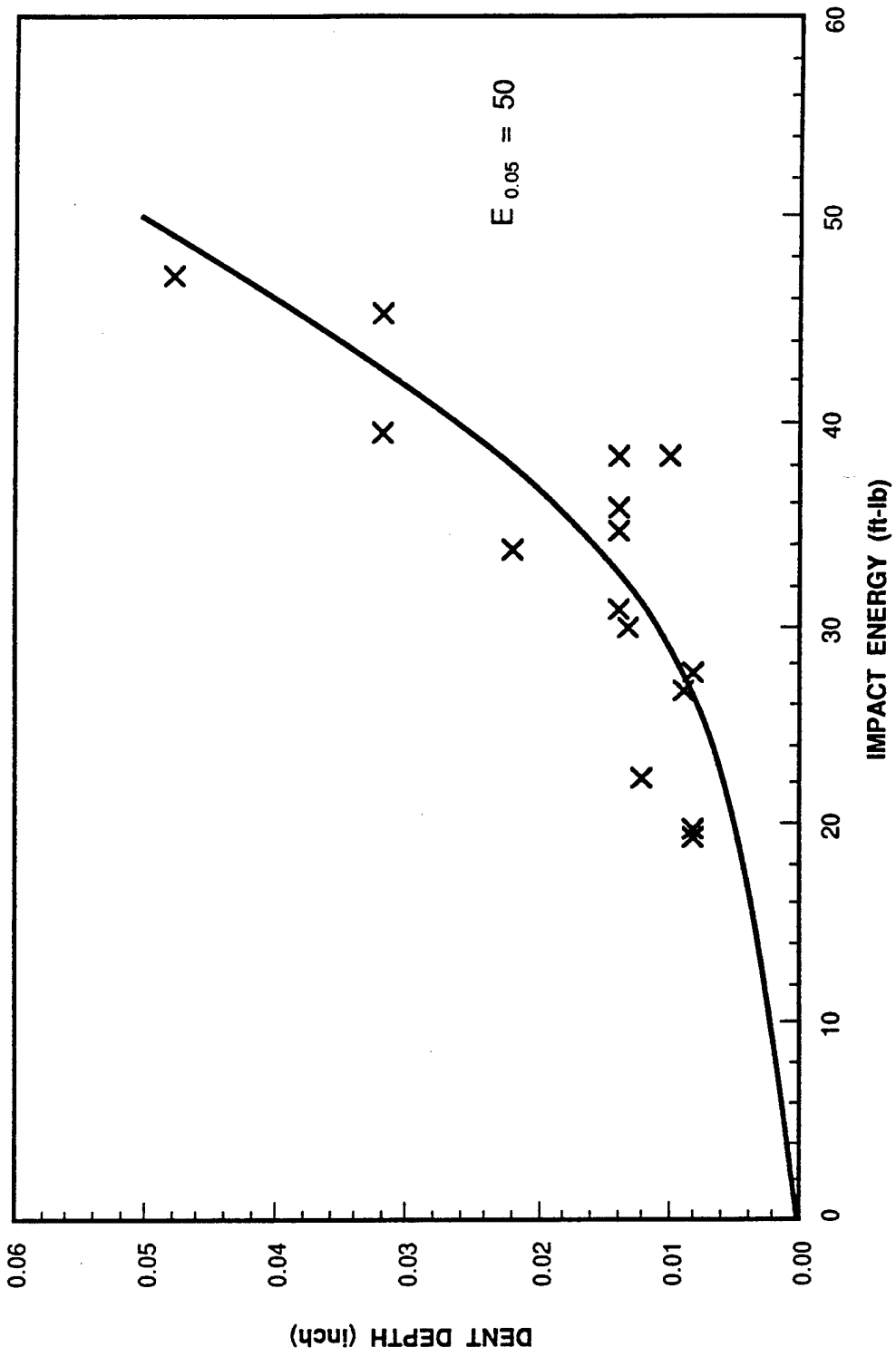

Figure 11. Relationship Between Dent Depth and Impact Energy for $0.20 \leq t \leq 0.25$ inch.

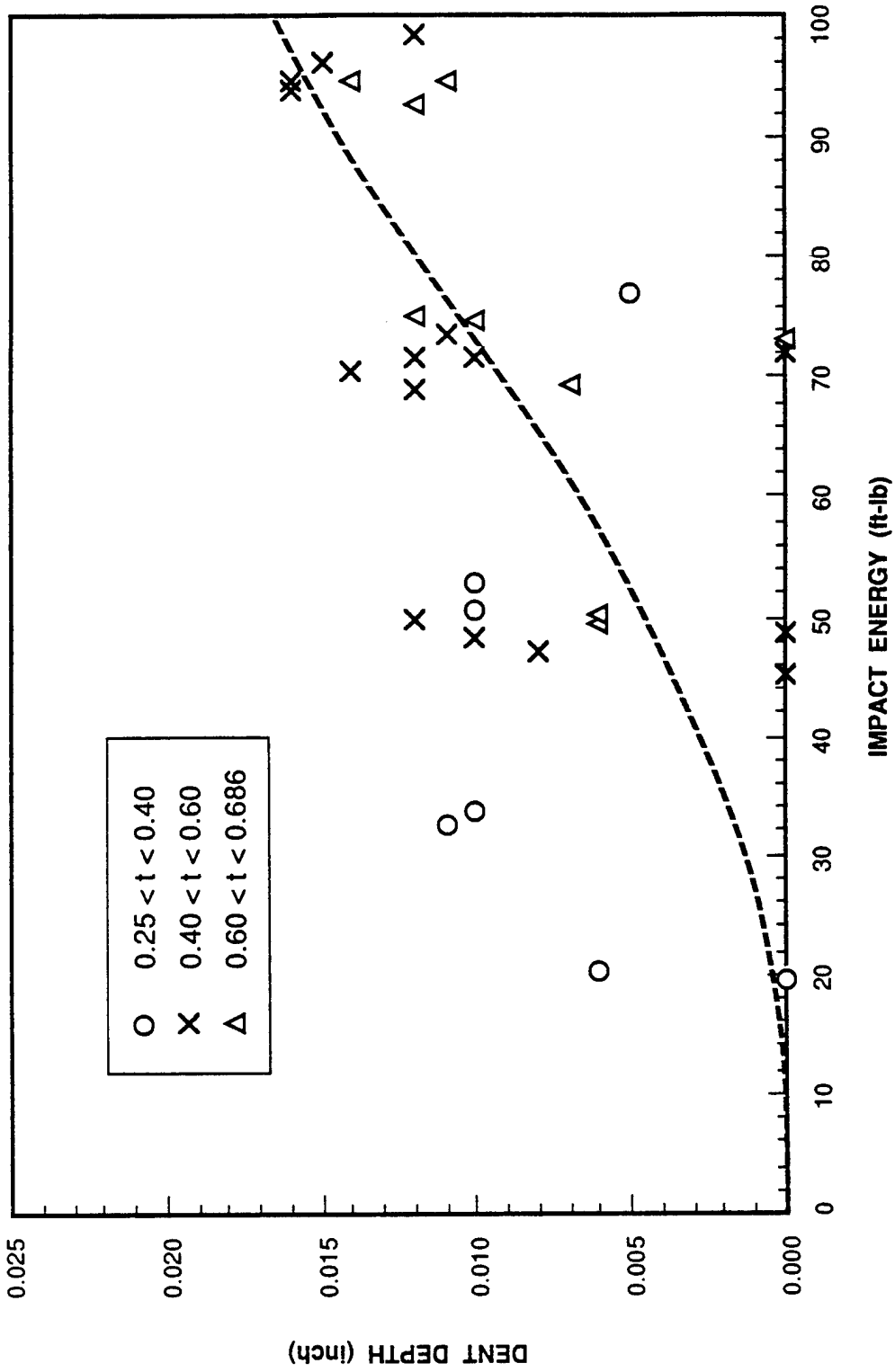

Figure 12. Relationship Between Dent Depth and Impact Energy for $0.25 < t < 0.686$ in.

The impact data discussed above were used to establish the critical energy for BVID. The results are shown in Figure 13. In this figure, the critical energy is expressed in terms of skin thickness. The skin thickness is divided into three regions. For laminates of 0.05 inch thick or thinner, a 0.05 inch deep dent would be a through-penetration damage and the cut-off energy is 30 ft-lb. For skin thicknesses between 0.05 and 0.40 inch the critical energy is between 30 and 100 ft-lb, and the relationship between critical impact energy and laminate thickness is shown in Figure 13. Beyond a skin thickness of 0.4 inch, the critical energy increases rapidly with skin thickness. In this region, the cut-off energy of 100 ft-lb is used as the critical energy.

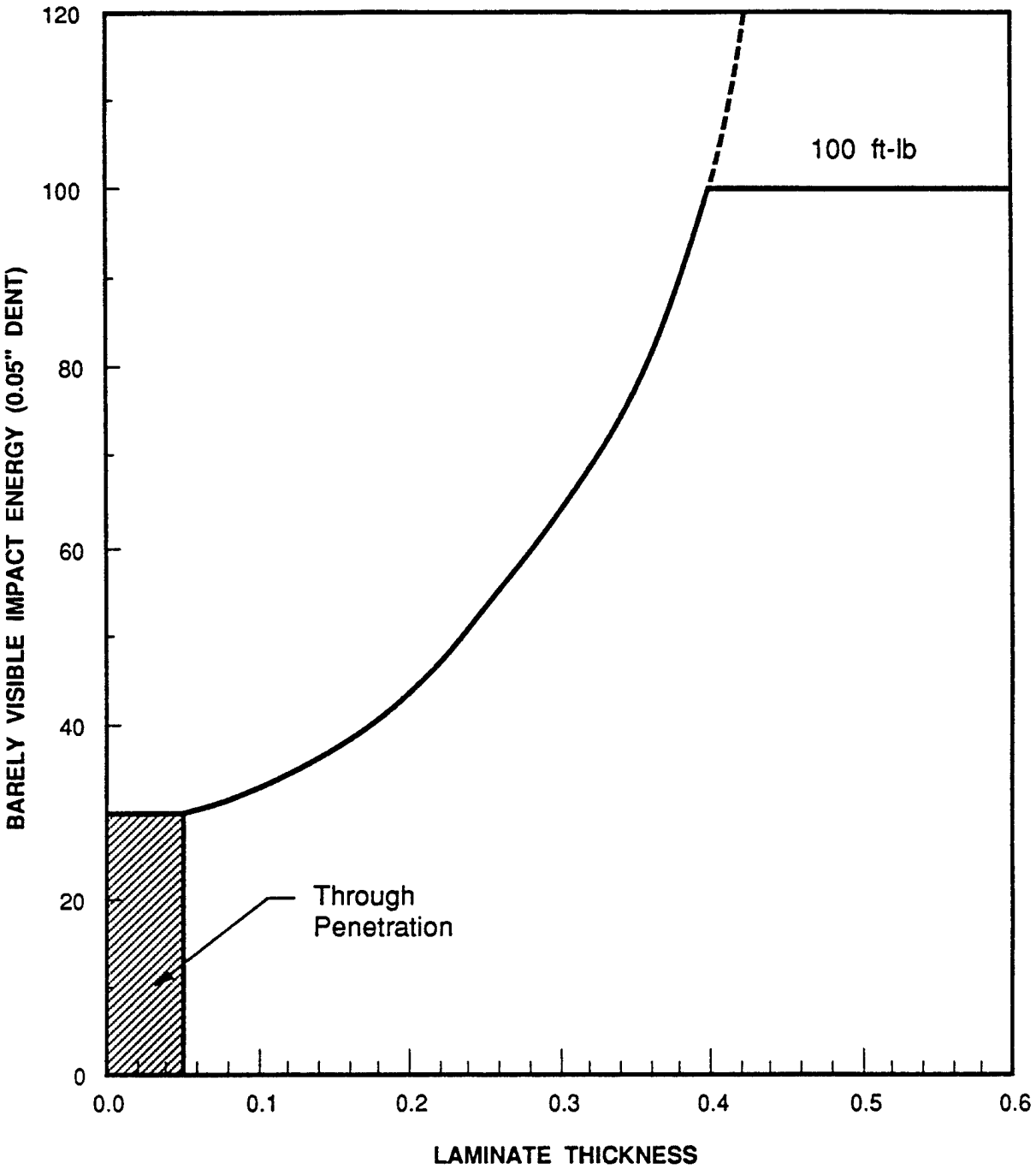

Figure 13. Critical Impact Energy for Barely Visible Impact Damage.

SECTION 3

IMPACT DAMAGE ANALYSIS

In this task, the state-of-the-art analysis methods used to characterize the nature and extent of damage caused by low-velocity impact and the post-impact strength prediction method were evaluated. A damage area based strength prediction method was developed. These analysis methods are discussed in the following paragraphs.

3.1 Damage Characterization

An accurate analysis method to characterize the nature and extent of damage caused by low-velocity impact of composites is not available at present. This is because of the extremely complex nature of the damage and the large number of variables involved. Analytical prediction of internal damage involves a complex three-dimensional stress analysis and development of well-defined failure criteria for different failure modes. The variables that need to be considered include: impact velocity, impactor mass, shape and material properties of the impactor, thickness, boundary conditions and mechanical properties of the target laminate, impact location, impact angle and the environmental conditions. The existing analytical approaches basically solve two problems simultaneously. These are a contact problem and a structural dynamics (or quasi-static) problem.

The contact problem is often approximated by an empirical relationship between the impactor and the laminate responses. The classical contact law derived by Hertz, for impact of an elastic sphere on an isotropic elastic half-space, has been modified by many investigators to study the responses of composite laminates (References 15-18). A typically assumed contact relation is that the force exerted by the impactor varies with the relative displacement (indentation) of the two bodies to a constant power, written as

$$F = k\alpha^n \tag{4}$$

where F is the contact force, α is the indentation, k and n are constants. The empirical constants k and n are determined in Reference 18 from

experimental data. The static indentation test data generated in Reference 18 confirmed that Equation (4) with n=1.5 is valid for the loading portion of the tests. The test results of the reference also indicated that the unloading curve is different from the loading curve because of the permanent indentation. The contact force in the unloading cycle is expressed in terms of the permanent indentation, α_o, as

$$F = S(\alpha - \alpha_o)^q \tag{5}$$

in Reference 18. In this equation S is an unloading rigidity written in terms of the contact force and indentation at the beginning of the unloading. The empirical contact law given by Equations (4) and (5) was used in a finite element program to investigate the low-velocity impact response of graphite/epoxy laminates. The analysis results correlates well with experimentally observed impact responses for laminated plate with free boundary conditions.

Although reasonable analytical/experimental correlation is obtained in Reference 18, it should be pointed out that the problem investigated in the reference is limited to impact energy where no significant internal damage is developed. Under such energy levels, the laminate response is basically elastic and slight modifications of the contact law derived for isotropic materials is valid. At higher impact energy levels or impact on supported plates, internal damage develops in the composite and the laminate response to impact is significantly different from an elastic response. Thus, the analysis method proposed in Reference 18 cannot be applied to impact problems that involve significant damage in the laminate (the real world case). The analysis methods given in References 15-17 are similar to that of Reference 18. These methods all have the same deficiency when applied to the impact energy that causes significant damage in the laminate.

The structural problem is often formulated as a higher order, two-dimensional plate problem. This analytical approach is discussed in References 12 and 18-25. In References 21-24, clamped circular composite plates are analyzed for static equivalent impact loads. A fine mesh finite element method is used to obtain ply stresses in Reference 21. These stresses are then used to calculate the failure region and modes using the Tsai-Wu and

maximum stress criteria. The failure modes considered in the reference are splitting and fiber breakage. A plate-membrane coupling model is developed in Reference 24 to obtain the deformation of a circular plate under quasi static point load. The deflected shape and the load-displacement curve determined from the analysis is then compared with the experimental data in Reference 24. No attempt was made to predict the impact damage in the reference.

The analysis approach in References 12, 20 and 22 are similar. The problem considered in these references is a rectangular, orthotropic plate under a localized applied load which simulate the impact force. The impact force is simulated by incorporating a modified Hertian contact law. Reference 20 presented the most sophisticated analysis which incorporated the static response into a dynamic analysis. The analysis is then used to predict the damage in clamped orthotropic plates caused by low velocity impact.

Despite the rigorous mathematical formulation and sophistication in the solution technique, limited success has been achieved in analytically characterizing the nature and extent of damage in a composite plate caused by the low-velocity impact. This is because of the inherent heterogeneous nature of the material system and the three-dimensional nature of the problem. The dynamics analysis in conjunction with a modified contact law provides a tool to describe the plate response up to the impact energy level that internal damage first occurs. Beyond this energy level, damage will occur in the form of delamination, matrix cracks, splitting and fiber breakage in the local region of the impact site. Thus, this region can no longer be described as a continuum, which all the analytical formulations assume.

From the above evaluation of the damage characterization analysis, it may be concluded that an analytical methodology that fully defines the state of damage in a composite laminate after an impact event is beyond the state-of-the-art. A practical approach would be to by-pass this analysis and use an empirical method such as the stiffness reduction model to directly predict the post-impact strength of the composite. This method was developed by Northrop in Reference 12, and will be discussed in the subsection below.

3.2 Stiffness Reduction Model

This semi-empirical method developed by Northrop in Reference 12 is based on an elastic stiffness reduction technique. It combines all internal damages resulting from a low-velocity impact into an equivalent region of reduced elastic stiffness, as shown in Figure 14. The localized stiffness reduction causes a stress concentration effect which perturbs the local stress field, thereby reducing the overall laminate strength. The severity of stiffness reduction, for a given material system and impact condition, depends on the impact energy level.

In the stiffness reduction model, the influence of other parameters that affect the post-impact compression strength of a laminate are empirically incorporated. The parameters considered are laminate layup, laminate thickness, material toughness (G_{IC}), support condition, and impactor size.

The empirical relationship between the post-impact compression strength and each parameter was obtained in a single functional form through extensive data correlation. The model is expressed as

$$\sigma_f = \sigma_o/[1 + C_1C_2C_3C_4C_5W_e] \tag{6}$$

where

σ_f is the failure stress of the impact-damaged laminate

σ_o is the failure stress of the undamaged laminate

C_1 is the laminate layup parameter

C_2 is the full penetration stress concentration parameter

C_3 is the laminate thickness parameter

C_4 is the material toughness parameter

C_5 is the impact energy parameter

W_e is the impactor size parameter

Empirical expressions for the influencing parameters were obtained in algebraic forms. These expressions are summarized below.

$$C_1 = 0.547\ (E_X/E_L)^{0.524} \tag{7}$$

$$C_2 = 3.707 \tag{8}$$

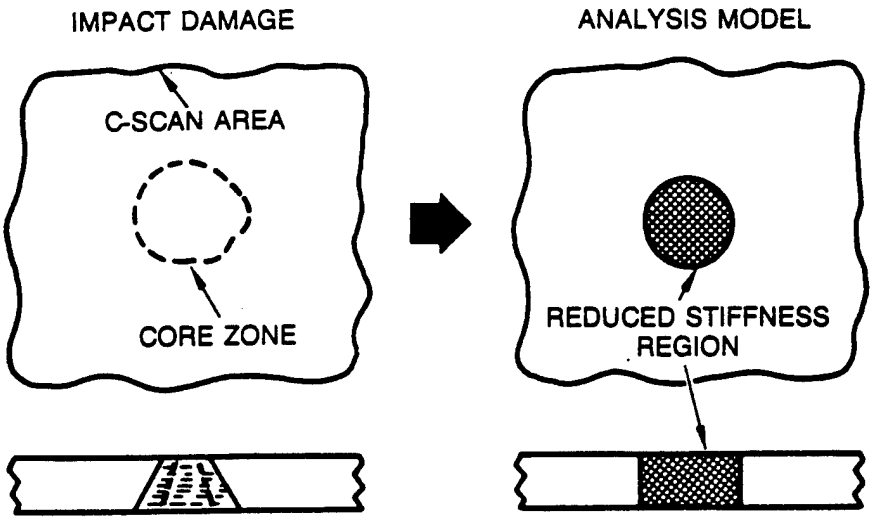

Figure 14. Stiffness Reduction Model.

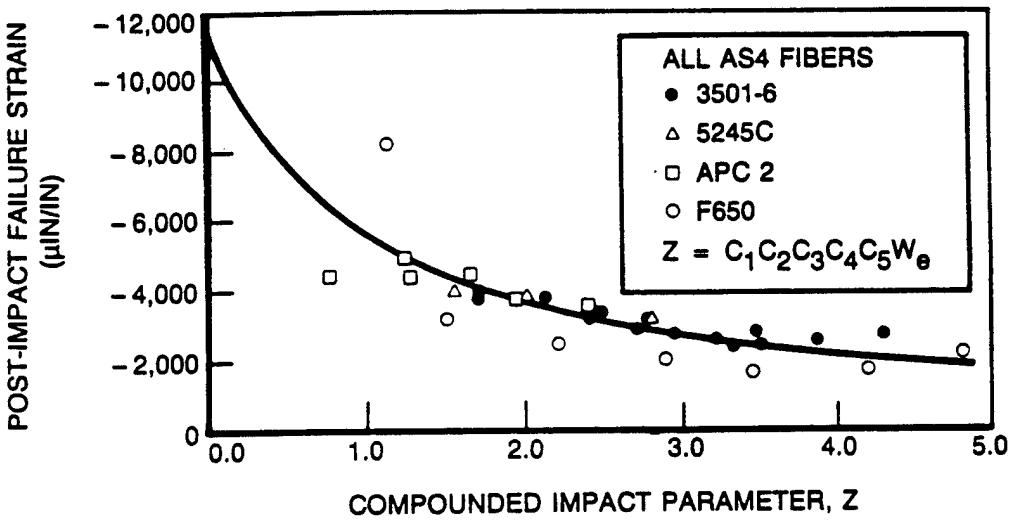

Figure 15. Comparison of Predicted and Observed Strength.

$$C_3 = 0.499/t^{0.5056} \quad (9)$$

$$C_4C_5 = A(kE)^B \quad (10)$$

$$A = 0.749/G_{IC} + 0.0145 \quad (11)$$

$$B = 0.4345 + 0.109\ G_{IC} - 0.0098\ G^2_{IC} \text{ for } G_{IC} \leq 5.55 \quad (12)$$

$$B = 0.737 \text{ for } G_{IC} \geq 5.55$$

where

E_x is the laminate Young's modulus in the loading direction

E_L is the longitudinal Young's modulus of the lamina

t is the laminate thickness

G_{IC} is the Mode I fracture toughness of the resin

k is the support condition coefficient.

The coefficient k is added in Equation (10) to account for the support condition effects. This coefficient is an indication of the amount of energy consumed for damage creation in an impact event. The value of k is taken as 1.0 for midbay impact of the 3-spar panel tested in Reference 12. The value of k is approximately 1.4 for the coupon impacted according to the NASA procedure. The spar-edge impact on the 3-spar panels is equivalent to k = 0.42.

To examine the overall predictive capability of the model, the failure strength in Equation (6) was expressed in terms of a single independent variable and written as

$$\sigma_f = \sigma_o/(1 + Z) \quad (13)$$

where

$$Z = C_1C_2C_3C_4C_5W_e$$

The experimental data were then correlated in terms of the compounded variable Z. The failure strains were plotted against the variable Z in Figure 15. The prediction using Equation (13) is also shown in the figure. The figure shows that, except for two data points, the model describes the general data trend very well.

3.3 Failure Analysis of Impact Damaged Composite Structures

The overall post-impact strength of a built-up composite structure is significantly influenced by the structural configuration. It was observed, during the static tests of the impact-damaged 3-spar panels (Reference 12), that failure in most of the specimens was in two stages. At the initial failure, the damage propagated to the spar fastener lines. The damage propagation was arrested by the spars, with final failure taking place at a higher applied load.

The damage propagation arrestment mechanism is provided by the stiffeners through (1) increased local stiffness due to the presence of the stiffeners and (2) the clamping force of the fastener that prevents out-of-plane displacement of the delamination. After the initial failure, further increase of the applied load will cause load redistribution within the structure. With the arrested damage zone acting as a stress concentrator, severe stress concentration builds up near the spars, and the final failure mode is compression failure outside the damaged bay. The failure load is controlled by the severity of the stress concentration, similar to the failure of specimens with an open hole.

Structural configuration effects on post-impact strength were incorporated semi-empirically in the stiffness reduction model in Reference 12. In this extension of the stiffness reduction model, the impact damage is assumed to act as a slit after initial failure and arrest as shown in Figure 16. Initial failure is determined using the stiffness reduction model. After the initial failure, the damaged bay is assumed to be totally ineffective, with the slit (representing the arrested impact damage) causing strain concentration in the spar and adjacent bays. Loss of load-carrying capacity of the damaged bay is a conservative assumption, since experimental data (Reference 12) indicate that a small amount of the load is transferred through the damaged area. From this assumption, the overall equilibrium of the structure requires

$$P_{TOT} = P_{sp} + P_1 + P_2 + P_3 \tag{14}$$

where P_{TOT} is the total applied load

P_{sp} is the amount of load carried by the spars

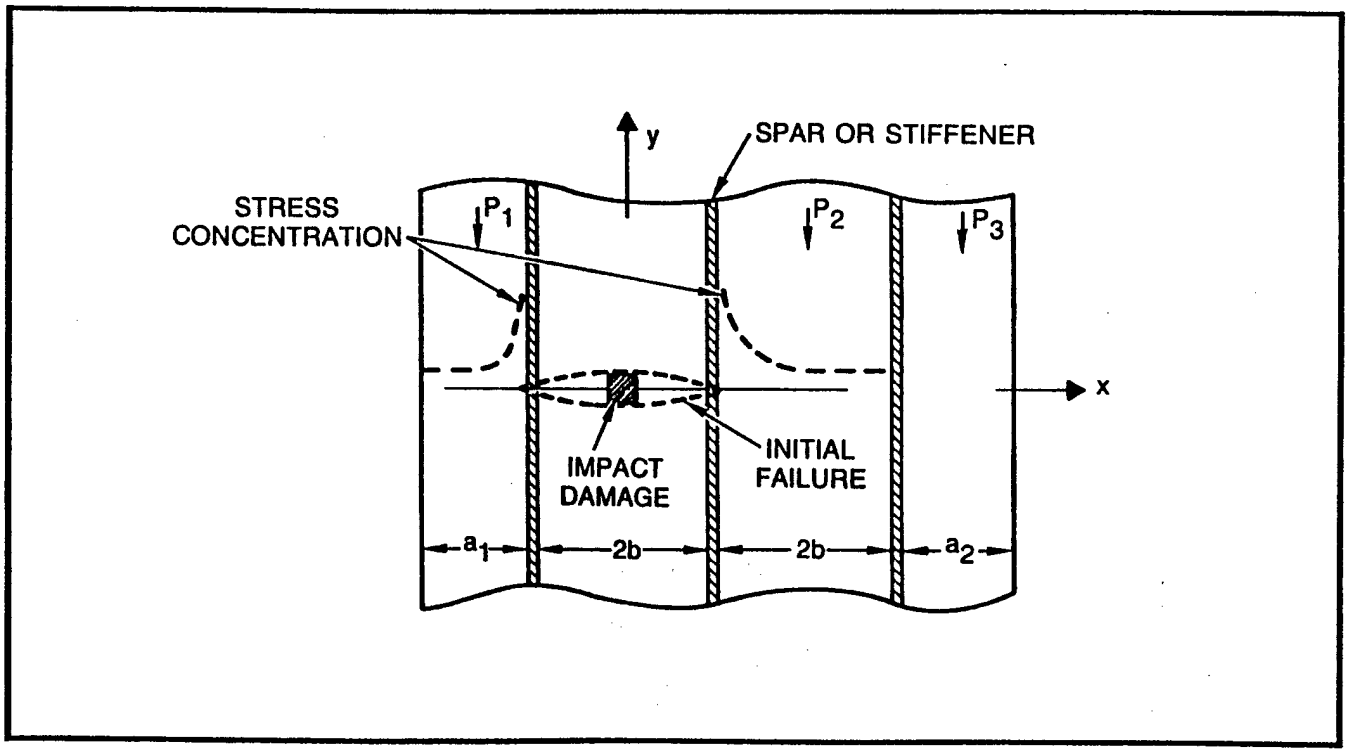

Figure 16. Structural Configuration Effects on Post-Impact Strength.

P_1 is the amount of load carried by the adjacent partial bay

P_2 is the amount of load carried by the adjacent full bay

P_3 is the amount of load carried by the remote partial bay

The load distribution (P_1, P_2, P_3) is obtained by integrating the stresses along the x-axis in Figure 16 with the stress distribution empirically determined from strain data generated in Reference 12. Final failure is then predicted using an average stress (strain) criterion similar to that used for strength prediction of laminates with an open or loaded hole. The influence of impact location (midbay, spar edge, or over spar) on post-impact strength is accounted for by using the support coefficient, k, (see Equation (10)).

The final failure strain (load) predicted by this method is then compared to the initial failure strain (load) predicted by the basic stiffness reduction model. If the initial failure strain is larger than the final failure strain, damage propagation will not be arrested by the structure and the initial failure coincides with the final structural failure. If the final failure strain is larger than the initial failure strain, the failure is a two-stage failure; that is, the initial unstable propagation of damage will be arrested by the structure. Thus, final failure will occur at a higher applied load.

Figure 17 shows a comparison of the predicted and observed failure strain for the 0.25 in. thick, AS4/3501-6 3-spar panels tested in Reference 12. The panel skin was (42/50/8) layup and the spar spacing was 5.5 in. with the total panel width of 18 in. The figure shows that the model predicts damage growth propagation will not be arrested by the structure when the impact energy is below 30 ft-lb or the initial failure strain is above 3800 micro-in/in. Above the energy level of 30 ft-lb., a two-stage failure will take place and the final failure strain is constant at 3800 micro-in/in. As shown in Figure 17, the predictions agree very well with the experimental data for both initial and final failure strains. Figure 18 shows the overall

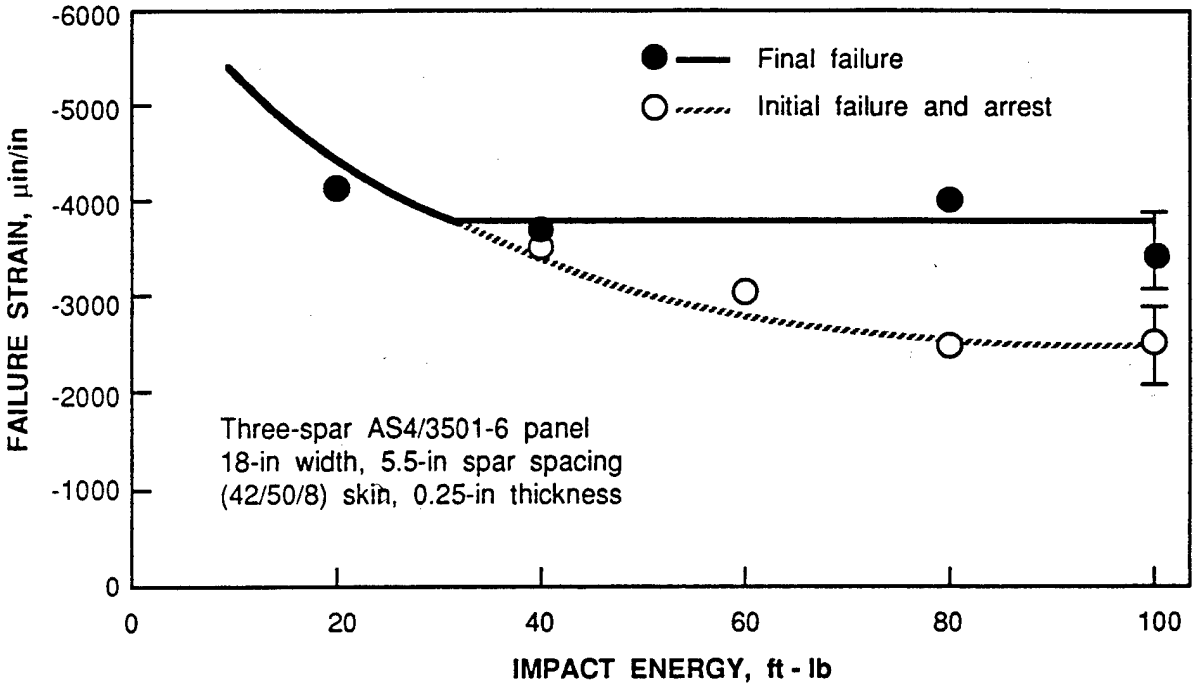

Figure 17. Comparison of Observed and Predicted Strain for AS4/3501-6 3-Spar Panels.

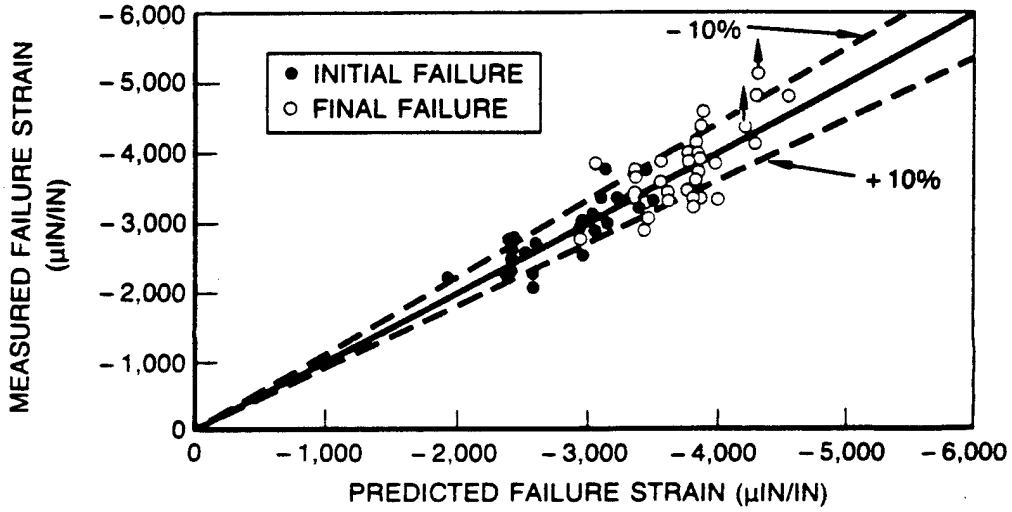

Figure 18. Overall Comparison of Measured and Predicted Structural Strength.

comparison of the measured and predicted post-impact structural strength. Both the initial and final failure strains are shown in the figure. The figure also shows a ±10% band about the predicted strain. It can be seen from the figure that the band covers a majority of the experimental data. This verifies the prediction capability of the model. This model forms the basis for the reliability analysis discussed in Section 4.

3.4 Damage Area Based Strength Prediction

The stiffness reduction model for post-impact compression strength prediction was modified to allow the C-scan damage area as an independent parameter. In its original form, the stiffness reduction is given by Equation (6). For the damage area based model, it is assumed that the influence of C_1, C_2, C_3 remain unchanged. That is the post-impact strength based on damage area is influenced by the laminate layup, thickness and full penetration stress concentration in the same manner as the post-impact strength based on impact energy. The parameters C_4, C_5 and W_e in the damage area based model are redefined as a single parameter which depends on the damage size and material fracture toughness (G_{IC}). Let $\lambda = C_4C_5W_e$ then Equation (6) can be rewritten as

$$\sigma_f = \sigma_o/(1+C_1C_2C_3\lambda) \tag{15}$$

the parameter λ as a function of damage area is determined by fitting strength data for each material to the expression

$$\lambda = m_1A^{m2} \tag{16}$$

where A is the damage area, m_1 and m_2 are material dependent fitting constants.

The parameter λ is determined by writing Equation (15) as

$$\lambda = \left[\frac{\sigma_o}{\sigma_f} - 1 \right] / C_1C_2C_3 \tag{17}$$

For the 0.25 inch thick, (42/50/8) layup laminate tested in Reference 12 and under a Northrop IRAD program, the constant $C_1C_2C_3 = 1.46$. The values of λ as a function of damage area for the AS4/3501-6 laminate data are shown in Figure 19. The values of λ are fitted to Equation (16) using the least squares method. The values of m_1 and m_2 are 0.79841 and 0.37084, respectively. As can be seen in Figure 19, the scatter for the value of λ is

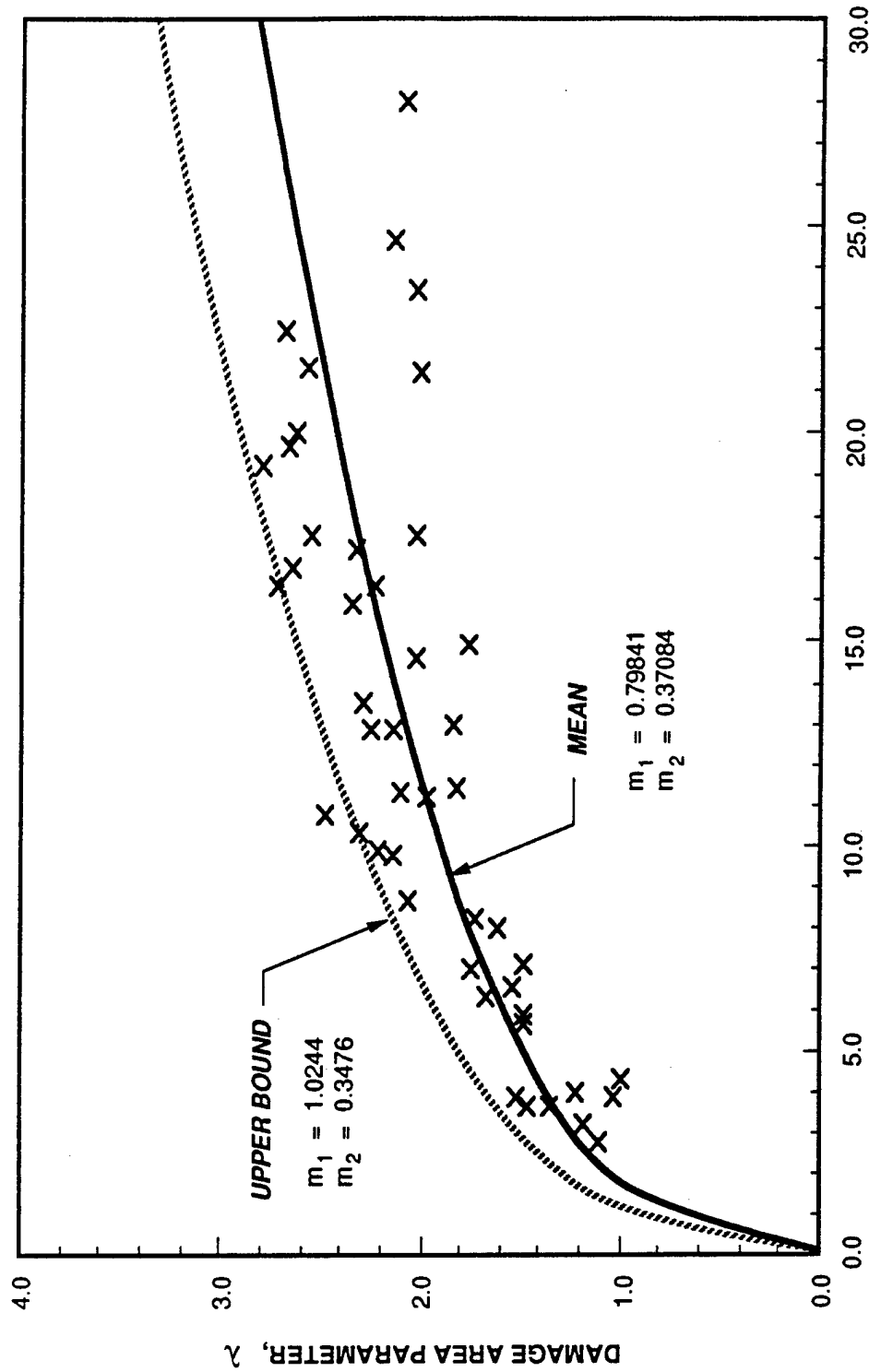

Figure 19. Damage Area Parameter for the AS4/3501-6 Data.

quite high. This type of high scatter in λ is consistent for all material systems. The high scatter in λ suggests that the post-impact strength based on damage area has higher scatter when compared to strength based on impact energy. In order that the strength scatter be incorporated in the modified stiffness reduction model, an upper bound fit of λ is also obtained. This upper bound λ predicts the lower bound post-impact strength. The values of m_1 and m_2 that fit the upper bound of λ are 1.02443 and 0.347566, respectively, for the AS4/3501-6 laminate.

This fitting technique was applied to post-impact strength data of other materials. The values of m_1 and m_2 for different materials are given in Table 5. These values show that m_1 decreases as the material fracture toughness increases; however, m_2 does not change significantly with G_{IC}. The overall data is then fitted into the equation

$$\lambda = m_1 A^{m_2} (G_{IC})^{m_3} \tag{18}$$

the value of m_1, m_2 and m_3 are obtained by using the least squares method and they are

$$m_1 = 0.78937$$

$$m_2 = 0.35139$$

$$m_3 = -0.17517$$

for the mean fit, and

$$m_1 = 1.09554$$

$$m_2 = 0.32620$$

$$m_3 = -0.16470$$

for the upper bound.

These values are incorporated into the stiffness reduction model for post-impact strength prediction. The results are shown in Figures 20-24 for different material systems. As can be seen from these figures, because of the

TABLE 5. FITTING CONSTANTS FOR THE DAMAGE AREA PARAMETER (λ).

MATERIAL	MEAN FIT		UPPER BOUND	
	m_1	m_2	m_1	m_2
AS4/3501-6	0.79841	0.37084	1.02443	0.34756
AS4/5250-3	1.01602	0.27090	1.30552	0.25434
AS4/5245C	0.67562	0.32014	0.88217	0.29426
R6451	1.43506	0.28737	1.81275	0.27512
AS4/APC2	0.58677	0.34408	0.77053	0.31390

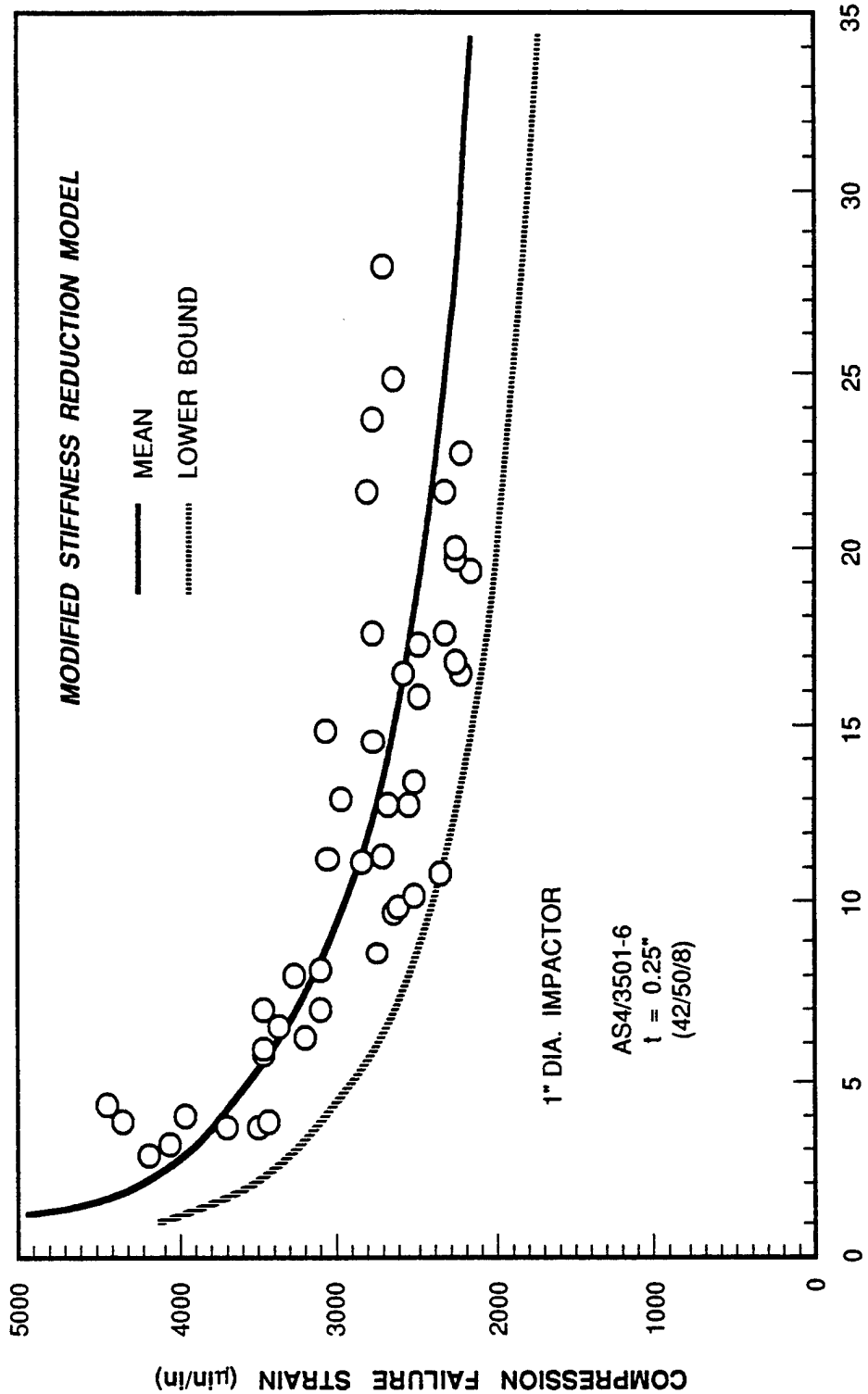

Figure 20. Predicted and Measured Post-Impact Compression Strength as a Function of Damage Area (AS4/3501-6).

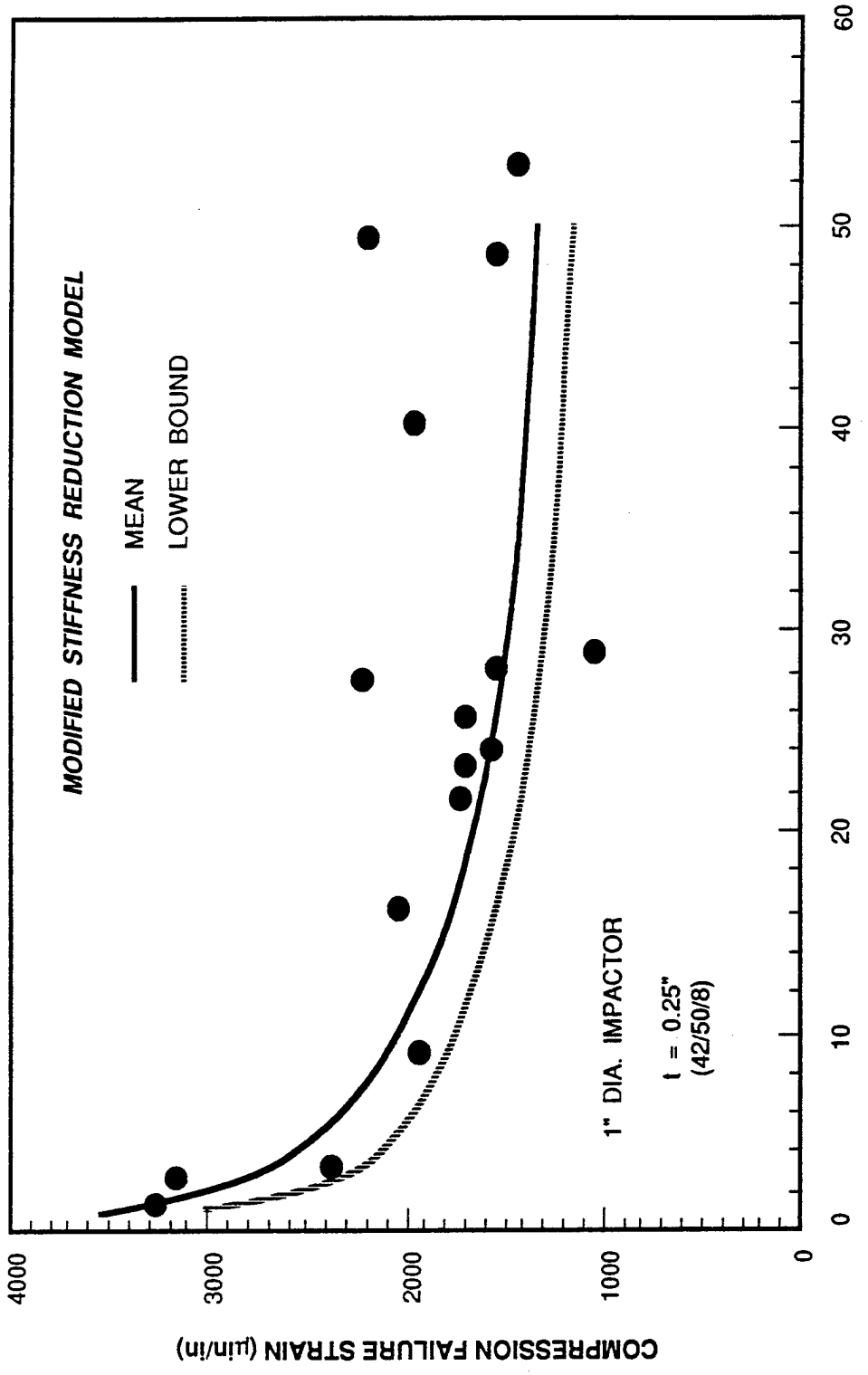

Figure 21. Predicted and Measured Post-Impact Compression Strength as a Function of Damage Area (R6451, F650, V378).

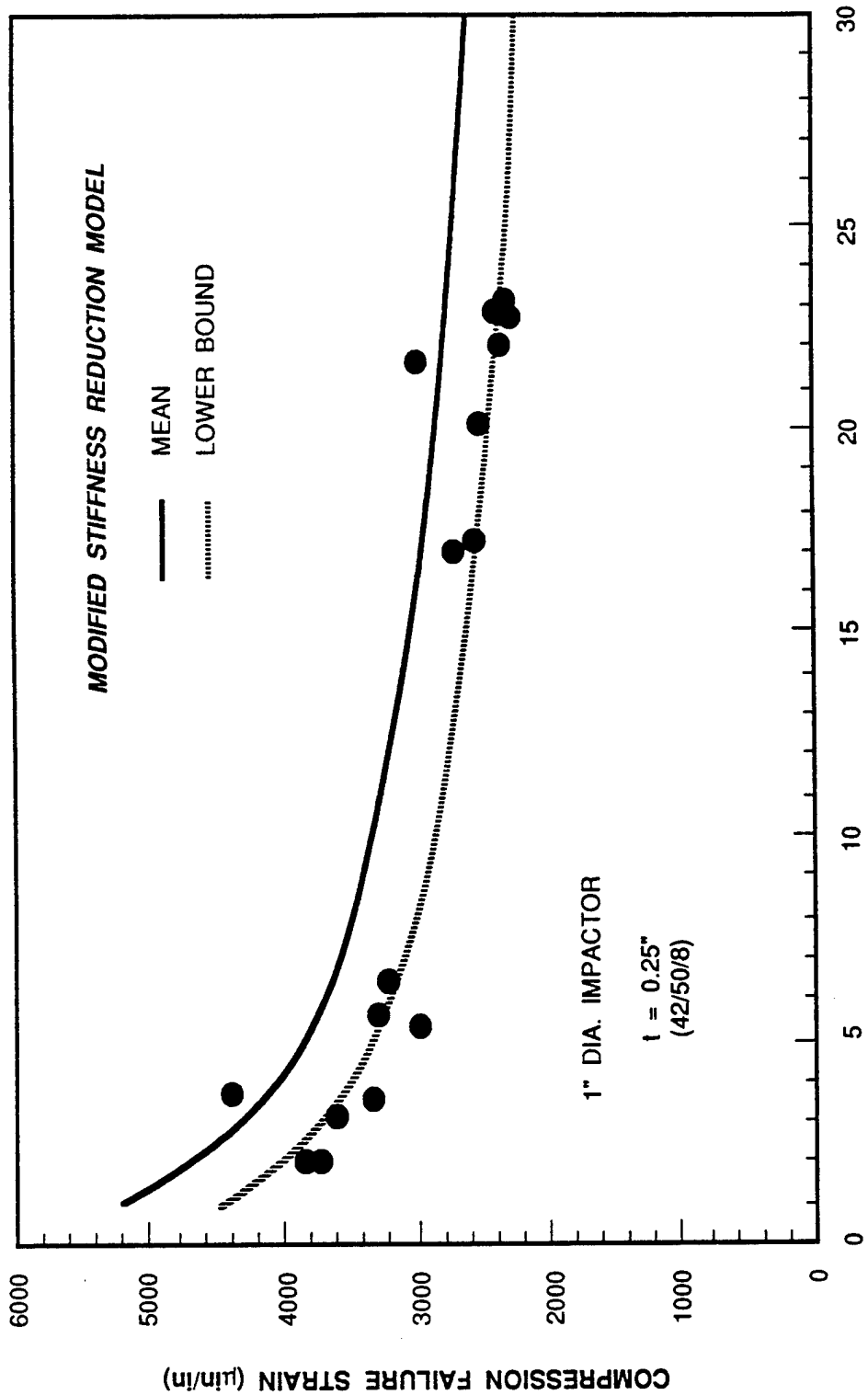

Figure 22. Predicted and Measured Post-Impact Compression Strength as a Function of Damage Area (AS4/5250-3).

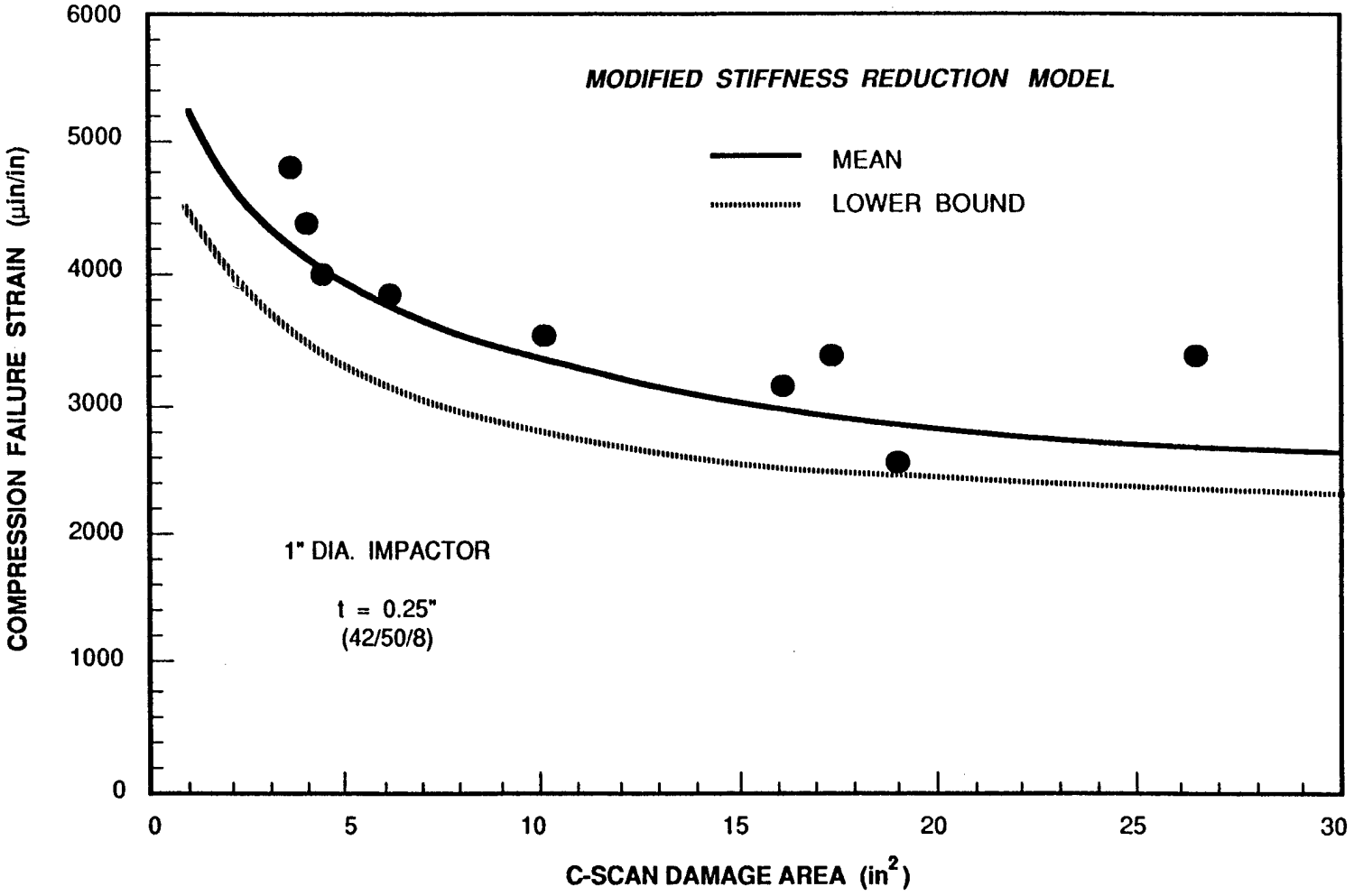

Figure 23. Predicted and Measured Post-Impact Compression Strength as a Function of Damage Area (AS4/5245C).

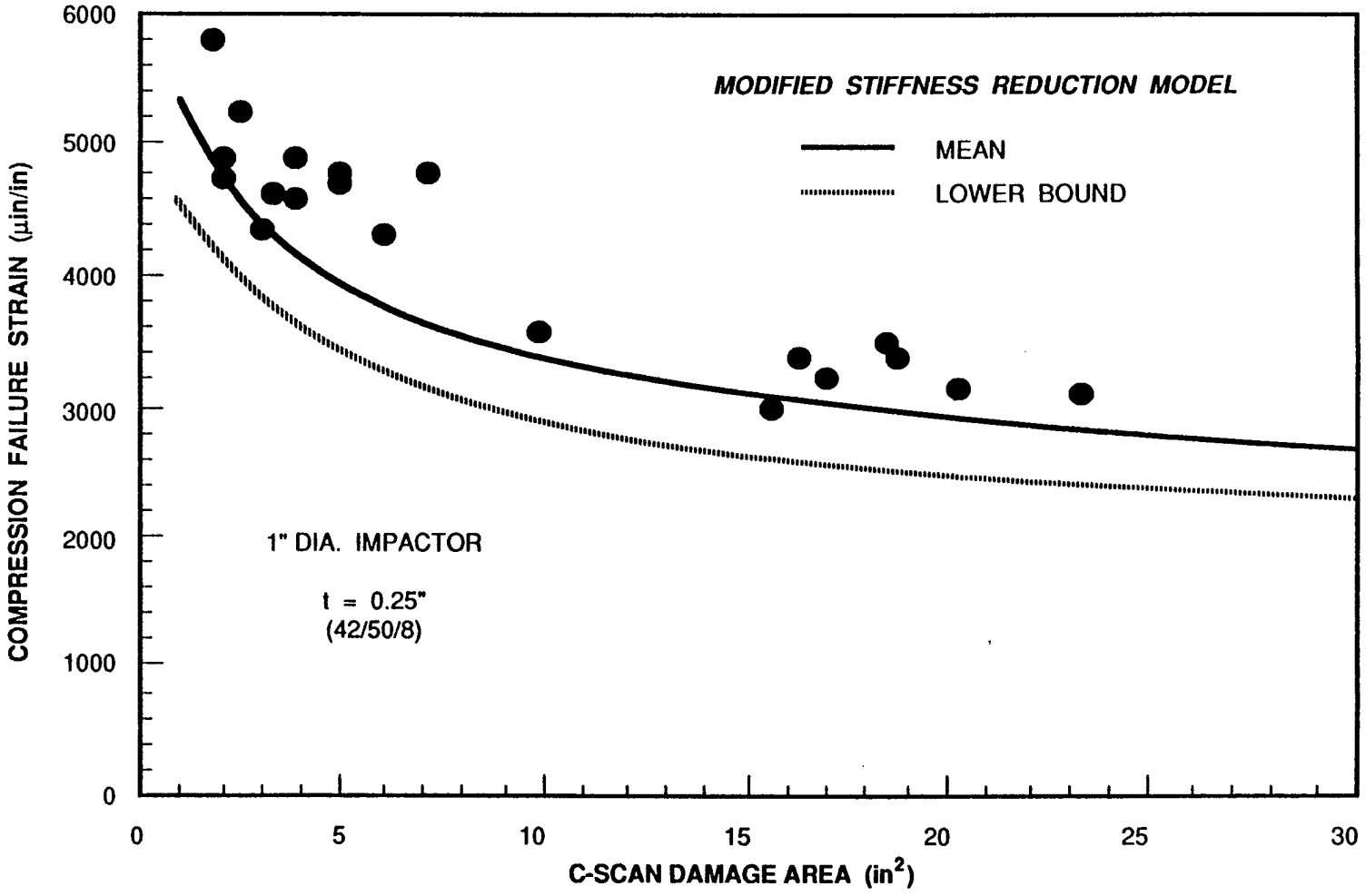

Figure 24. Predicted and Measured Post-Impact Compression Strength as a Function of Damage Area (AS4/APC2).

higher scatter in the test data, the lower bound prediction provides a more conservative post-impact strength.

This modified stiffness reduction model will be used as a baseline for structural reliability analysis.

SECTION 4

DAMAGE TOLERANCE METHODOLOGY

During Task IV of this program, an integrated reliability analysis method was developed. In this analysis, the reliability of a composite structure, under a given impact threat, was evaluated at various applied stress (strain) levels. The method integrates the post-impact strength analysis technique, the post-impact strength data scatter and the impact threat distribution into a single reliability computation. The analysis procedure is schematically shown in Figure 25. Figure 25a shows the relationship between the post-impact strength and the impact energy. Also shown in Figure 25a are the post-impact strength data scatter at different impact energy levels. The stiffness reduction model discussed in Section 3-2 was used to establish the relation between the post-impact strength and the impact energy. The strength scatter is described by a Weibull distribution and will be discussed in Section 4.1. In Figure 25b, the impact threat distribution is shown as a Weibull distribution (Section 2.3). The post-impact strength and the impact threat are combined to form a compounded distribution to determine the damage tolerance strength reliability at given applied stress (strain), as shown in Figure 25c, which will be discussed in Section 4.2.

4.1 Post-Impact Compression Strength Scatter

The post-impact compression strength test data generated in Reference 12 and under a Northrop IR&D program were statistically analyzed to determine the data scatter. Individual and joint Weibull methods were used for the analysis. Post-impact compression failure strains were obtained after the specimens were impacted at energy levels between 20 to 100 ft-lb. The materials tested in the references included four composite systems. The results of the joint Weibull analysis are summarized in Table 6. The table also shows the total number of data points and number of impact energy levels for each material system. As can be seen from the table the joint Weibull shape parameter (α) ranges from 12.65 for the CE12K or AS6/5245C system to 40.81 for the AS4/5250-3 material. However, it may be noted that the total number of data points is limited. The high value of α or low scatter observed for the AS4/5250-3 material may not be representative.

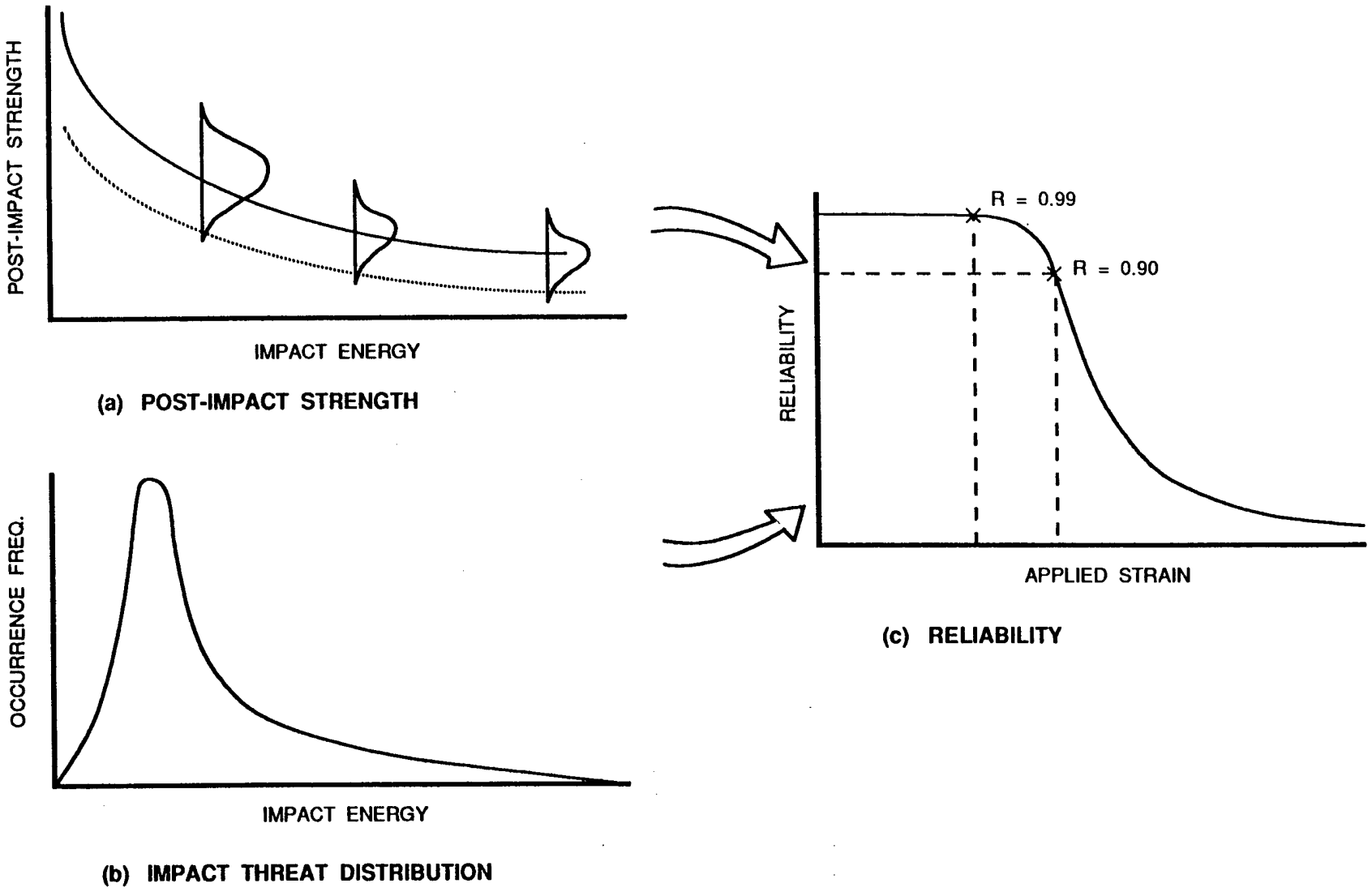

Figure 25. Schematic of the Integrated Reliability Analysis Method.

TABLE 6. SUMMARY OF POST-IMPACT STRENGTH DATA SCATTER.

MATERIAL	TOTAL No. DATA POINTS	No. OF IMPACT ENERGY LEVELS	JOINT WEIBULL α
AS4/3501/6	50	7	12.87
AS4/5250-3	14	4	40.81
CE12K AS6/5245C	10	3	12.65
AS4/APC2	19	5	17.59

The AS4/3501 material was more thoroughly tested. Therefore, more realistic statistics may be obtained from this data set. A more detail statistical analysis was then conducted on this data set. Strength data for this material were obtained after 20, 40, 50, 60, 70, 75 and 100 ft-lb of impact. The average post-impact compression failure strain and the individual Weibull distribution of the strength after different levels of impact are shown in Figure 26. The figure also shows the predicted post-impact strength using the stiffness reduction model. In addition, the B-basis strength computed from the joint Weibull analysis is also given in the figure. The results of the individual Weibull analysis show that the shape parameter ranges from 8.2 to 22.9. Figure 26 shows that the scatter varies randomly with the impact energy. No relation can be established between α and impact energy.

Based on the above scatter analysis, a Weibull shape parameter α = 12.0 is tentatively selected for use in the analysis that follows.

4.2 Integrated Structural Reliability Analysis

The post-impact probability of survival of a structure under an applied strain ϵ is $p(\epsilon)$. The probability is dependent upon the impact energy and the post-impact strength scatter, in addition to the impact parameters discussed in Section 2.2. The mean strength after a given impact is obtained from the stiffness reduction model. The post-impact strength distribution with Weibull parameters α_{pI} and β_{pI} can then be defined using the results of the post-impact strength data analysis of Section 4.1. It may be noted that the value of α_{pI} is assumed to be constant, but the value of β_{pI} varies with impact energy.

The probability of occurrence at energy level E under a given impact threat is defined by the Weibull distribution discussed in Section 2.3. This probability is denoted by P(E). By integrating $p(\epsilon)$ and P(E) over the entire range of impact energies the impact damage strength reliability is then given by the joint probability function

$$R(\epsilon) = \int_0^\infty p(\epsilon)\ P(E)\ dE \qquad (19)$$

The reliability $R(\epsilon)$ in Equation (19) is evaluated using a numerical integration technique. A computer program was written to compute $R(\epsilon)$. Results of the reliability computations are discussed below.

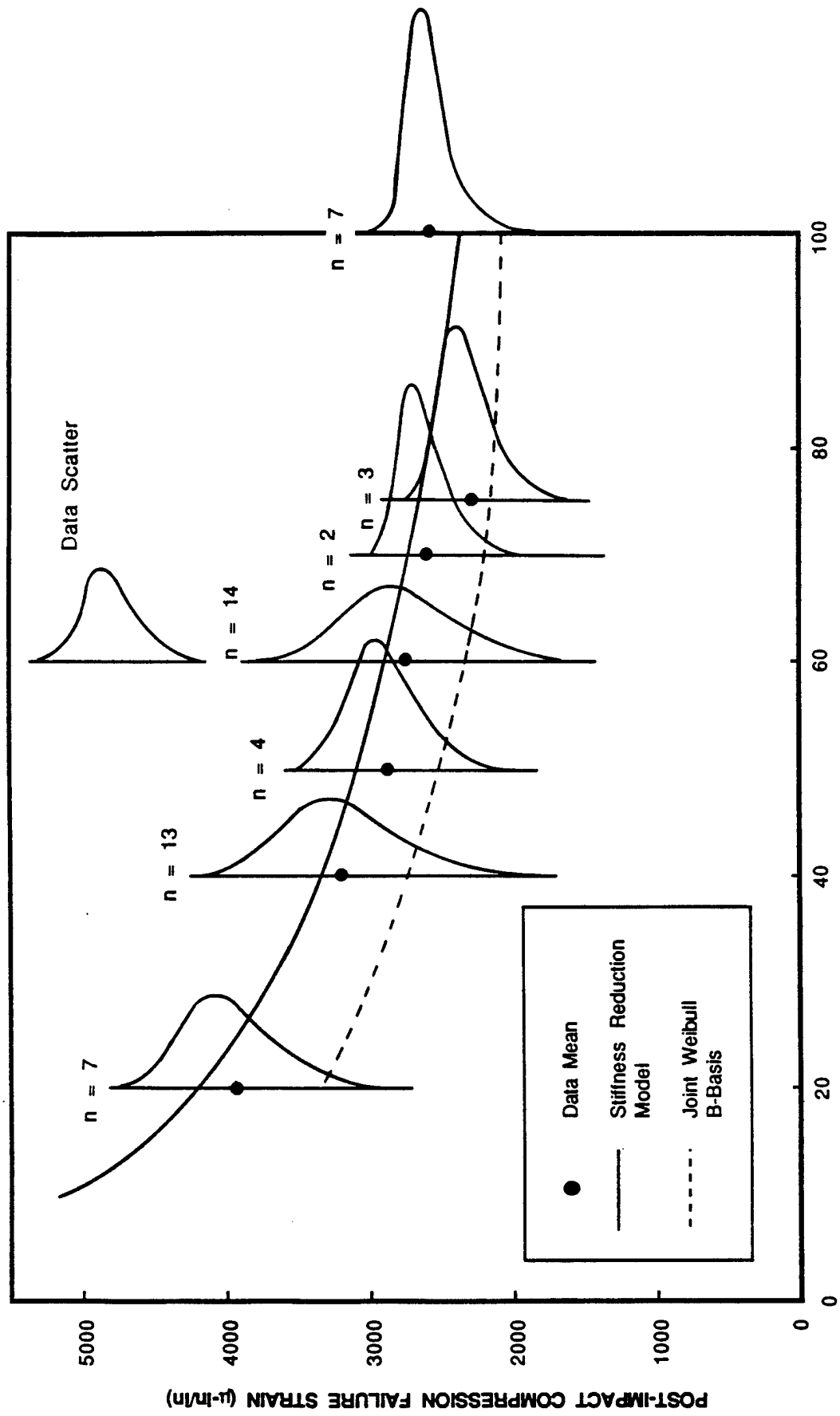

Figure 26. Post-Impact Failure Strain Distribution for AS4/3601-6 Laminate.

The influence of impact threat on the post-impact strength reliability is shown in Figure 27. The three levels of impact threat defined in Section 2.3 were used in the reliability computations. The composite laminate considered was the typical wing skin construction used in Reference 12. Namely, 0.25 inch thick, (42/50/8) layup, AS4/3501-6 laminate with a G_{IC} of 0.75 in-lb/in^2. The reliability shown in Figure 27 includes a 95% confidence. The post-impact strength scatter parameter used in the analysis was α = 12.0. As shown in the figure, the reliability is strongly influenced by the impact threat level. For the low impact threat, the applied strains associated with 90% and 99% reliability are 3464 and 2650 micro-in/in, respectively. These applied strains are reduced to 2856 and 2150 micro-in/in under the medium impact threat. Under the high level of impact threat, they are further reduced to 2288 and 1720 micro-in/in. These results indicate that structural zoning based on impact threat is very important in impact damage tolerance design of composite structures. A single impact damage tolerance knockdown factor is not sufficient and may result in over-conservative design.

The influences of the impact threat parameters on the post-impact strength reliability are shown in Figures 28 and 29. In Figure 28, the probability of occurrence for a 100 ft-lb impact, p(100), was fixed at 0.01. The post-impact strength reliability was computed for different values of modal impact energies (X_m). The figure shows that the reliability increases with decreasing X_m; however, the applied strain associated with a 90% reliability is not significantly changed for the range of X_m considered. The strain decreases from 2860 micro-in/in for X_m = 4.0 ft-lb to 2760 micro-in/in for X_m = 20 ft-lb. Figure 29 shows the post-impact strength reliability for different values of p(100) as X_m is fixed at 6 ft-lb. As the value of p(100) increases from 0.0001 to 0.1, the post-impact strength reliability decreases and the applied strain with 90% reliability decreases from 3480 to 2280 micro-in/in.

The influence of the post-impact strength data scatter (α_{pI}) on the post-impact strength reliability is shown in Figure 30. The figure shows the reliability for α_{pI} ranges from 8.0 to 20.0. It can be seen that the reliability increases as the scatter decreases (α_{pI} increases). However, in the range of α_{pI} between 10 and 20 the influence of α_{pI} on the reliability is small. The post-impact strength reliability is more significantly influenced by α_{pI} when the value of α_{pI} is smaller (higher scatter).

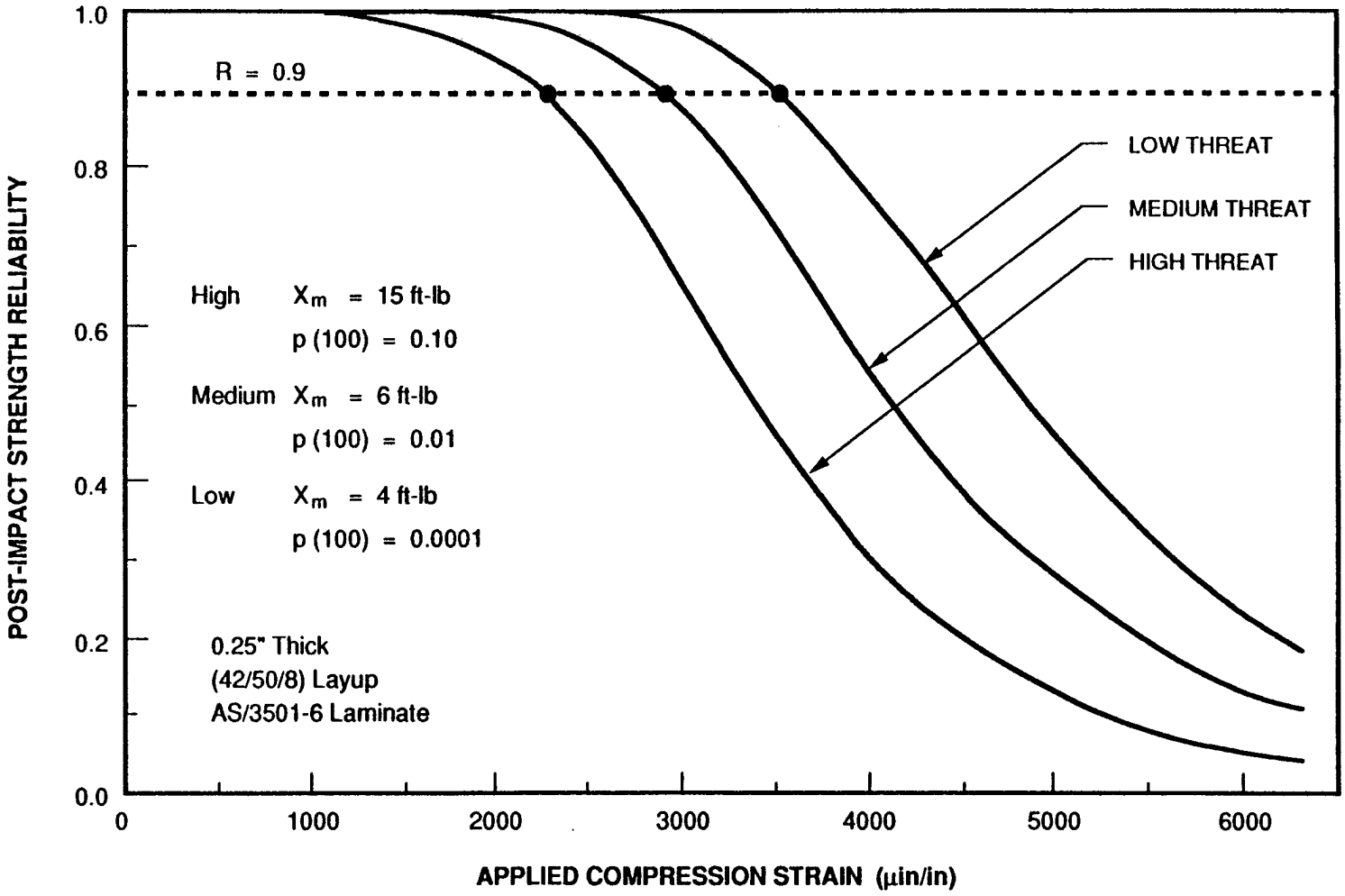

Figure 27. Influence of Impact Threat on the Post-Impact Strength Reliability.

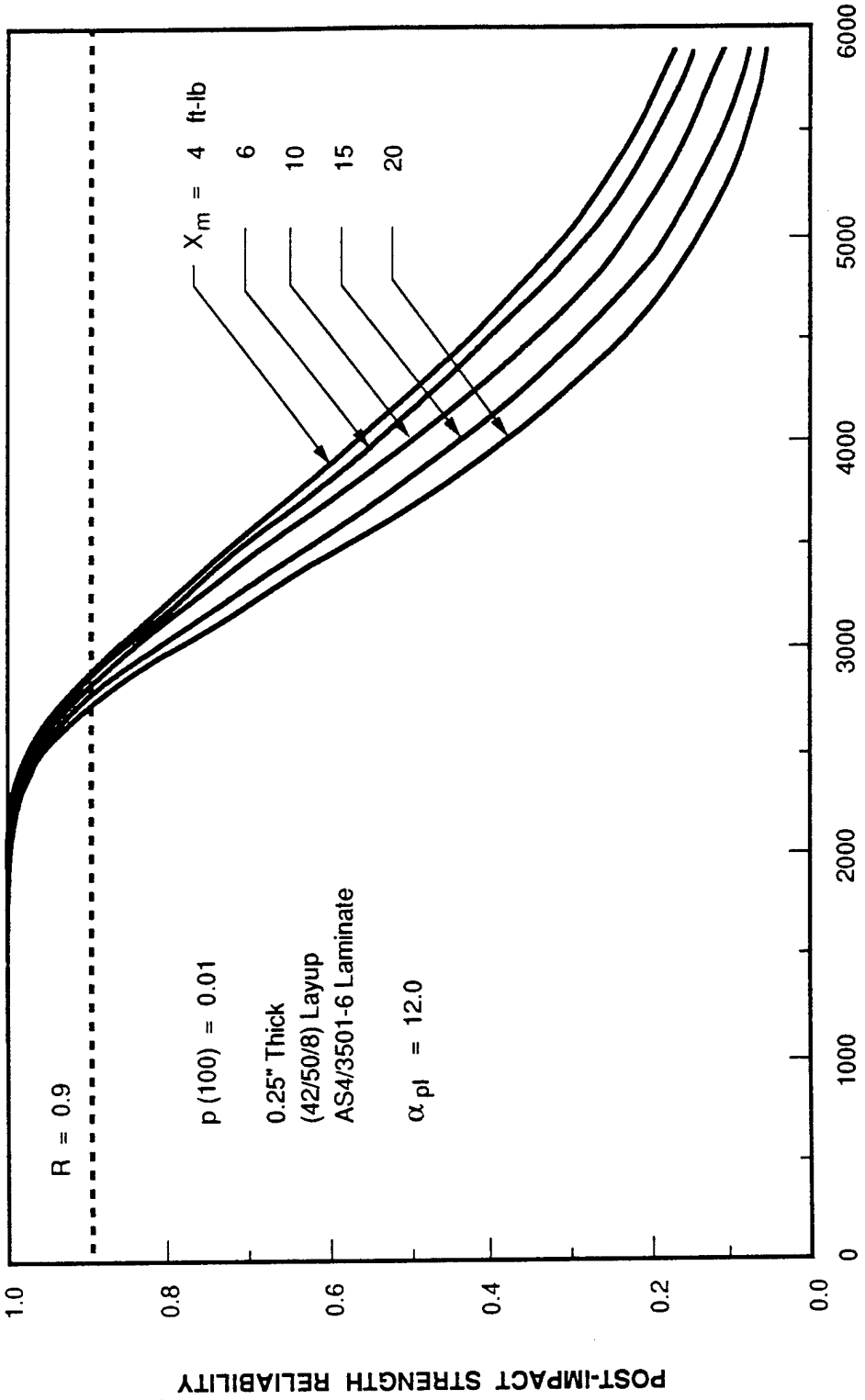

Figure 28. Influence of Modal Impact Energy on the Post-Impact Strength Reliability.

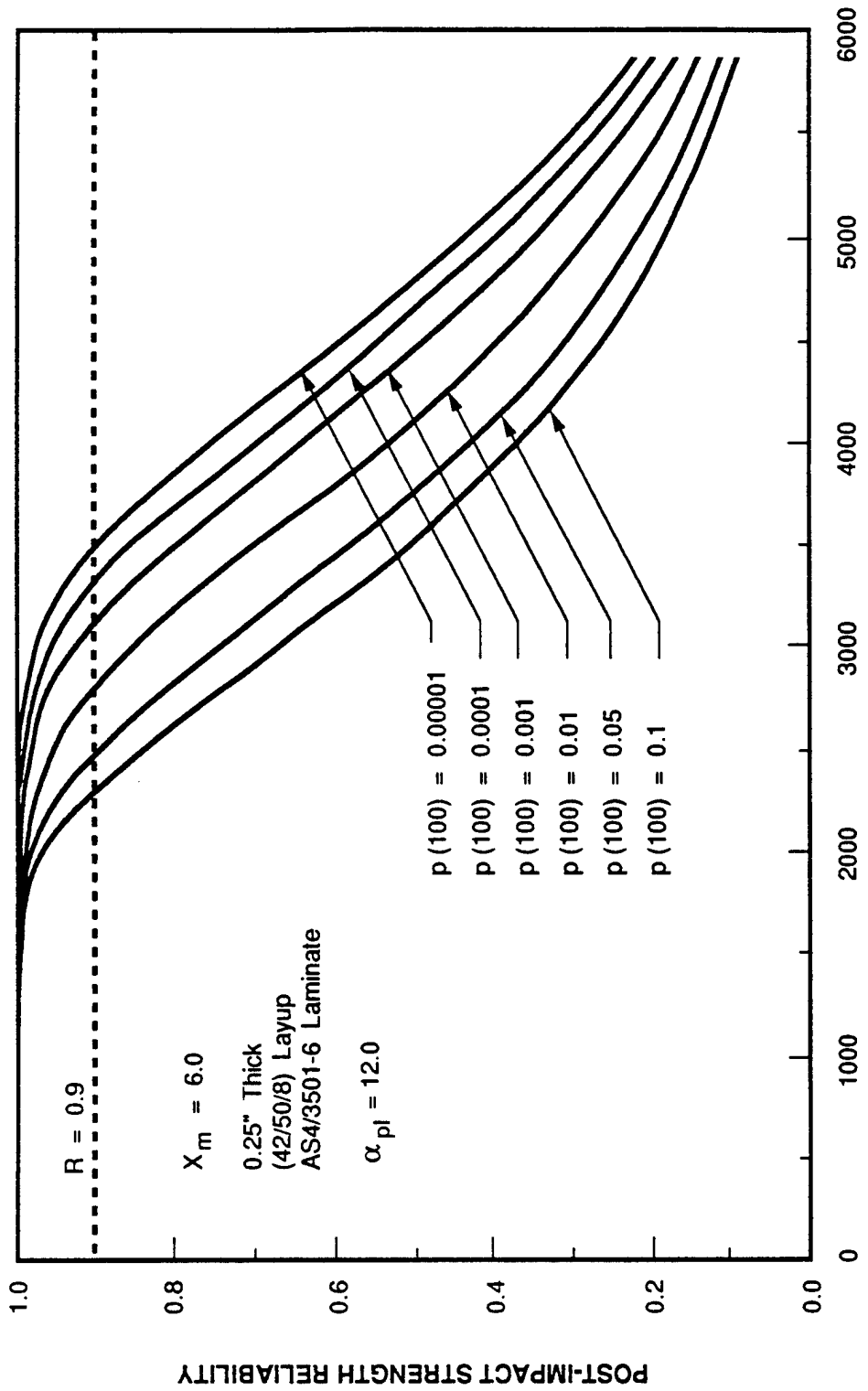

Figure 29. Influence of Remote Probability of Occurrence on the Post-Impact Reliability.

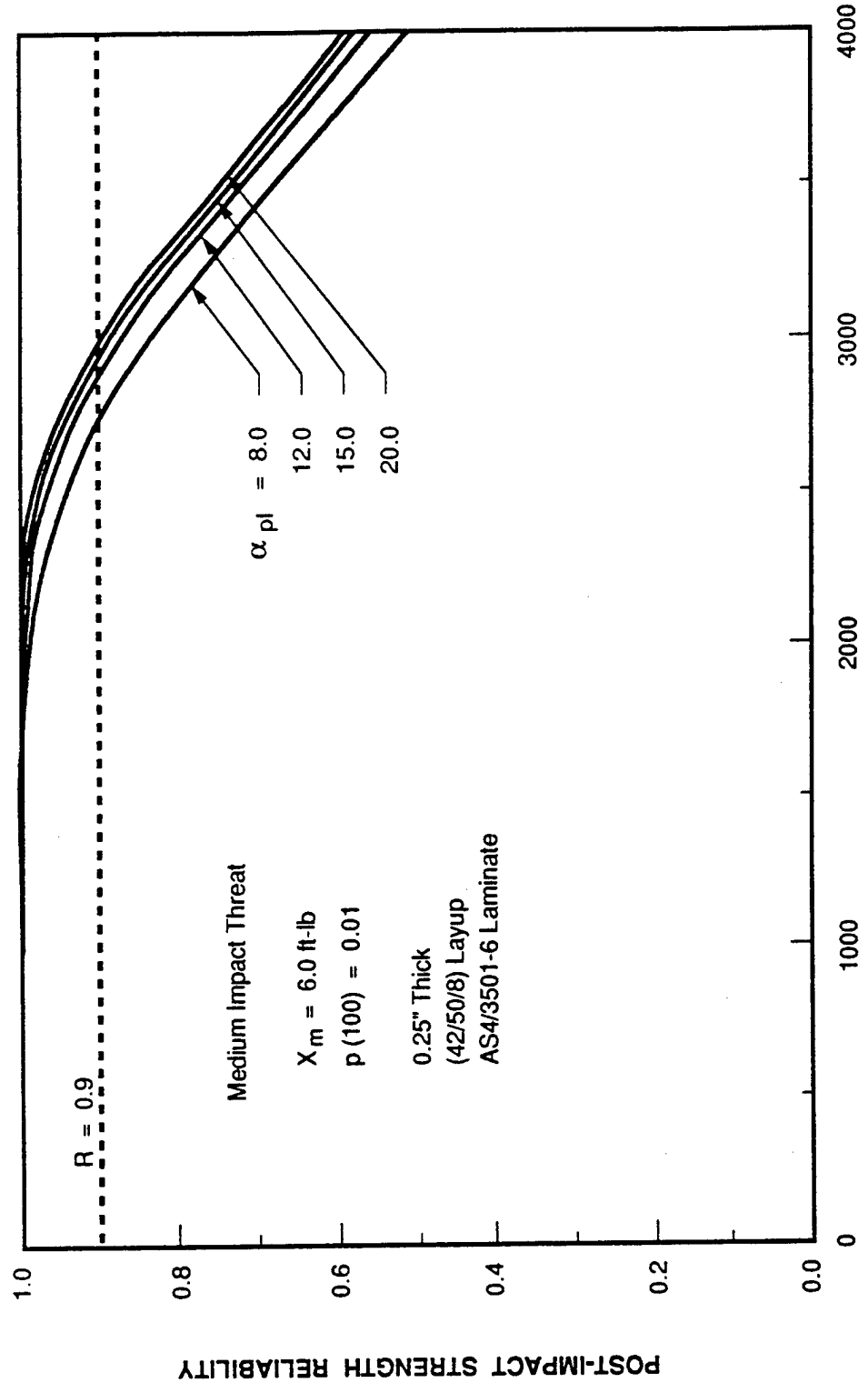

Figure 30. Influence of Post-Impact Strength Scatter on Damage Tolerance Reliability.

Figure 31 shows the influence of material G_{IC} on the post-impact strength reliability. The value of G_{IC} varies from 0.75 to 6.0 in-lb/in^2. This range covers most of the commonly used composite material systems. As shown in the figure, the post-impact strength reliability is significantly influenced by material for the same impact threat.

A sensitivity study was also conducted to determine the influence of various parameters on the reliability of impact damaged built-up structures. The parameters investigated include: impact threat level, threat parameters X_m and $p(X_p)$, fracture toughness (G_{IC}), stiffener spacing, stiffener stiffness and post-impact strength scatter α. The final (structural) failure strain data in Reference 12 was statistically analyzed to determine the scatter; the limited amount of data available in Reference 12 showed a Weibull shape parameter of 15.

Figure 32 shows the effects of structural configuration on the reliability. The structure is exposed to a high threat defined in Figure 5. The structure considered is a 21-in. wide 3-spar panel. The spar spacing is 7 in. and the spar stiffness (AE) is 5.696×10^6 lb. The skin material is AS4/3501-6 with a fracture toughness of 0.75 in-lb/in^2. The laminate layup is (42/50/8) with a thickness of 0.25 in. As shown in Figure 32, at low applied compression strain (<1600 micro-in/in) the reliability is high and the effects of structural configuration is insignificant. At high applied strain (>3800 micro-in/in) the reliability is dominated by initial (coupon level) failure and the structural configuration has no influence on the reliability. Figure 32 shows that the reliability is significantly influenced by the structural configuration for the applied compression strains between 1600 to 3800 micro-in/in (shaded area in the figure). The applied strain for the 95% confidence and 90% probability (B-basis reliability) is 2290 micro-in/in for initial (coupon) failure and 3090 micro-in/in for final (structure) failure.

Figure 33 shows the structural configuration effects on the reliability for the 3-spar panel described above exposed to low impact threat. The figure shows that the structural configuration has a minimal influence on the reliability. This is because the low impact threat defined in Figure 5 contains mostly low energy impact events. The post-impact strength at lower impact energy is governed by single step failure as shown in Figure 17.

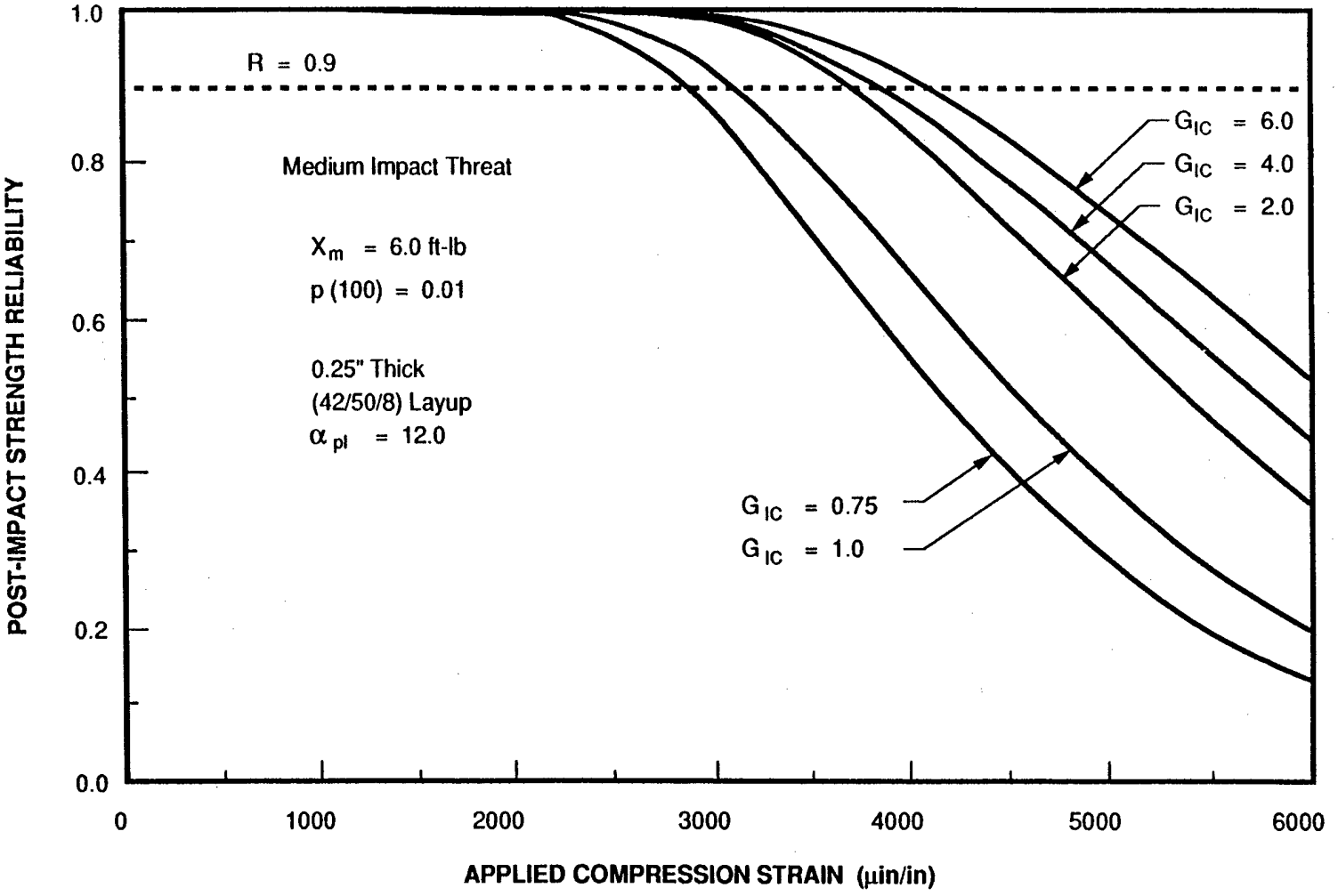

Figure 31. Influence of Fracture Toughness (G_{IC}) on Damage Tolerance Reliability.

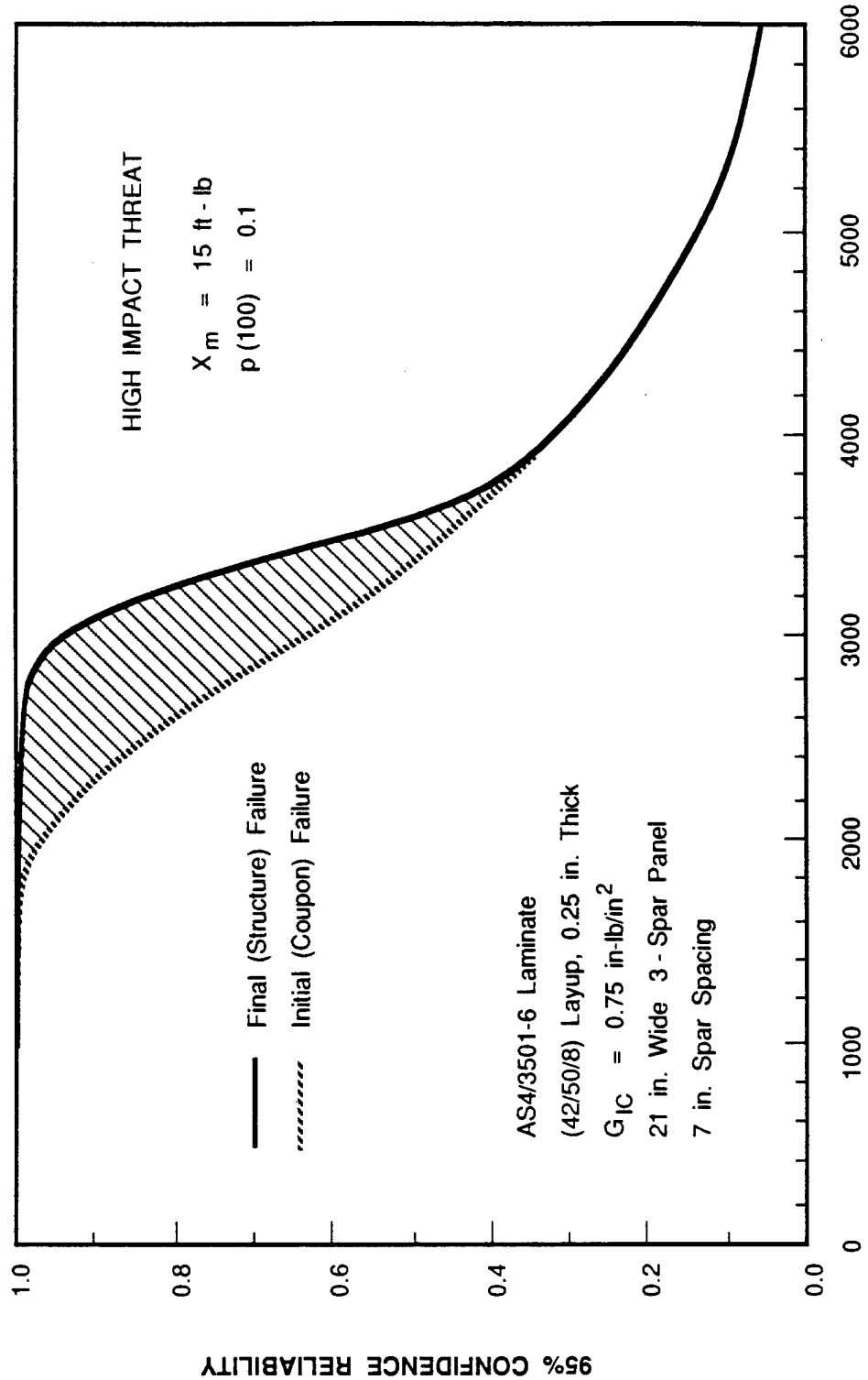

Figure 32. Structural Configuration Effects on Reliability of a 3-Spar Panel Exposed to High Impact Threat.

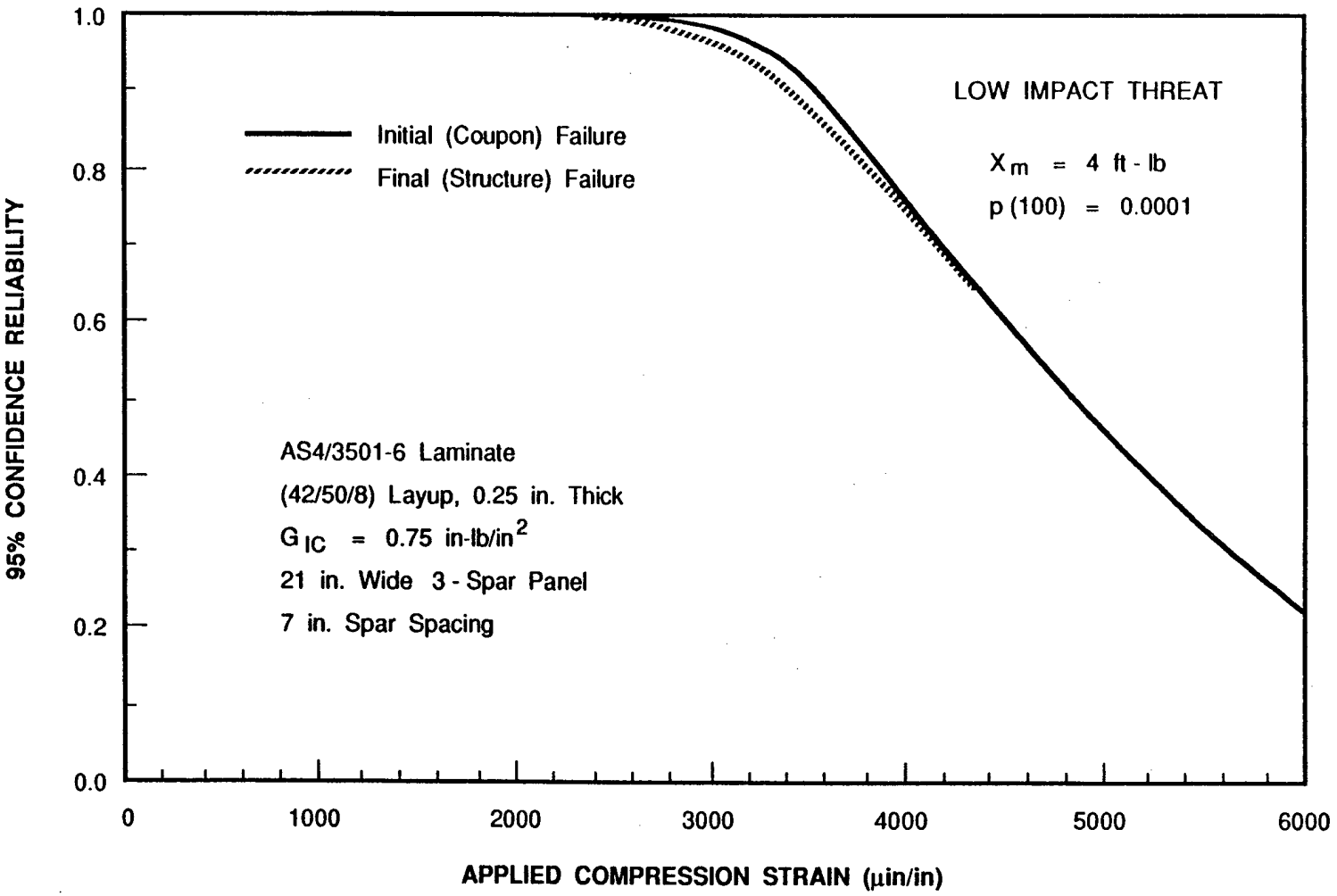

Figure 33. Structure Configuration Effects on Reliability of a 3-Spar Panel Exposed to Low Impact Threat.

The influence of impact threat on the structural reliability is shown in Figure 34 for the 3-spar panel described earlier. The figure shows that the reliability is higher when the structure is exposed to a low impact threat. The applied compression strength for a B-basis reliability are 3086, 3223 and 3510 micro-in/in for the high, medium and low impact threat, respectively. These values compare to 2288, 2856 and 3464 micro-in/in when structural configuration effects are not considered.

The influence of fracture toughness (G_{IC}) on damaged structural reliability is shown in Figure 35. The value of G_{IC} varies from 0.75 to 6.5 in-lb/in^2. This range covers most of the commonly used composite material systems. As shown in the figure, G_{IC} has a significant influence on the damaged structural reliability. The B-basis applied strain increases from 3223 micro-in/in for G_{IC}=0.75 in-lb/in^2 to 4171 micro-in/in for G_{IC}=6.5 in-lb/in^2.

The influence of spar (stiffener) spacing on the damaged structural reliability is shown in Figure 36. The figure shows that the spar spacing has a strong influence on the reliability. This is because the damage propagation arrestment capability of the structure depends on the spar spacing. For closely spaced spars, the damage is likely to be contained in a small region of the structure and it requires higher applied load to cause final failure of the structure. For widely spaced spars, the differential load between the final failure and the initial failure is small and therefore the structural configuration effect is less significant. The B-basis applied compression strains for 2.5 in spar spacing is 4816 micro-in/in and is decreased to 2979 micro-in/in when the spar spacing increases to 9 in.

4.3 Damage Area Based Structural Reliability

The scatter in the post-impact compression strength data in terms of C-scan damage area was incorporated into the damage area based strength prediction model, Equation (15), for structural reliability computation. This scatter is relatively higher in comparison to the impact energy based post-impact strength data. This was shown in Figures 20 through 24. This scatter was analyzed using a normalization technique and the Weibull distribution. In this scatter analysis, the post-impact compression mean strengths were first predicted using Equation (15). The experimental data were then normalized with respect to the predicted mean strength. A Weibull analysis was then

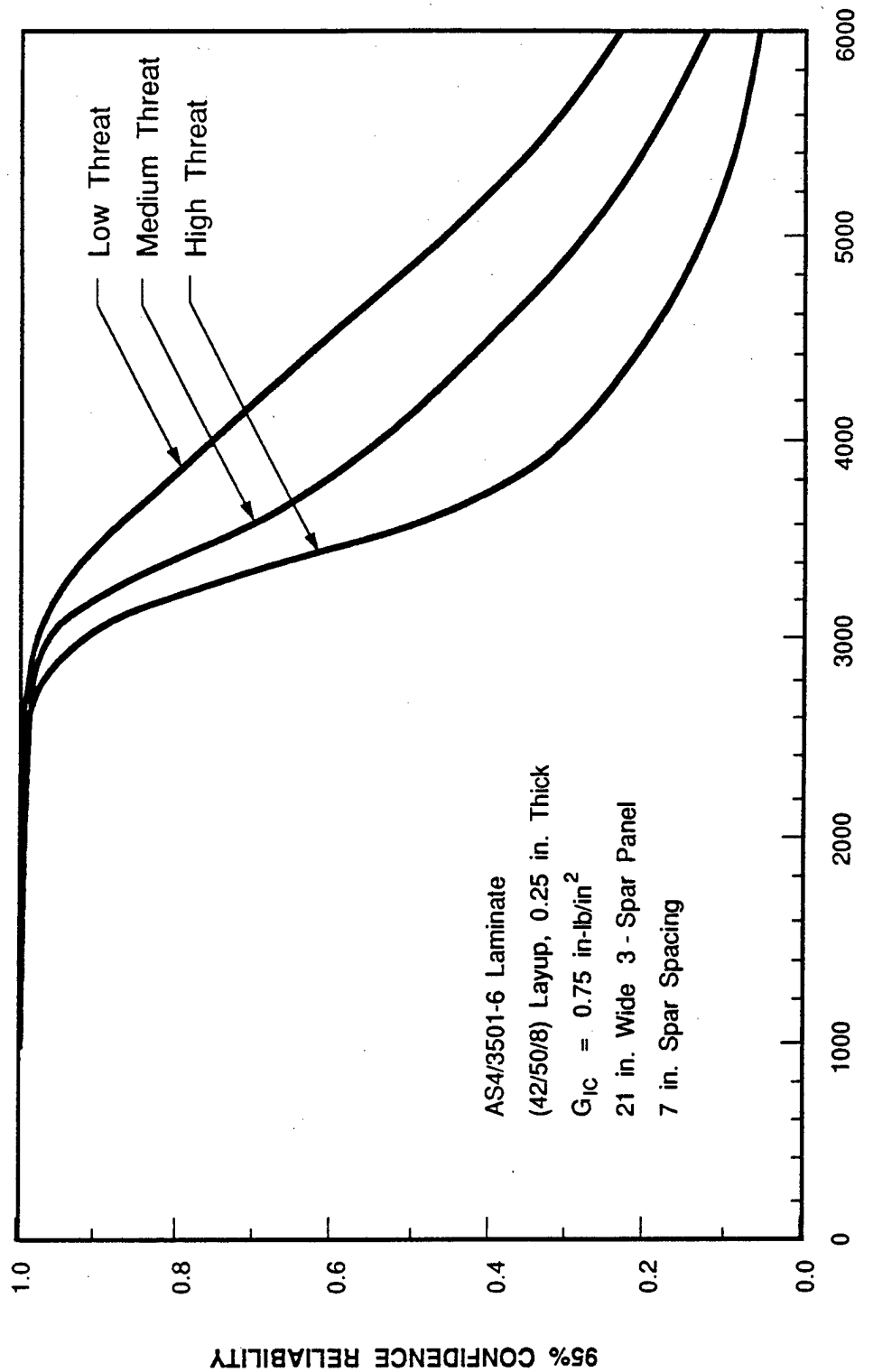

Figure 34. Influence of Impact Threat on Structural Reliability.

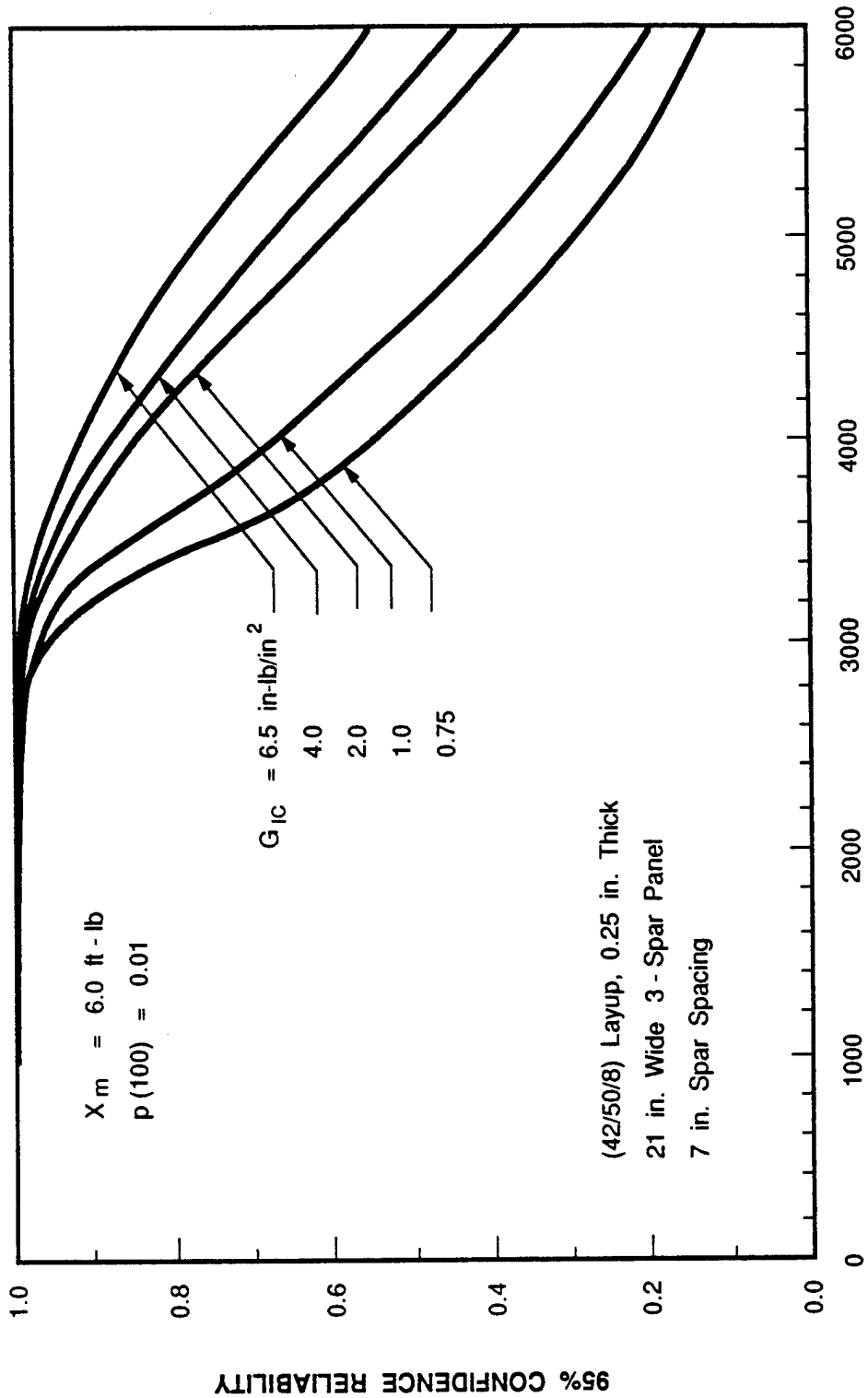

Figure 35. Influence of Fracture Toughness on Post-Impact Structural Reliability.

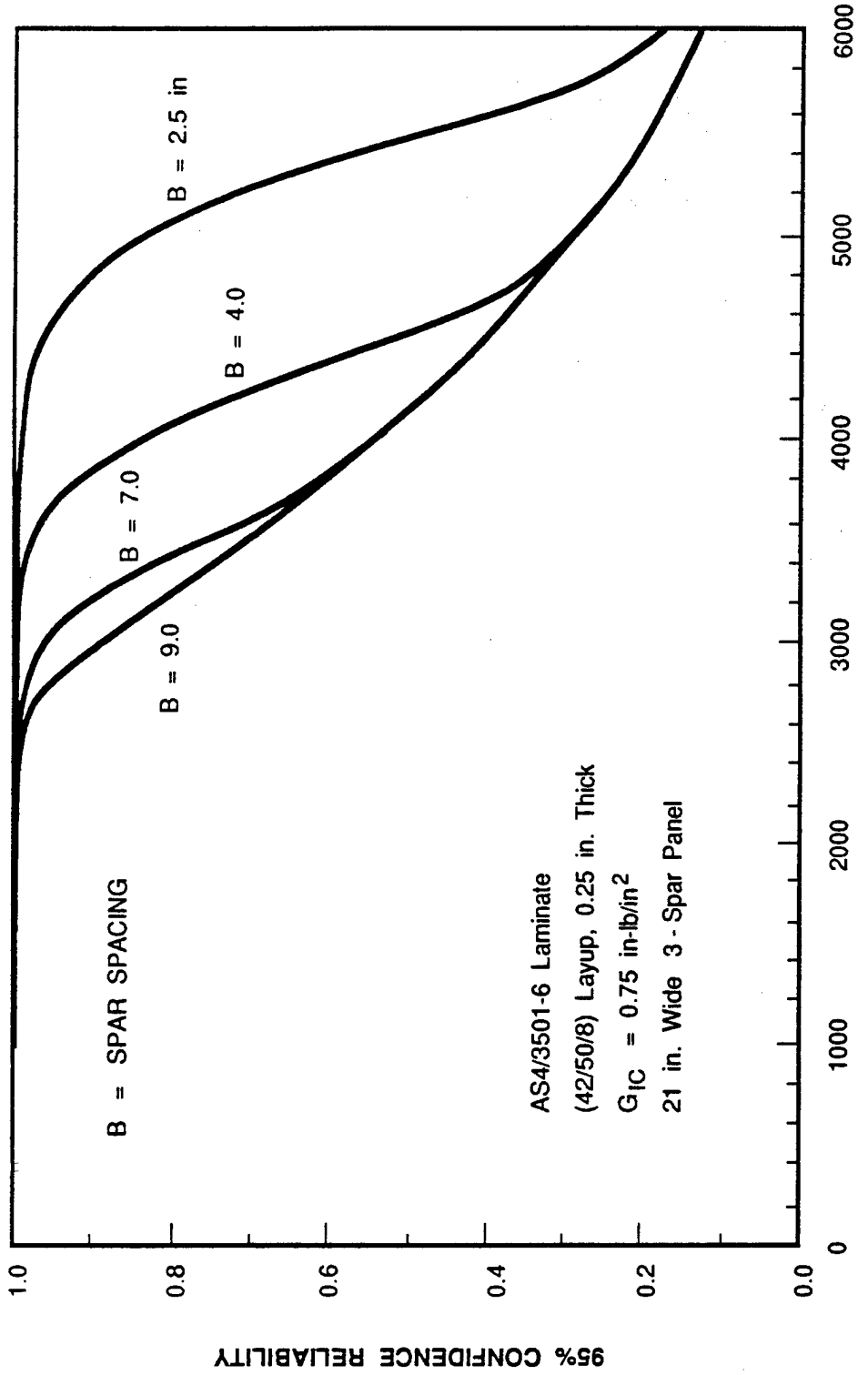

Figure 36. Influence of Spar Spacing on Post-Impact Structural Reliability.

conducted on the overall normalized strength. The Weibull shape parameter determined from the normalized strength data is 8.5. This scatter parameter was used in the reliability analysis discussed below.

The post-impact reliability of a composite laminate under a given applied compression strain is determined based on a Weibull distribution. The 95% confidence reliability is given by

$$R = \text{Exp}\ [\ -\ (\epsilon_{app}/\ \overset{\vee}{\beta})^{\alpha}] \tag{20}$$

Where ϵ_{app} is the applied strain

$\overset{\vee}{\beta}$ is the 95% confidence Weibull scale parameter

$\alpha = 8.5$ is the Weibull shape parameter.

The relationship between the mean post-impact strength

ϵ_f and $\overset{\vee}{\beta}$ can be written as (Reference 1)

$$\overset{\vee}{\beta} = \epsilon_f/\ \{\ \Gamma\ (1 + 1/\alpha)\ [\chi^2\ (2n)/2n]^{1/\alpha}\} \tag{21}$$

where n is the number of specimens

$\Gamma\ (x)$ is the Gamma function

$\chi^2(x)$ is the chi-square distribution

ϵ_f is the mean failure strain given by Equation (15)

The post-impact reliability for a damaged laminate can now be determined from Equations (15), (20), and (21).

Structural configuration effects were incorporated into the damage area based structural reliability analysis. This was done based on the assumption that after the initial failure was arrested by the substructure, further increase of the applied load will cause load redistribution within the structure. With the damage zone acting as a stress concentrator, severe stress concentration builds up near the spars, and the final failure mode is compression failure outside the damaged bay. The failure load is controlled by the severity of the stress concentration. Therefore, the analysis of

structural effects after the initial failure is identical for both the energy based and the damage area based models.

Structural reliability was computed using the method discussed in Subsection 4.2. Figure 37 shows the effects of structural configuration on the damaged structural reliability. The structure considered is a 21 in. wide, 3-spar panel. The spar spacing is 7 in. and the spar stiffness (AE) is 5.696×10^6 lb. The skin material is AS4/3501-6 with a fracture toughness of 0.75 in-lb/in^2. The laminate layup is (42/50/8) with a thickness of 0.25in. As shown in the figure, the structural reliability is not influenced by the substructure when the damage area is small. This is because the initial failure strain is large for small damage area. Under such a large initial failure strain, the damage propagation will not be arrested by the substructure and the final (structural) failure takes place at the same strain level as the initial failure. For large damage area between two spars, the structural reliability is controlled by the substructural arrangement and independent of the damage size. Therefore, the reliability is a constant. The results shown in Figure 37 indicate that under an applied compression strain of 2500 micro-in/in, the structural reliability remains at 0.94 for damage area larger than 5.5 in^2. Under a compression strain of 3000 micro-in/in the structural reliability remains at 0.76 for damage area larger than 5.5 in^2.

Figure 38 shows the influence of C-Scan damage area on the structural reliability. The structural reliability is plotted as a function of the applied compression strain in the figure. The figure shows that the structural reliability is influenced by the impact damage area (A) only when A is smaller than 5.5 in^2, for the configuration and material considered. For a single bay damage with damage area greater than 5.5 in^2, the structural reliability is not affected by size of the damage area. As can be seen in the figure, the applied compression strain for a 90% reliability (R=0.9) for damage area larger than 5.5 in^2 is 2650 micro-in/in. That is, for the particular structural configuration considered, the minimum applied compression strain with 90% reliability is 2650 micro-in/in for any damage area that is contained between two spars.

The influence of fracture toughness (G_{IC}) on the structural reliability is shown in Figure 39. The figure shows the results for G_{IC}

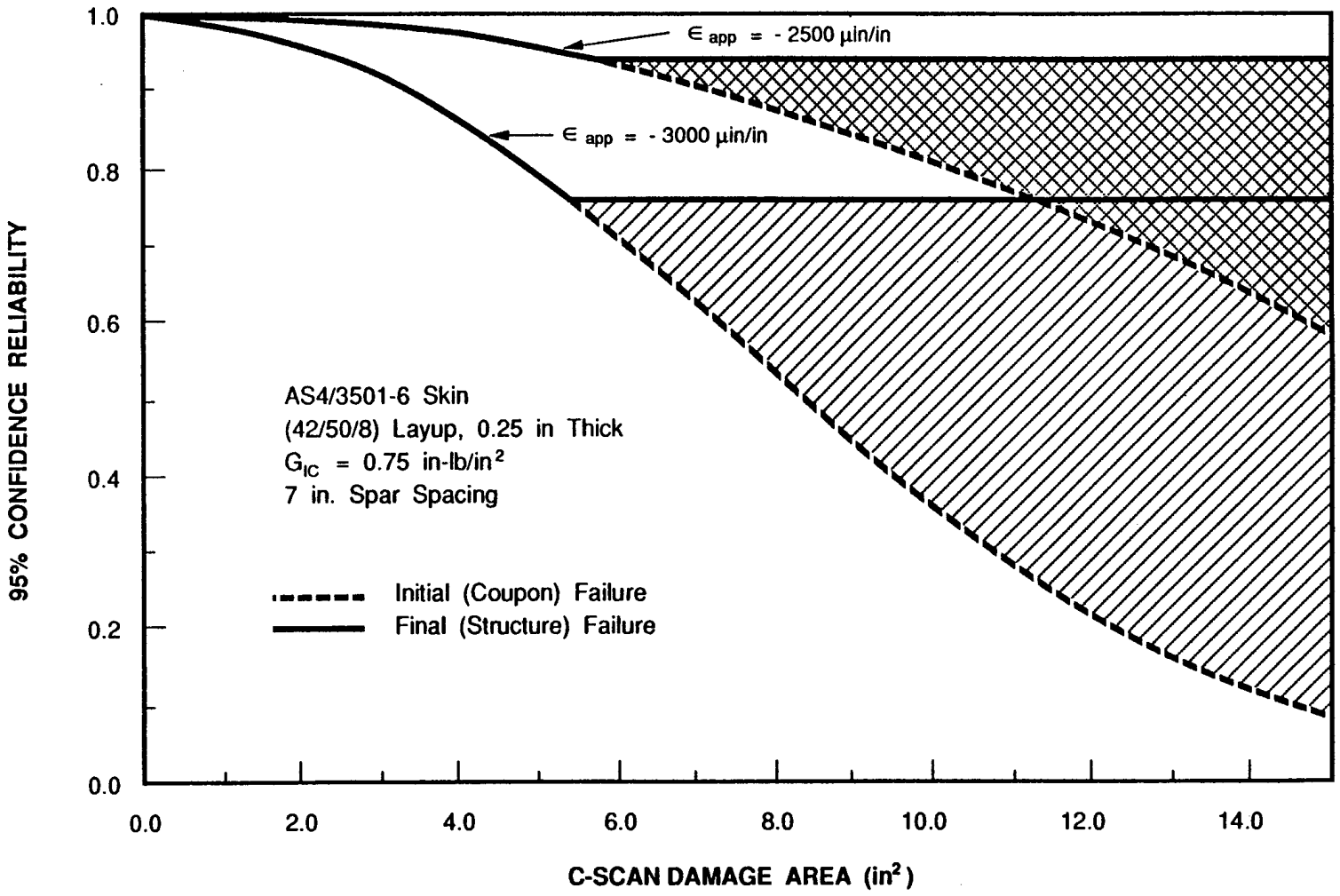

Figure 37. Effects of Structural Configuration on Damaged Structural Reliability.

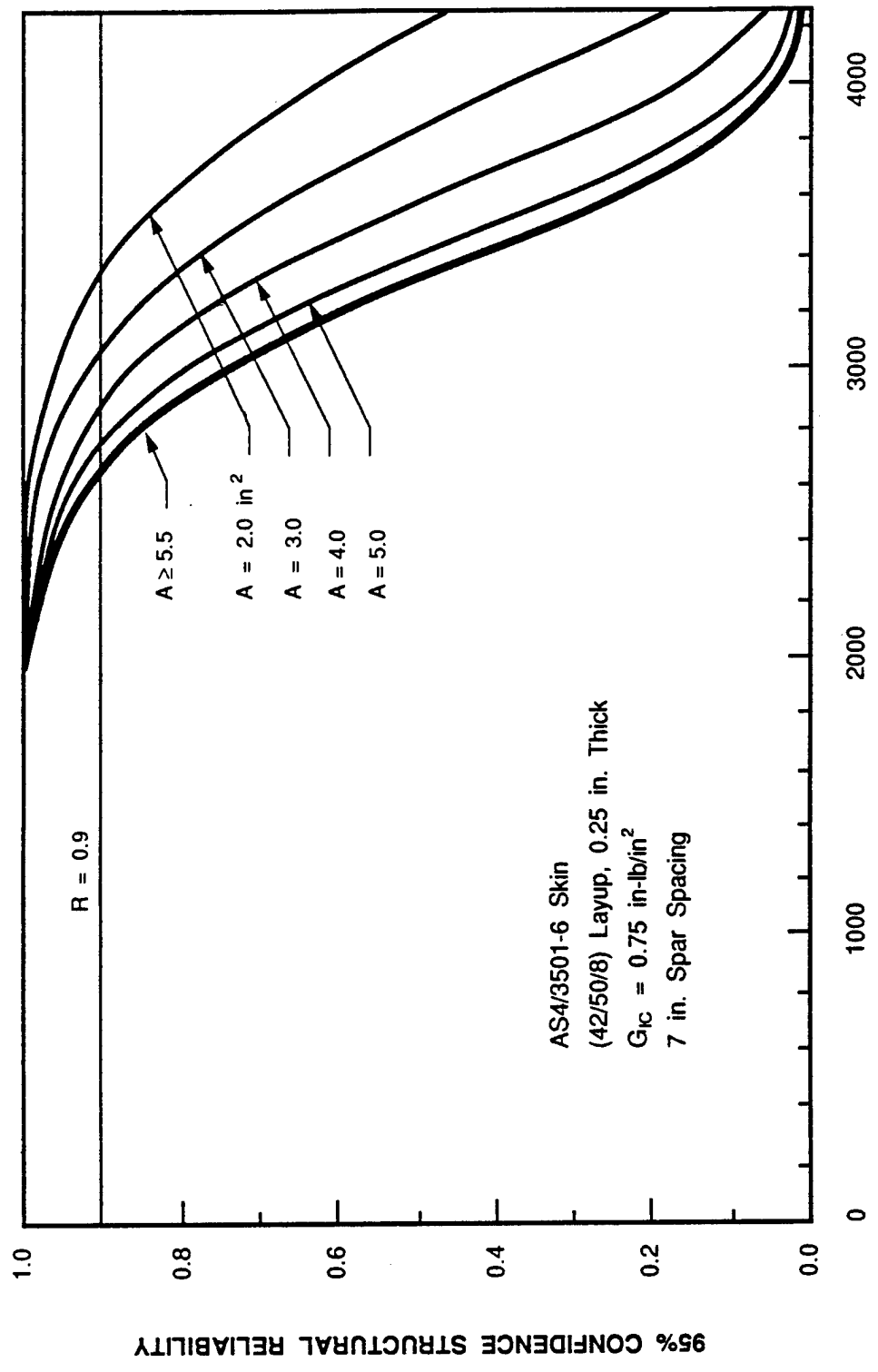

Figure 38. Influence of C-Scan Damage Area on Structural Reliability.

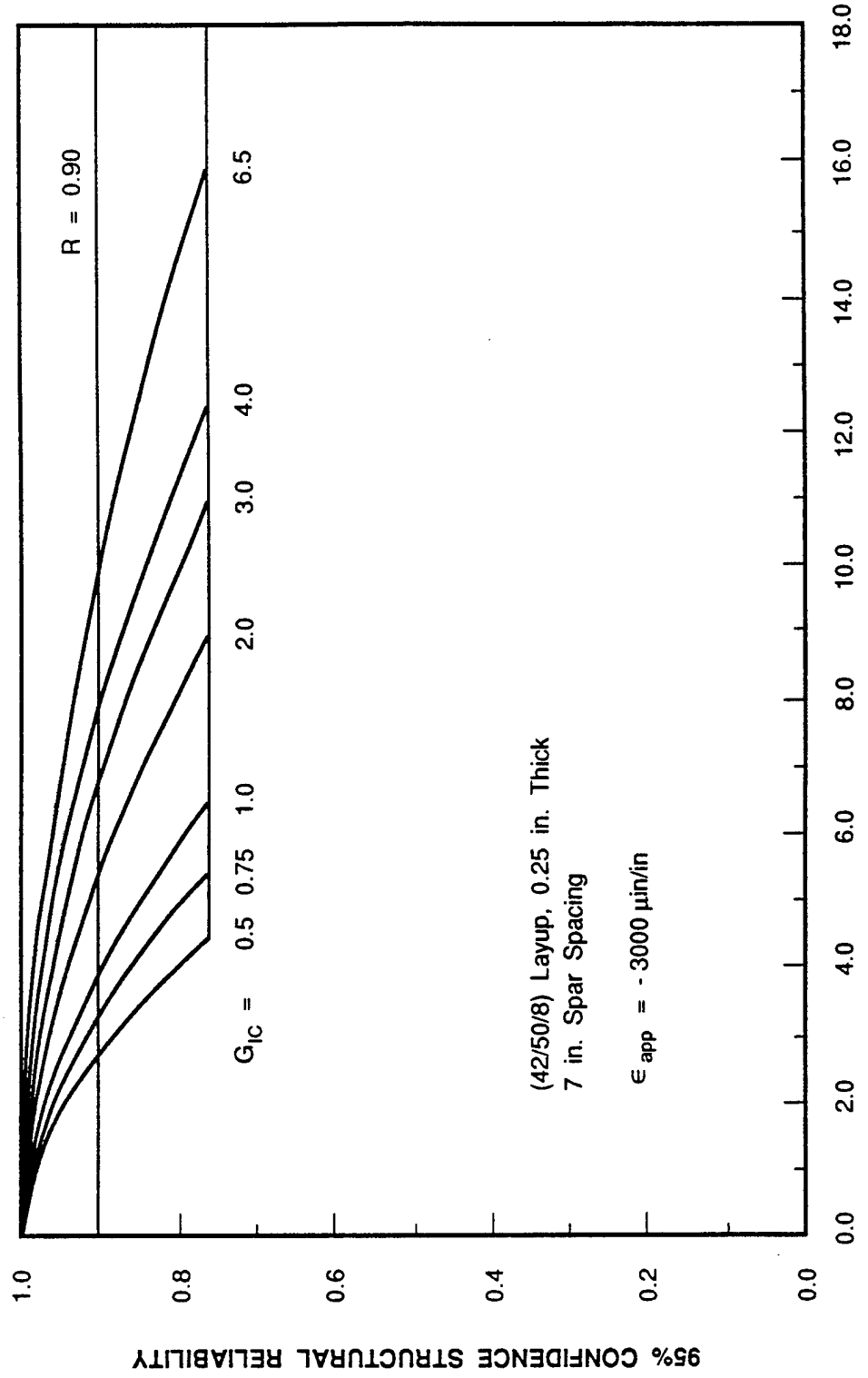

Figure 39. Influence of Fracture Toughness (G_{IC}) on Structural Reliability.

ranges from 0.5 to 6.5in-lb/in^2. The applied compression strain is 3000 micro-in/in. As shown in the figure, the minimum reliability is independent of the fracture toughness. The reliability for a large damage area for all values of G_{IC} is a constant at 0.76. This is because the final failure is controlled by the structural configuration and independent of G_{IC}. The figure also indicates that the under applied compression strain of 3000 micro-in/in the damage area with 90% reliability is controlled by initial failure and therefore depends upon the fracture toughness. The 90% reliability damage area increases with G_{IC}. For G_{IC} = 0.5 in-lb/in^2 it is 2.75 in^2 and increases to 10.0 in^2 for G_{IC} = 6.5 in-lb/in^2.

Figure 40 shows the influence of spar spacing (B) on the structural reliability. The figure shows the results for an applied compression strain of 3000 micro-in/in. These results indicate that the final failure is significantly influenced by the spar spacing. For large damage area the reliability, controlled by spar spacing, decreases as B increases. The critical damage area with 0.9 reliability is 3.3 in^2 for B > 6 in. With spar spacing of less than 5 in., the structural reliability remains above 0.9 as long as the damage area is contained in one bay.

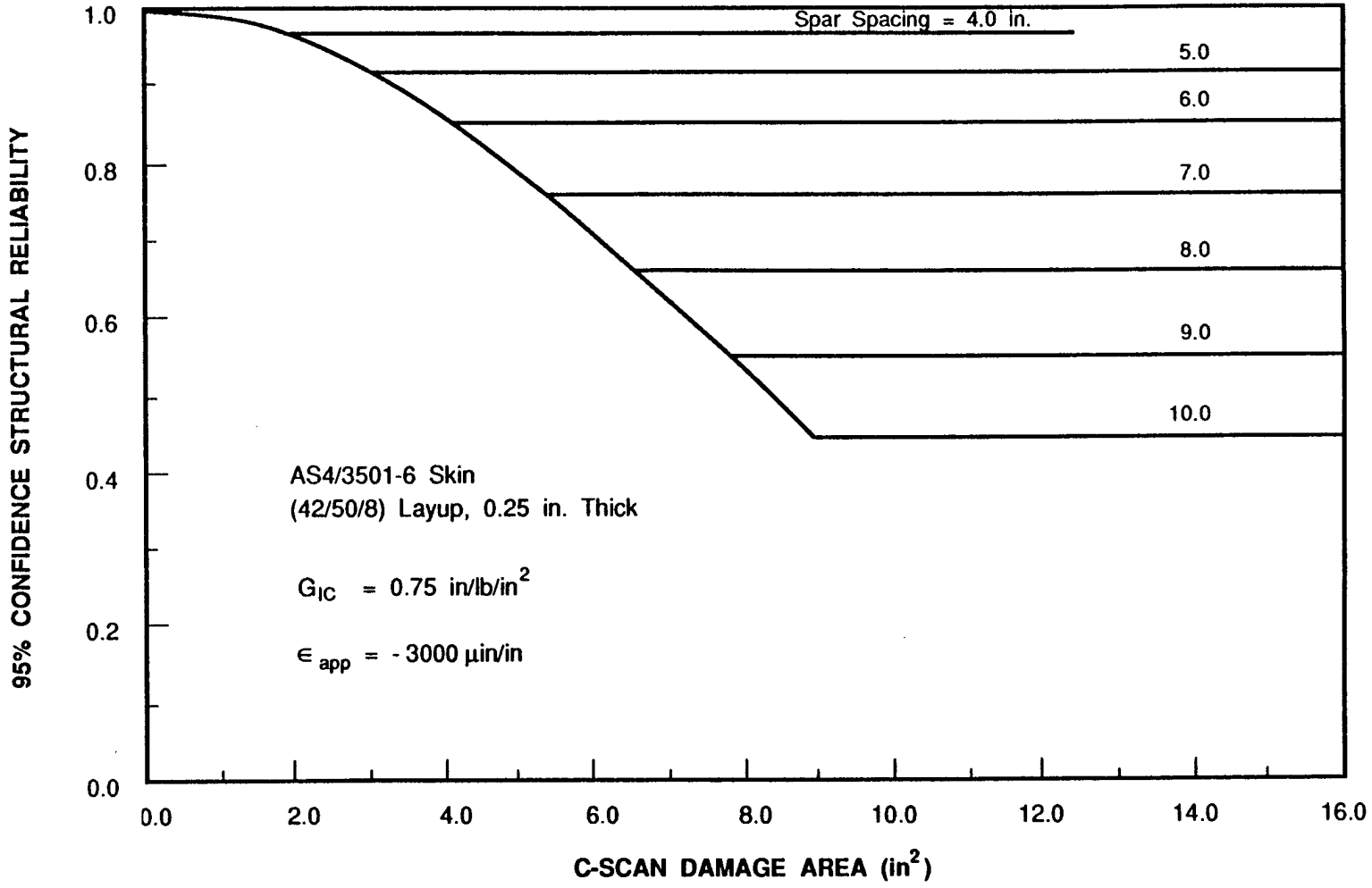

Figure 40. Influence of Spar Spacing on Structural Reliability.

SECTION 5

METHODOLOGY DEMONSTRATION

The F/A-18A upper wing skin was selected for damage tolerance evaluation. The methodology discussed in Section 4 was applied to evaluate the reliability of the structures exposed to impact threat. The baseline threat scenario used in the evaluation was the medium threat defined in Section 2. A sensitivity study was then conducted to examine the influence of various parameters on the damaged structural reliability. The results of these evaluations are discussed in the following paragraphs.

5.1 Baseline F/A-18A Inner Wing

The F/A-18A inner wing upper skin assembly drawing is shown in Figure 41. The wing span, from wing root to wing fold, is approximately 106 in. The skin width at wing root is approximately 45 in. and at wing fold is 31 in. The skin material is AS4/3501-6 with thickness ranging from 0.36 to 0.78 in. The skin layup is basically (48/48/4) and varies from (39/50/11) to (48/48/4). The substructure consists of the front, rear and four intermediate spars. The compression strain at maximum design ultimate load (DUL) of the skin ranges from below 2500 micro-in/in to above 3500 micro-in/in. The strain distribution is shown in Figure 42.

The inner wing skin was subdivided into forty-five regions for damage tolerance evaluation. The subdivision was based on the substructure arrangement and the thickness distribution of the skin. These subdivisions are shown in Figure 43. The skin layup, thickness and spar spacing for each subdivision are tabulated in Table 7.

Figure 44 shows the 95% confidence structural reliability of the upper wing skin subjected to DUL. As shown in the figure, the reliability at DUL is very high for the entire upper skin. The majority of the area has a reliability between 0.95 and 0.99, and the reliability of the entire skin exceeds 0.90. This indicates that the F/A-18A inner wing upper skin can reliably withstand the medium impact threat when subjected to design ultimate load.

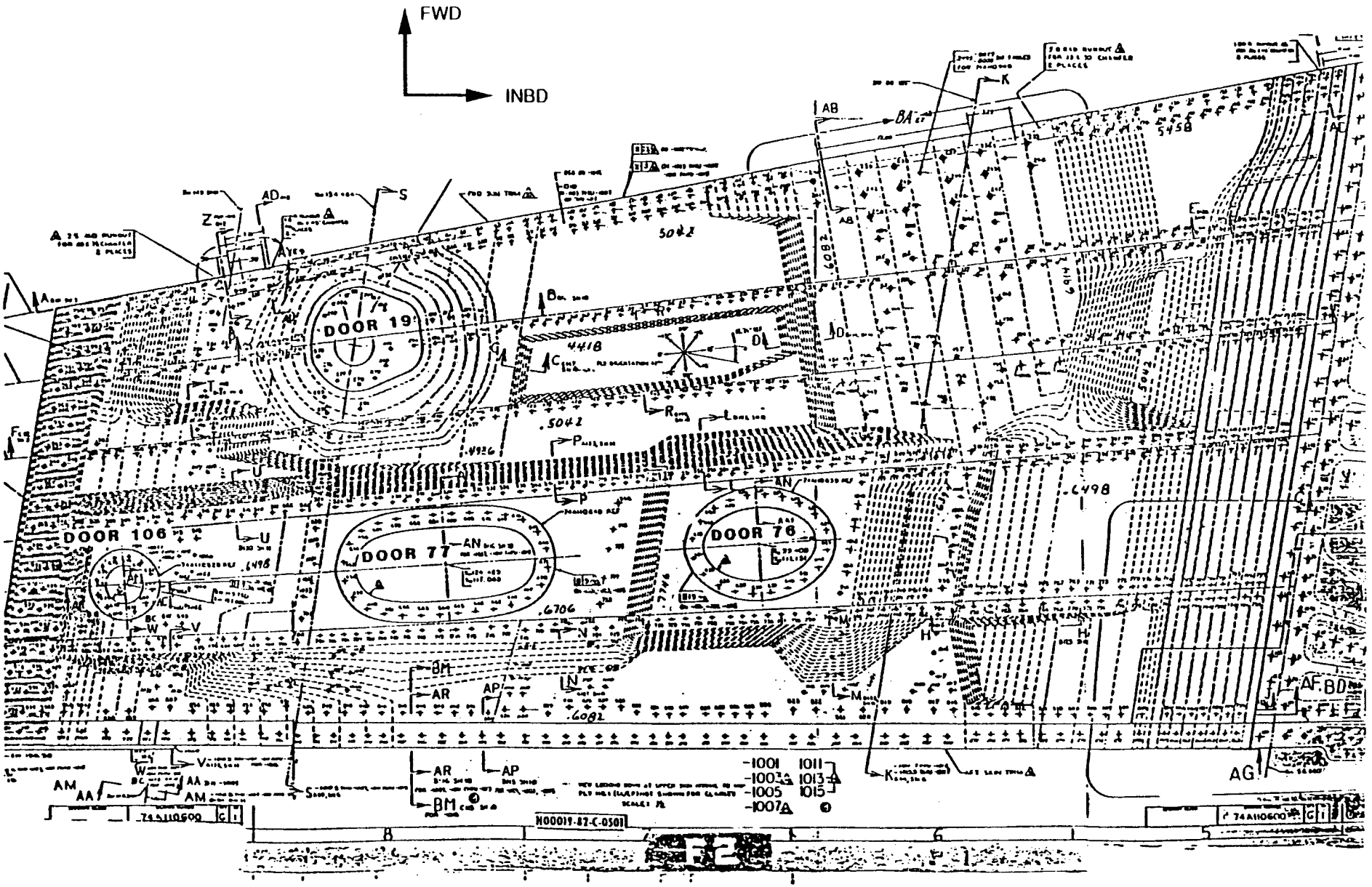

Figure 41. F/A-18A Inner Wing Upper Skin Assembly Drawing.

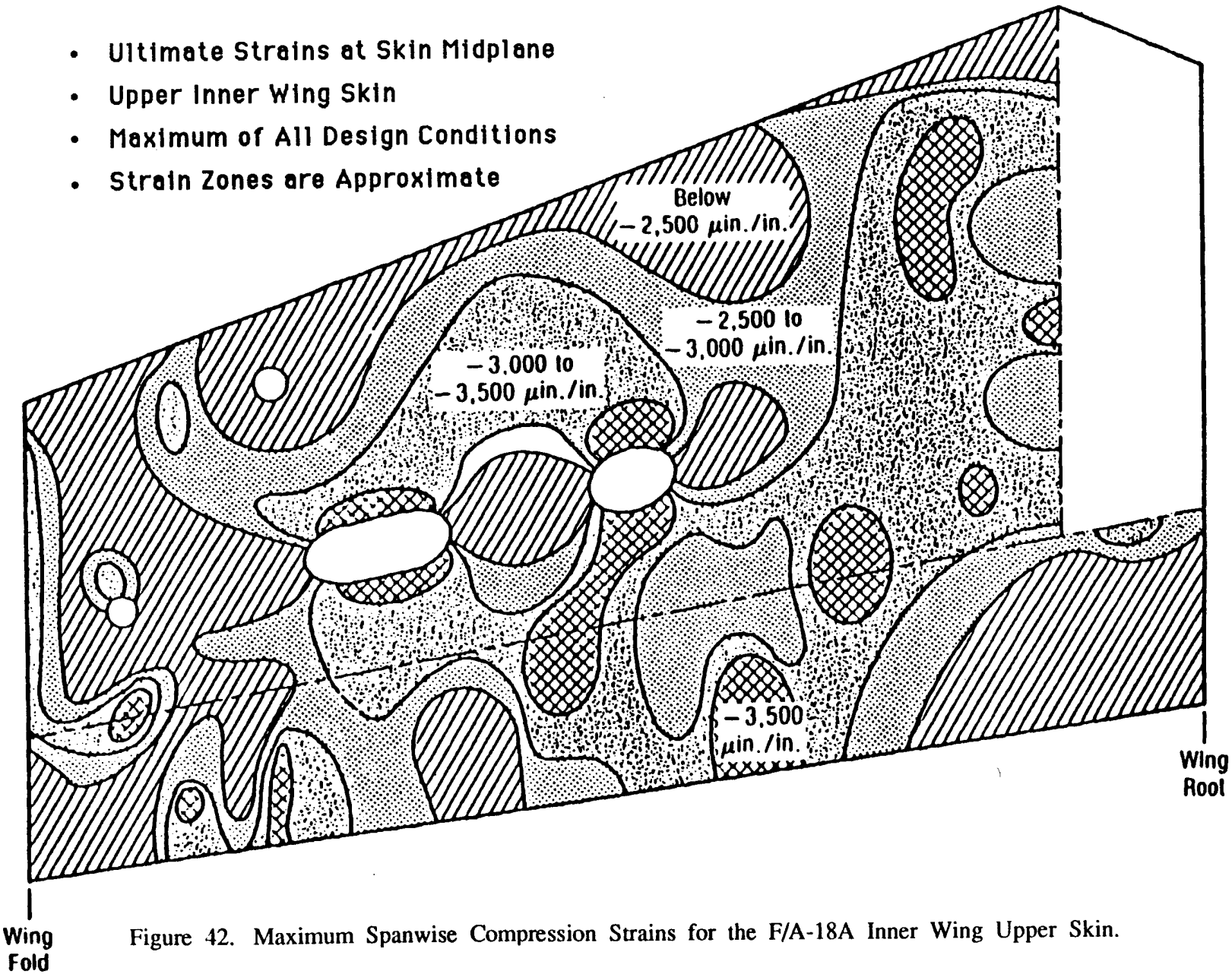

Figure 42. Maximum Spanwise Compression Strains for the F/A-18A Inner Wing Upper Skin.

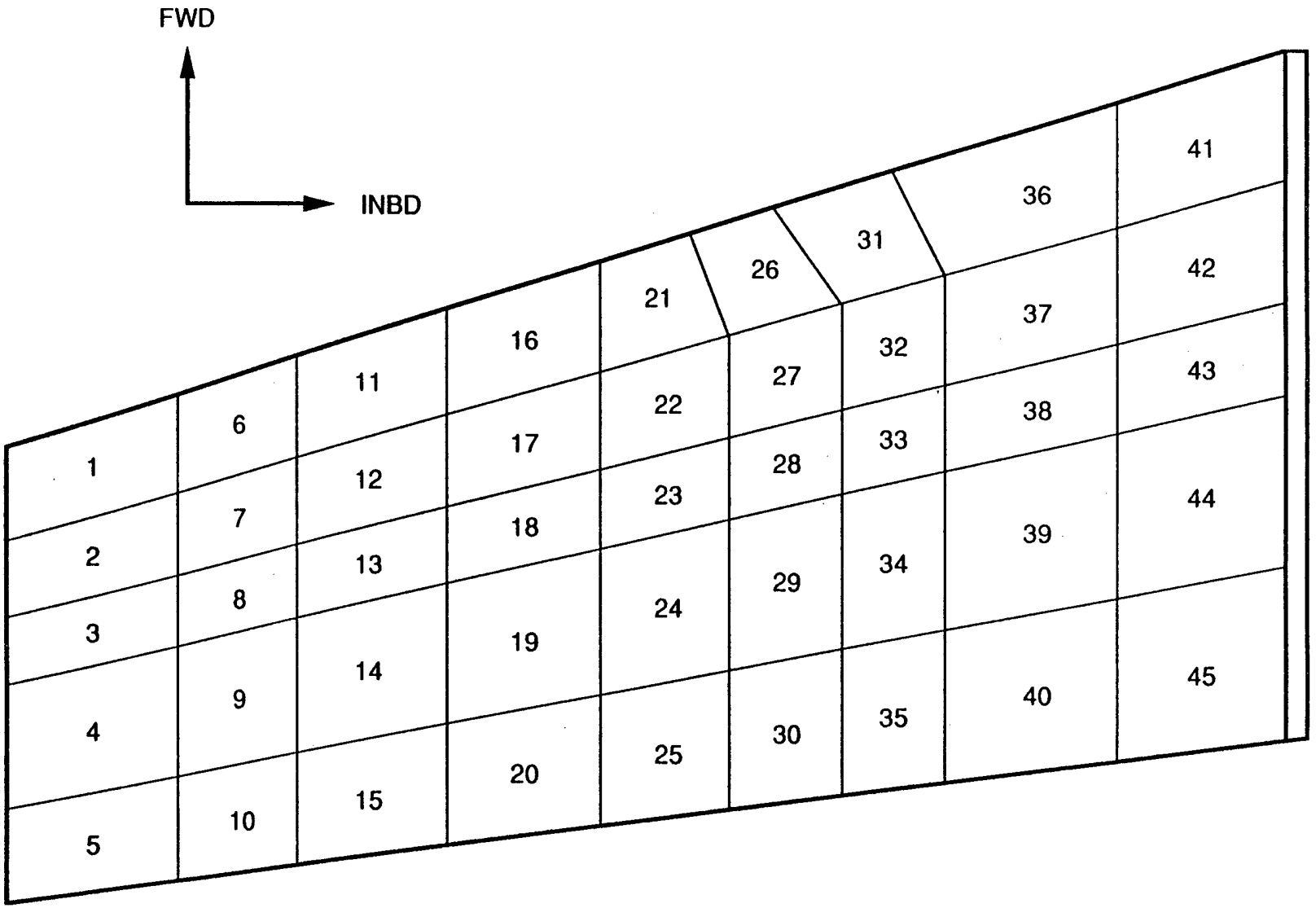

Figure 43. Subdivision of the F/A-18A Inner Wing Skin for Damage Tolerance Evaluation.

TABLE 7. F/A-18A INNER WING LAYUP, THICKNESS AND SPAR SPACING FOR DAMAGE TOLERANCE SUBDIVISIONS.

SUBDIVISION	LAYUP	THICKNESS	SPAR SPACING
1	(47/47/6)	0.3586	4.500
2	(47/47/6)	0.3586	6.500
3	(48/48/4)	0.5250	5.375
4	(45/52/3)	0.6498	9.000
5	(46/48/6)	0.5250	5.125
6	(47/47/6)	0.3586	5.375
7	(47/47/6)	0.3586	6.725
8	(48/48/4)	0.5250	5.650
9	(45/52/3)	0.6498	9.300
10	(44/48/8)	0.5250	5.575
11	(46/50/4)	0.5042	6.125
12	(45/50/5)	0.4210	7.000
13	(44/52/4)	0.4834	5.875
14	(44/50/6)	0.6706	9.750
15	(39/50/11)	0.5874	6.000
16	(46/50/4)	0.5042	6.250
17	(48/48/4)	0.4418	6.425
18	(46/50/4)	0.5042	6.075
19	(44/50/6)	0.6706	10.200
20	(42/48/10)	0.6082	6.550
21	(46/50/4)	0.5042	6.750
22	(48/48/4)	0.4418	6.675
23	(46/50/4)	0.5042	6.200
24	(44/50/6)	0.6706	10.500
25	(42/48/10)	0.6082	7.025
26	(45/48/7)	0.6082	7.500
27	(45/48/7)	0.6082	7.000
28	(45/48/7)	0.6082	6.200
29	(46/49/5)	0.7746	10.800
30	(42/48/10)	0.6082	7.375
31	(42/52/6)	0.6498	7.500
32	(42/52/6)	0.6498	6.500
33	(42/52/6)	0.6498	7.500
34	(41/50/9)	0.6706	10.250
35	(42/48/10)	0.6082	8.000
36	(42/52/6)	0.6498	8.500
37	(41/53/6)	0.6706	7.000
38	(41/53/6)	0.6706	7.625
39	(41/55/4)	0.6082	10.250
40	(40/56/4)	0.5250	7.875
41	(42/54/4)	0.5458	9.250
42	(46/50/4)	0.5042	7.250
43	(46/50/4)	0.5042	8.125
44	(39/58/3)	0.6498	10.875
45	(40/55/5)	0.6082	9.000

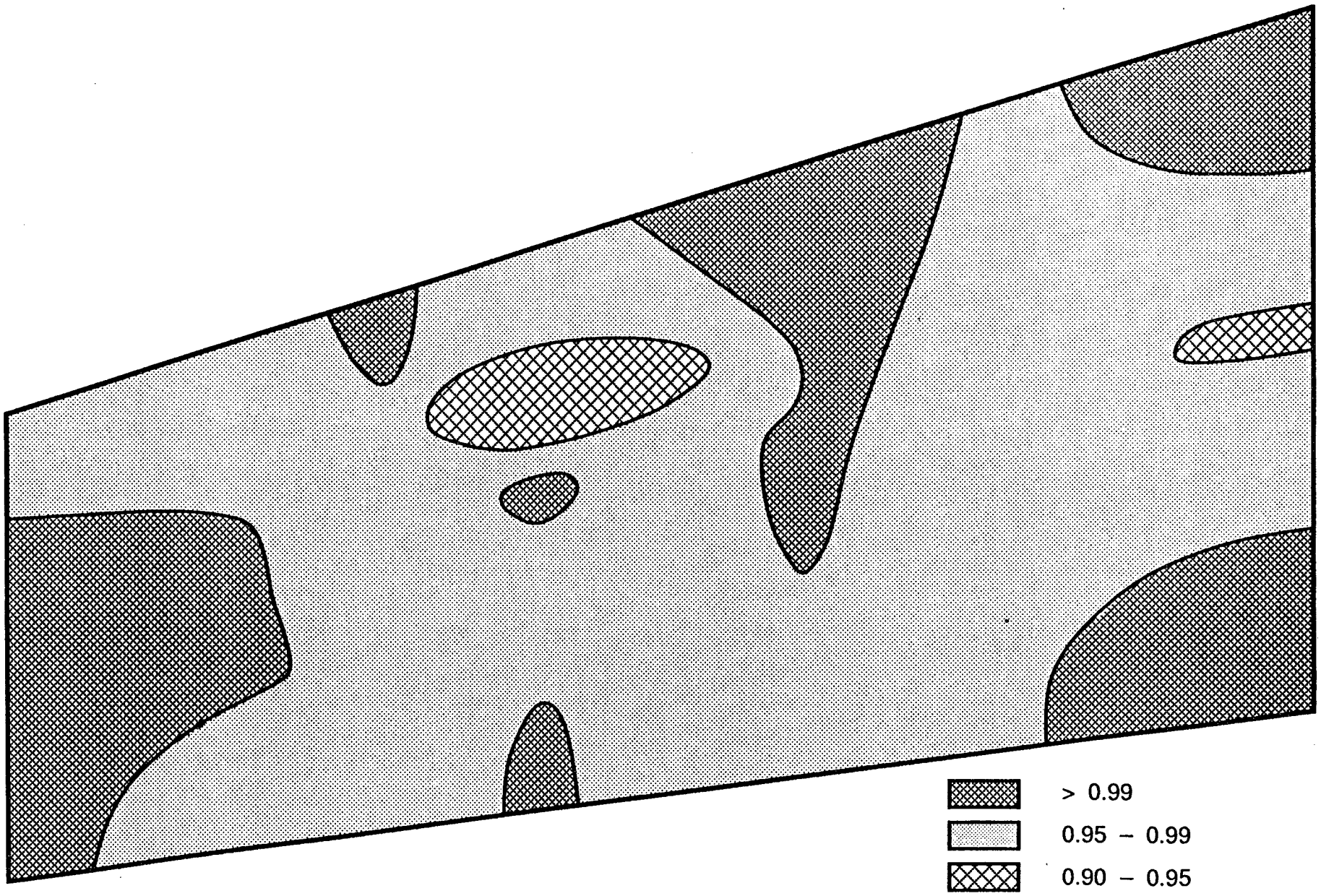

Figure 44. 95% Confidence Reliability of the F/A-18A Inner Wing Upper Skin at DUL Exposed to Medium Impact Threat.

Figure 45 shows the 95% confidence, 0.9 reliability strain contours for the upper wing skin against the medium impact threat. The compression strains shown in this figure range from 3100 to 4000 micro-in/in. Comparing the strains in Figure 42 and Figure 45, it can be seen that the strains in Figure 45 are significantly higher than that shown in Figure 42. This comparison is shown in Figure 46 in terms of margin of safety (M.S.) The M.S. was computed for each subdivision using the values shown in Figure 45 as B-basis allowables and the values shown in Figure 42 as ultimate strain. Figure 46 shows the margin of safety ranges from 0.02 to 0.52. This again indicates the high damage tolerance capability of the skin.

5.2 Sensitivity Study

Sensitivity studies were conducted to examine the influence of various parameters on the impact damage tolerance capability of composite structures. The influence of threat scenarios and the influence of damages tolerance requirements were examined separately. The B-basis (95% confidence and 0.9 reliability) strain based on different threat scenarios were computed and compared to determine the threat sensitivity. The design requirements sensitivity were determined by comparing the margin of safety using different design requirements.

The threat scenarios considered in the sensitivity study were:

1. 100 ft-lb mid-bay impact
2. Barely visible impact damage
3. High threat
4. Medium threat
5. Low threat
6. MCAir survey threat

Subdivisions 1, 2, and 3 from the F/A-18A inner wing were selected for this study. Analysis were conducted on these subdivisions for each of the impact threat scenario to compute the B-basis allowables. The results of this study are shown in Figure 47. This figure shows a general trend for the severity of the impact threat. As can be seen from this figure, the 100 ft-lb impact is the most severe threat and the MCAir survey threat is the least

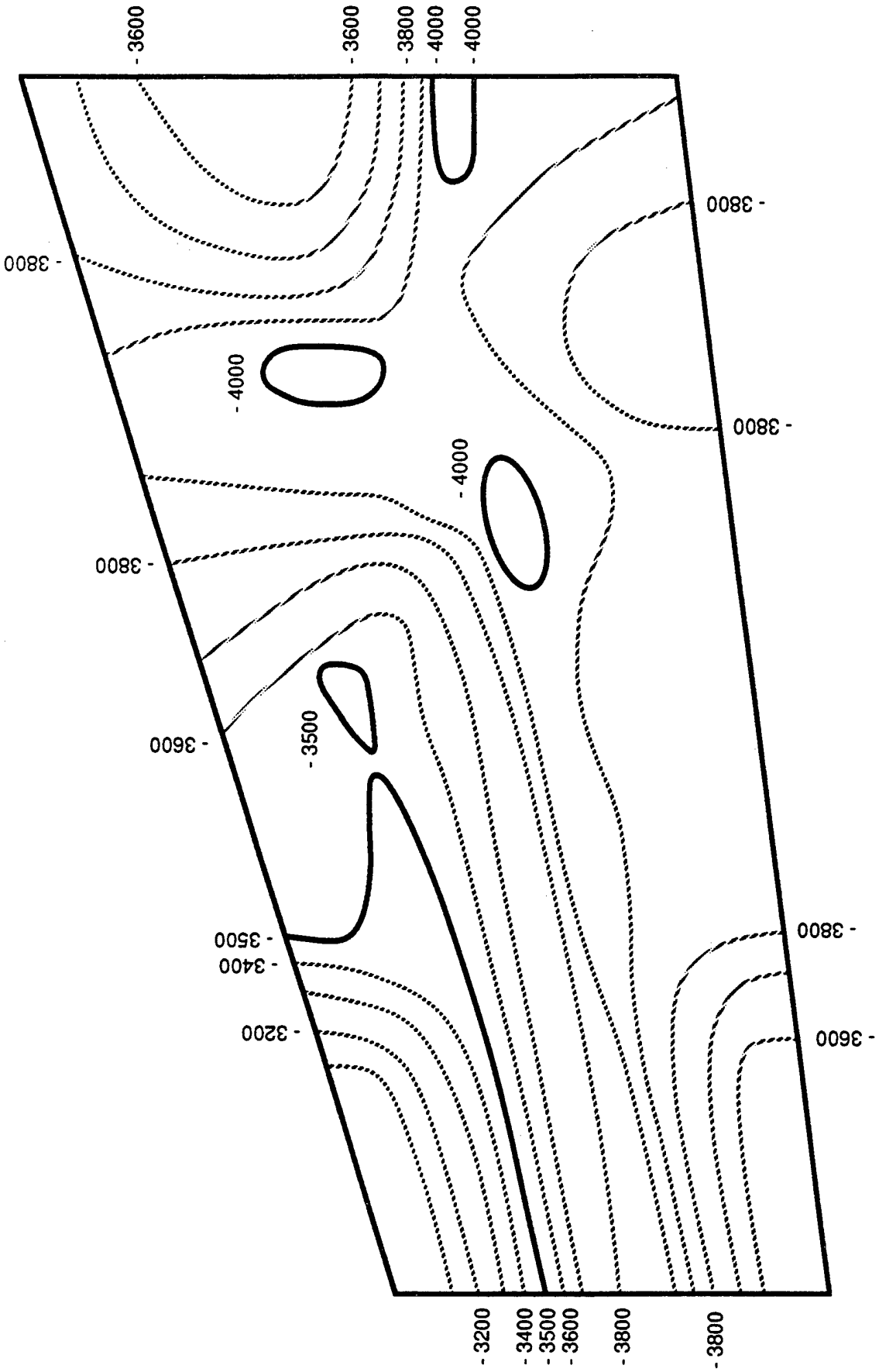

Figure 45. 95% Confidence, 0.9 Reliability Strain for the F/A-18A Inner Wing Upper Skin Exposed to Medium Impact Threat.

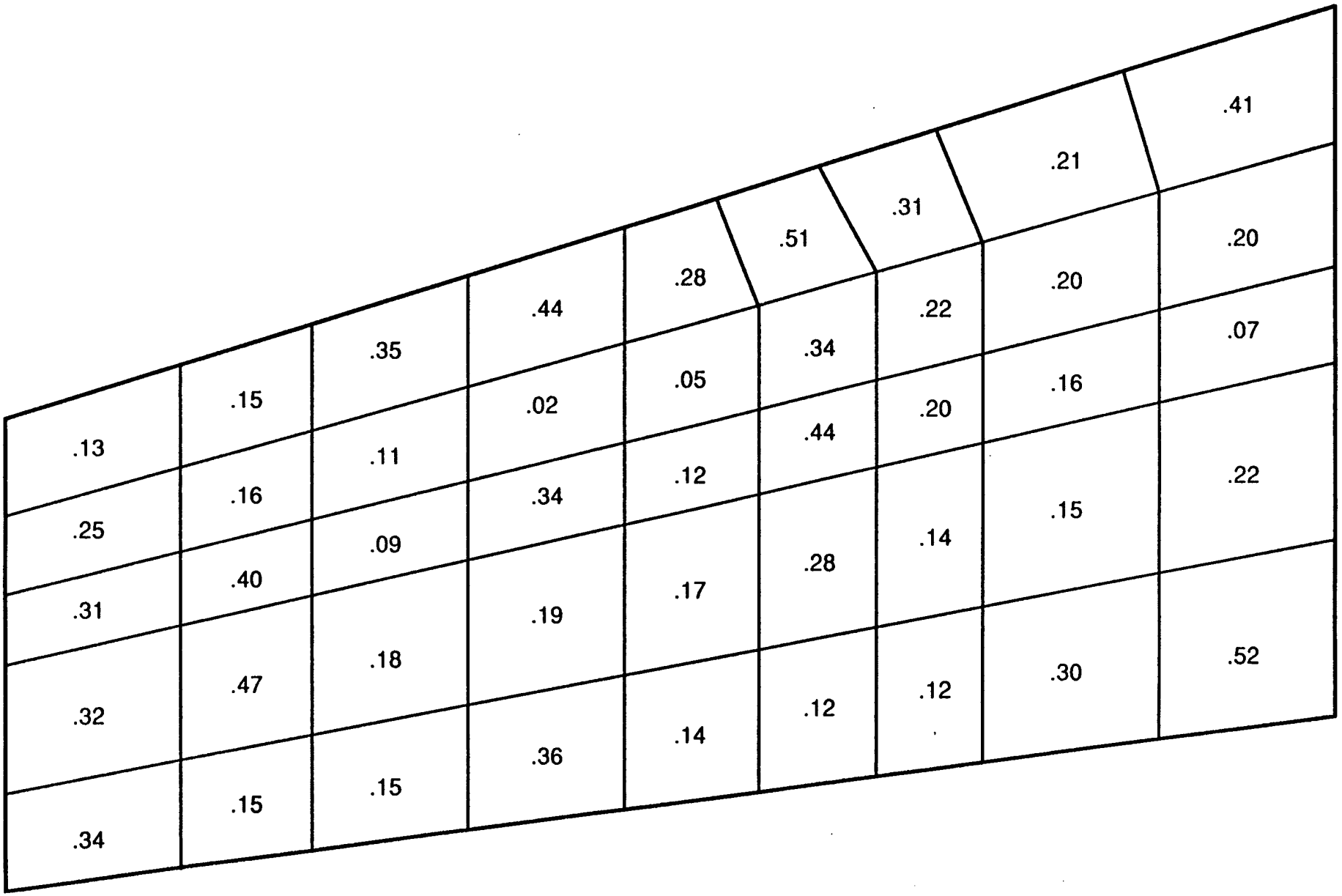

Figure 46. B-Basis Margin of Safety for the F/A-18A Inner Wing Upper Skin.

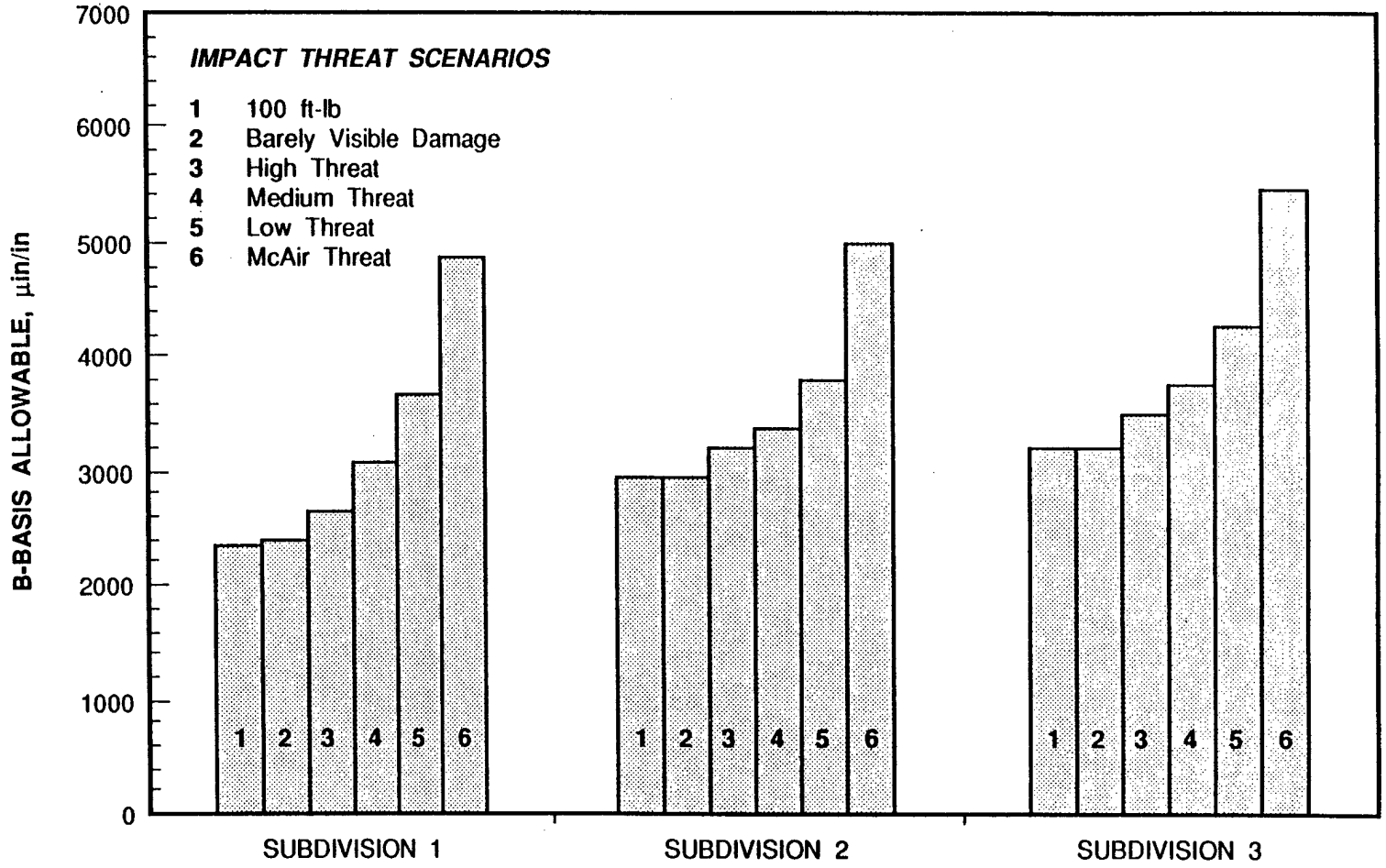

Figure 47. Sensitivity of Threat Scenarios on the B-Basis Allowable for the F/A-18A Inner Wing.

severe threat. The B-basis allowable for Subdivision 1 ranges from 2338 micro-in/in for the 100 ft-lb impact to 4870 micro-in/in for the MCAir survey threat. This shows that a factor of 2.08 in the allowable may result depending on the impact threat. This trend is similar for the other subdivisions. The barely visible impact damage threat is slightly less or equally severe as the 100 ft-lb impact for the thickness range of these subdivisions. The B-basis allowable based on high threat ranges from 1.08 to 1.14 times higher than that based on 100 ft-lb impact. The slight difference in this ratio is due to structural configuration effects. The structural configuration effects are less significant in Subdivision 1 and, therefore, the ratio is higher. The B-basis strain determined based on the medium threat ranges from 1.15 to 1.31 times higher than that based on 100 ft-lb impact. This ratio increases to 1.29 to 1.58 for low threat and further increases to 1.71 to 2.08 for the MCAir threat.

The damage tolerance design requirement sensitivity study was conducted by examining the influence of damage tolerance requirements on the margin of safety of the structure. This was done by analyzing the same three subdivisions on the F/A-18A inner wing using the seven requirements below.

1. No catastrophic structural failure below DUL

   or $P_F^S \geq DUL$ (22)

   where P_F^S is the structure failure load

2. No catastrophic structural failure below maximum service load (MSL) with maximum service load defined as 20% above design limit load (DLL)

   or $P_F^S \geq 1.2\ DLL$ (23)

3. No catastrophic structural failure below DUL for structure containing barely visible impact damage (BVD)

   or $P_{BVD} \geq DUL$ (24)

4. No catastrophic structural failure below MSL for structures containing BVD

or $P_{BVD} \geq 1.2$ DLL (25)

5. No local failure below DLL and no catastrophic structural failure below MSL

or $P_{IF} \geq$ DLL and $P_F^S \geq 1.2$ DLL (26)

where P_{IF} is the initial (or local) failure load.

6. No local failure at DUL

or $P_{IF} \geq$ DUL (27)

7. No catastrophic structural failure below DUL for structures containing a 2-inch diameter circular internal damage (C-scan damage area)

or P (2" DIA) $\geq$ DUL (28)

Requirements 1, 2, 5, and 6 depend on the impact threat assumed in the analysis. In this study, the baseline threat (medium threat) was used. The results of this study are shown in Figure 48. In this figure, both the margins of safety computed based on the B-basis allowable strain and based on the average value are shown. The results in Figure 48 show consistently that the margin of safety is lowest for the BVD requirement (Requirement 3). They also show that Requirements 2 and 5 result in the highest M.S. and they are in general equal.

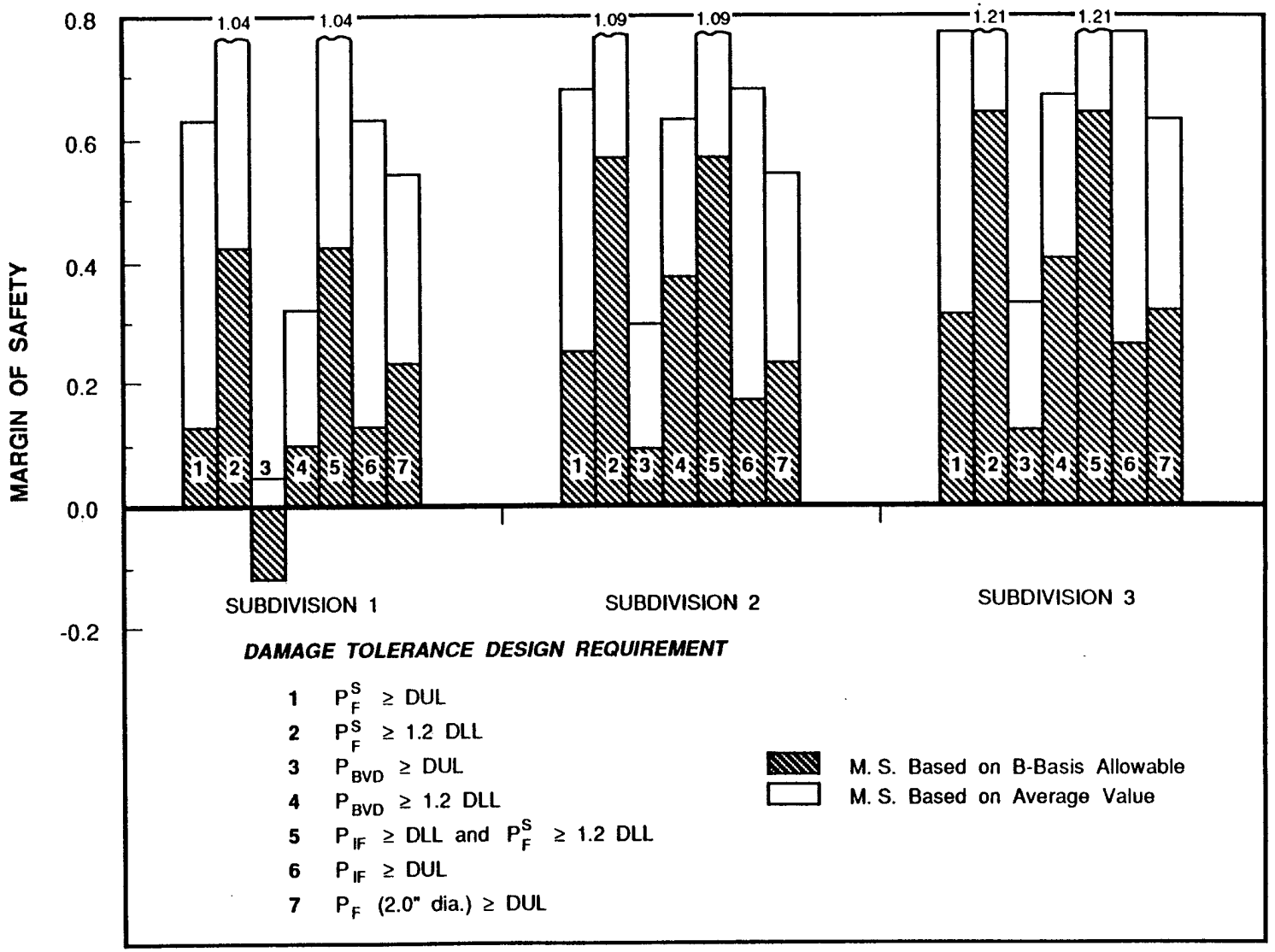

Figure 48. Influence of Damage Tolerance Design Requirement on the Margin of Safety – F/A-18A Inner Wing.

SECTION 6

CERTIFICATION METHODOLOGY

The methodology developed in this program can be easily integrated into the composite structures certification methodology developed in Reference 1. The methodology developed in Reference 1 has general applicability to all aircraft types and is very flexible. As such, it is ideally suited for efficient incorporation of the effects of impact damage and cocured/bonded structures.

The procedure to certify cocured/bonded structures is identical to that of bolted structures, except at higher data scatter (lower Weibull shape parameter, α) should be used. The static strength Weibull shape parameter for laminates and bolted structures of current composite systems was determined to be 20 in Reference 1. Using this value of α, the B-basis allowable to mean strength ratio is 0.9, based on a sample size of 15. From the scatter analysis of the bonded joint data (Appendix A), the modal value of α is 9. The B-basis to mean strength ratio is reduced to 0.79. Therefore, a larger knockdown should be applied for the bonded structures in determining the allowable static strength. However, this will not change the certification procedures. Similar analysis/testing requirements are applicable for cocured/bonded structures.

The overall certification procedure for composite aircraft structures include three steps. These are: (1) Static strength, (2) durability, and (3) damage tolerance. The static strength and durability certification procedures are discussed in details in Reference 1 and they are briefly summarized in Sections 6.1 and 6.2. The damage tolerance methodology developed in this program is given in Section 6.3.

6.1 Static Strength Certification

The building-block approach was adopted in Reference 1 for both static and durability certification. The testing requirements in this approach include testing for design allowables, design development testing and full-scale testing. This approach fully utilizes coupon, element, subcomponent, and component level test data so that a limited number of full-scale structural test data can be interpreted statistically. The number of

tests decreases from the coupon level to the component level. A relatively large number of tests is required at the coupon level to establish the data scatter and B-basis statistics for different loading mode, failure mode, and environments for both static and fatigue tests. A smaller number of tests is required at the element and subcomponent level to determine the failure mode interaction and a sufficient number of component tests to demonstrate the variability in structural response. This information is then used for interpretation of the full-scale structural test data.

The purpose of design allowable tests is to evaluate the material scatter and to establish strength parameters for structure design. Because composites are environmental sensitive, design allowables should be obtained for the entire range of the environmental service envelope of an aircraft. Statistical analysis methods must be used to compute the design allowables.

In planning a design allowable testing, it is important that a sufficient number of tests be conducted to generate meaningful statistical parameters. In general, the number of specimens required depends on the scatter of the data. The higher the data scatter, the larger number of specimens are required. Based on the scatter analysis performed in Reference 1, the number of specimens recommended for B-basis allowables is 15 and for A-basis is 30. This is because within the range of α for typical composites (α=20 - 30) the B-basis knockdown factor remains approximately constant for sample size greater than 15. The A-basis knockdown factor stabilizes for sample sizes larger than 30.

The design allowable tests should be planned to develop the strength to temperature envelope relationship for the full range of the service temperature of aircraft. The moisture level for the test specimens should be either end-of-lifetime level or the maximum level in the design lifetime, whichever is higher. The tests should also provide data for each failure mode. Tension, compression and shear strengths test should be conducted at each environment. The design allowable tests should be conducted at both lamina and laminate levels. The purpose of the lamina test is to establish the mechanical properties such as Young's moduli, shear modulus and Poisson ratio. These tests should include longitudinal and transverse tension and compression and shear tests. At the laminate level, two laminates representing the practical fiber dominated and matrix dominated lay-ups should

be selected. The test specimens should include unnotched specimens to determine the laminate design strain. Other tests such as open and filled holes, bearing and bolt bearing by-pass should also be included.

The philosophy for design development testing should be that the test environment used is the one that produces the failure mode which gives the lowest static strength. That is the worst case environment, or the temperature associated with the most critical load should be used.

The extent of the static test effort will be different from aircraft to aircraft and also from component to component. The number of replicates for each test should be sufficient to identify the critical failure mode and provide a reasonable estimate of the mean strength of the element. The test effort should be concentrated on the most critical design feature of the structure. The number of replicates should be increased for the critical design features. A cost trade-off is usually involved in deciding the levels of complexity and the number of replicates.

If mixed failure modes are observed in a certain specimen type, more tests are required to establish the worst failure mode and the associated mean strength. The following recommendations are made for specimen complexity simulation in design development testing:

1. Use the design/analysis of the aircraft structure to select critical areas for test verification.
2. Specimen complexity should be controlled by the requirement to simulate the correct (full-scale structure) failure mode(s) in the specimen.
3. Special attention should be given to matrix sensitive failure modes, such as compression, bondline and hole wear.
4. Potential "hot spots" caused by out-of-plane loads should be carefully evaluated.

The full-scale static test is the most crucial qualification test for composite structures for the following reasons. Secondary loads are virtually impossible to eliminate from complex built-up structure. Such loads can be produced by eccentricities, stiffness changes, discontinuities, fuel pressure loading and loading in the post-buckled range. Some of these sources of

secondary loads are represented for the first time in the full-scale structural test article. These loads are not a significant design driver in metallic structures. However, the poor interlaminar strength of composites makes them extremely susceptible to out-of-plane secondary loads. It is very important, therefore, to carefully account for these loads in the design of composite structures.

In addition, a detailed correlation in terms of measured load and strain distributions, structural analysis data and environmental effects between the design development and full scale test data will be necessary to provide assurance of composite static strength. Static test environmental degradation must be accounted for separately either by adverse condition testing, by additional test design factors or by correlation with environmental design development test data.

6.2 Durability Certification

The fatigue design allowables may be determined by the load factor approach, life factor approach or the ultimate strength approach. The individual or joint Weibull analyses are recommended for computation of design allowables. These approaches for fatigue allowable determination are detailed in Reference 1.

In planning the fatigue allowable tests, the main consideration is the test environment. The test environment depends on the relationship between the load/temperature spectrum and the material operation limit. The recommended approach is to use simple conservative constant temperature tests with a constant moisture level. The stress levels used in the fatigue tests should be selected so that the fatigue threshold can be established. For typical graphite/epoxy composites under typical fighter aircraft spectra, the threshold stress level would be approximately 60% of the mean static strength. This would require a minimum of four stress levels for each test condition. From these considerations, using the same number of specimens required for the static allowable tests (15 for B-basis and 30 for A-basis) a large test matrix would result. However, as discussed in Volume 1 of Reference 1, the fatigue life scatter does not depend on the stress level for a given test condition. Therefore, the pooling techniques for statistical data condition can therefore be reduced. The recommended number of tests for each test condition is 6 for B-basis and 10 for A-basis.

The environmental complexity necessary for fatigue design development testing will depend on the aircraft hygrothermal history. Three factors must be considered. These are: Structural temperature for each mission profile, the load/temperature relationships for the aircraft, and the moisture content as a function of the aircraft usage and structure thickness. In order to obtain these data, it is necessary to derive the real time load-temperature profiles for each mission in the aircraft's history. These relationships will have a significant influence on the environmental fatigue test requirements.

As discussed in Reference 1, the use of fatigue test data to verify fatigue life on subcomponents require long test duration because of the high fatigue life scatter observed in composite structures. The load enhancement factor approach or the ultimate strength approach is recommended in planning the fatigue design development testing.

The number of replicates to be used in the fatigue design development testing should be determined using the same philosophy as in the static tests. A sufficient number must be used to verify the critical failure modes and to reasonably estimate the required fatigue reliability.

The work in Reference 26 and other USAF sponsored programs have shown that composites possess excellent durability. In particular, the extensive data base developed in Reference 26 showed that composite structures, which demonstrated adequate static strength, were fatigue insensitive.

Therefore, it is recommended in Reference 1 that no durability full-scale test is required for all composite structures or mixed composite/metal structures with non-fatigue critical metal parts, provided the design development testing and full-scale static tests are successful. For mixed structure, with fatigue critical metal parts, a two-lifetime ambient test will be required to demonstrate durability validation of the metal parts.

6.3 Damage Tolerance Certification

The building-block approach is equally applicable for impact-damaged structures. This was verified by the test results of Reference 12. In the reference, residual strength tests were conducted on impact-damaged 5 by 10 inch coupons and 3-spar panels. Based on the results of these tests, the residual strength of the impact-damaged full-scale wingbox was analytically predicted. The predicted initial failure strain was 2,750 micro-in/in. This

was verified during the wingbox fatigue test, where the initial failure and arrestment occurred, as predicted, at a gross strain of 2,730 micro-in/in. The results of Reference 12 indicate that the building-block approach can be used to adequately address the threat of in-service impact during the structural certification process. The key elements of damage tolerance certification of composite structures are discussed in the following paragraphs.

6.3.1 Testing Requirements

The purpose of damage tolerance tests is to establish residual strength capability and strength scatter for damage tolerance analysis. Two levels of tests should be conducted on representative laminates and structural elements.

The coupon tests should be conducted on the 5 by 10 inch coupons of representative laminate. In planning these tests, a range of impact energy should be first identified. The range of impact energy depends on the laminate thickness and material system. For composite materials commonly used in primary aircraft structures, a 20 to 100 ft-lb range is recommended. These specimens should be impacted according to the NASA procedure (Reference 13). The impact damaged specimens are then tested for post-impact strength in compression.

The number of specimens required for the coupon tests should be sufficiently large so that the trend of strength degradation and the scatter in strength can be confidently established. The results shown in figure 26 is a typical example. A minimum of five impact energy levels and ten specimens at each level should be used in the impact test. The joint Weibull analysis method discussed in Reference 1 should be used to determine the scatter parameters.

Representative structural elements should be impacted and tested for residual strength in compression. A typical example for structural elements is the 3-spar panels tested in Reference 12. The purpose of these tests is to determine the structural configuration effects on the strength of the impact damaged structure. The results in Reference 12 indicated that the spar

spacing has a significant effect on the damage arrestment capability of the structure. The stiffness of the spars strongly influenced the first failure load but does not significantly affect the final failure strain.

The results of element tests should provide data to determine the damage containment capability of the structure. A typical example is shown in Figure 17. The number of impact energy levels used in the tests should be planned in a way so that the critical energy for a two-stage failure can be established. The critical impact energy depends on the skin thickness and stiffener spacing. A preliminary analysis, using the method discussed in Section 3 should be used in planning these tests.

6.3.2 Impact Threat Definition

A Weibull representation of the impact threat distribution was illustrated in Section 2.3. In this representation, a modal impact energy and an energy level associated with a rare impact event are required. These impact energy levels and the probability of occurrence of the rare impact event are used to determine the Weibull parameters of the impact threat, given by Equations (1) and (2).

Three impact threat distributions were defined in Section 2.3. As discussed in Section 2.3, the medium threat is a conservative estimate of impacts received by structural areas exposed to both operational and maintenance induced impact damage. The conservatism of this threat scenario was demonstrated by comparing the MCAir results of impact survey of in-service aircraft. This impact threat distribution is recommended for damage tolerance design.

6.3.3 Damage Tolerance Design Requirements

The influence of damage tolerance requirements on the structural margin of safety was examined by the sensitivity study discussed in Section 5. the seven damage tolerance design requirements used in the sensitivity are:

1. No catastrophic structural failure below DUL.
2. No catastrophic structural failure below MSL.
3. No catastrophic structural failure below DUL for structure with BVD.

4. No catastrophic structural failure below MSL for structure with BVD.

5. No local (initial) failure below DLL and no catastrophic structural failure below MSL.

6. No local (initial) failure below DUL.

7. No catastrophic structural failure below DUL for structure containing 2.0 inch diameter circular internal damage (detectable by nondestructive inspection method).

Requirements 1, 2, 5, and 6 should be evaluated based on specific impact threat. The medium threat is recommended for evaluation because of its conservatism in representing the in-service and maintenance impact threats.

Requirements 1, 3 and 6 use design ultimate load as design criterion and, therefore, are very conservative requirements. If a B-basis reliability is also required for the impact damaged structure, these design requirements may result in additional weight to the structure. This is because B-basis reliability at DUL is usually required for the undamaged structure. If the margin of safety at DUL was 0.0 for the undamaged structure, a negative margin for damage tolerance would generally result.

In order to assure the high degree of confidence in structural reliability for impact damaged composite structures without significant weight penalty, requirements such as 2, 4, and 5 are recommended. These requirements assures high structural reliability at DLL and MSL for impact damaged structures.

Requirement 7 should be used as maintenance and part acceptance criterion. Structures containing 2-inch diameter circular internal damage (or damage with equal damage area) should be treated as undamaged structure. therefore, the reliability should be equivalent to that of undamaged structure. For this reason, the high reliability at DUL should be retained.

6.3.4 Impact Damage Analysis

The analysis methodology developed in Section 4 is recommended for damage tolerance evaluation of composite structures. The methodology was demonstrated in Section 5 on actual aircraft structures. The procedures are given below.

1. Divide the structure into small subdivisions. The structure should be divided according to the substructure arrangement and the skin thickness.

2. Select a damage tolerance design requirement. The requirements are discussed in the previous subsection. Requirement 5 is recommended for damage tolerance design.

3. Define an impact threat scenario. The medium threat defined earlier is recommended for a baseline analysis.

4. Conduct damage structural reliability analysis for each subdivision.

5. Determine the B-basis strain for the damaged structure from the analysis results.

6. Compare the B-basis strain with the DUL strain to determine the margin of safety for damage tolerance.

SECTION 7

SUMMARY AND CONCLUSIONS

7.1 Summary

The results of this research program are summarized below:

1. An extensive data analysis has been conducted to establish the static strength and fatigue life data scatter for typical bonded joints.
2. A statistical distribution was used to describe the impact threat scenarios. Based on this distribution, realistic impact damage requirements for structural certification were defined.
3. A damage tolerance evaluation methodology was developed. The methodology has the capability to assess the reliability of an impact damaged composite structure.
4. The methodology was demonstrated on the F/A-18A wing.
5. The results of this program has been integrated into the certification methodology developed in Reference 1. The improved methodology permits certification of bonded and cocured composite structures with the same level of confidence as bolted structures. This methodology also ensures that the threat of in-service low-velocity impact is adequately addressed.

7.2 Conclusions

The following conclusions may be drawn from the investigations undertaken in this program:

1. The certification methodology developed in Reference 1 has general applicability to all aircraft types and is very flexible. As such, it is ideally suited for efficient incorporation of the effects of impact damage and cocured/bonded structures.
2. The procedure to certify cocured/bonded structures is identical to that of bolted structures, except a higher data scatter should be used.

3. The building-block approach for certification is equally applicable for impact-damaged composite structures.

4. The key elements in damage tolerance evaluation of composite structures are the definition of impact threat and the selection of design requirements.

5. The damage tolerance analysis methodology developed can be utilized for initial design, trade studies, scenario sensitivity studies and in-service damage assessment of composite structures.

APPENDIX A

BONDED JOINT SCATTER ANALYSIS

The scatter in static strength and fatigue life of adhesively bonded composite joints was statistically characterized. This scatter was then compared with that observed in composite laminates and bolted joints. The two-parameter Weibull distribution was used in the data analysis. Details of the Weibull analysis can be found in Reference 1. Experimental data on bonded joints from References A.1 and A.2 provide a data base sufficient for statistical analysis. The results are discussed in the following paragraphs.

A.1 Static Data Analysis

In Reference A.1, composite-to-titanium adhesively bonded step-lap joint specimens were tested. The basic design of the specimen was a three-step joint similar to that used in the F/A-18 horizontal tail. The composite material used was AS/3501-5 graphite/epoxy and the solid composite section was a 27-ply, $(0_3/90/0_3/\pm45/0_2/\pm45/90)_s$ laminate. The adhesive material was American Cynamid FM-400. The parameters investigated in the reference included:

1. Loading frequency
2. Load truncations
3. Stress level
4. Extended life
5. Loading direction
6. Environment

More than 70 static and residual strength test series were conducted. Among these test data, 65 sets were found adequate for statistical analysis. These test data and the respective Weibull parameter α values are summarized in Table A.1. Each test series consisted of 20 or more specimens, except for the real time tests which had only 10 specimens in a test series. All static strength data were included in the scatter analysis. For the fatigue test specimens, only the residual strength of the surviving specimens was analyzed.

TABLE A.1. SUMMARY OF α's FOR REFERENCE A.1 DATA.

TEST SERIES	ENVIRONMENT	LOAD	TEST PARAMETER	NUMBER OF SPECIMENS	α
1	RTD	TENSION	STATIC	30	10.37
3	"	"	RESIDUAL, BASELINE 2LT	29	8.63
3 - 1	"	"	RESIDUAL, DRYING OUT	10 + 10 [1]	8.28
4	"	"	" , BASELINE 1LT	20	8.01
5	"	"	" , FREQUENCY	16	8.98
6	"	"	" , HIGH LOAD RATE	16	10.10
7	"	"	" , LOW LOAD RATE	11	9.27
8	"	"	" , DWELL TIME	16	6.95
9	"	"	" , REAL TIME	4 + 6 [2]	--
22	"	"	" , STRESS LEVEL	20	9.19
23	"	"	" , STRESS LEVEL	19 + 1 [1]	7.03
28	"	"	" , TRUNCATION	20	17.44
29	"	"	" , TRUNCATION	18 + 2 [1]	10.03
30	"	"	" , TRUNCATION	19 + 1 [1]	16.74
101	"	"	" , STRESS LEVEL	8 + 12 [1]	15.80
104	"	"	" , BASELINE 15LT	12 + 8	12.26
2	RTD	COMPRESSION	STATIC	20	13.72
10	"	"	RESIDUAL, BASELINE	20	10.18
10 A [3]	"	TENSION	" , FREQUENCY	12	12.93
10 A [3]	"	COMPRESSION	" , "	7 + 1	13.91
11	"	"	" , "	19 + 1	8.97
12	"	"	" , "	20	15.25
12 A	"	"	" , "	19 + 1	8.82
13	"	"	" , REAL TIME	10	11.98
24	"	"	" , STRESS LEVEL	19 + 1	6.91
25	"	"	" , "	12 + 8	7.73
31	"	"	" , TRUNCATION	20	7.55
32	"	"	" , "	18 + 2	8.20
32 A	"	"	" , "	20	8.84
102	"	"	" , STRESS LEVEL	19 + 1	10.45
105	"	"	" , BASELINE 15LT	19 + 1	16.80
60	RTW	TENSION	STATIC	20	19.83
107	"	"	RESIDUAL, BASELINE	13 + 7	10.57
107 - 1	"	"	, FREQUENCY	11 + 9	15.99
108	"	"	, "	11 + 9	13.61
109 - 1	"	"	, "	5 + 9	--
110	"	"	RESIDUAL, FREQUENCY	19 + 1	19.21
111 T	"	"	, REAL TIME	10	13.48
123	"	"	, TRUNCATION	4 + 16 [2]	--
124	"	"	, "	6 + 14 [1]	14.21
61	RTW	COMPRESSION	STATIC	20	14.97
111 C	"	"	RESIDUAL, REAL TIME	10	18.10
112	"	"	, FREQUENCY 2LT	15 + 5 [1]	11.42
113	"	"	, " 1LT	20	9.43
114	"	"	, DWELL TIME	17 + 3 [1]	12.28
125	"	"	, TRUNCATION	19 + 1 [1]	15.32
126	"	"	, "	20	11.08
129	"	"	, BASELINE 15LT	7 + 12 [1]	11.70

TABLE A.1. SUMMARY OF α's FOR REFERENCE A.1 DATA (CONCLUDED).

TEST SERIES	ENVIRONMENT	LOAD	TEST PARAMETER	NUMBER OF SPECIMENS	α
63 -1	LTW	TENSION	STATIC	20	14.13
66	HTW	"	"	20	20.32
131 - 1	MPTW	TENSION	RESIDUAL, BASELINE 2LT	14 + 6 (1)	9.85
132	"	"	" , FREQUENCY 1LT	12 + 8 (1)	10.62
132 - 1	"	"	" , BASELINE 1LT	17 + 3 (1)	12.73
133	"	"	" , FREQUENCY	10 + 10 (1)	6.75
142	"	"	" , STRESS LEVEL	13 + 7 (1)	11.41
64	LTW	COMPRESSION	STATIC	20	7.87
67	HTW	"	"	20	19.56
134 C	MPTW	COMPRESSION	RESIDUAL, REAL TIME	6 + 4	7.40
135	"	"	" , BASELINE 2LT	17 + 3 (1)	10.89
136	"	"	" , BASELINE 1LT	19 + 1 (1)	24.39
137	"	"	" , DWELL TIME	15 + 5 (1)	16.68
143	"	"	" , STRESS LEVEL	11 + 9 (1)	10.09
146	"	"	" , TRUNCATION	16 + 4 (1)	15.47
146 A	"	"	" , "	18 + 2 (1)	11.25
149 - 1	"	"	" , BASELINE 15LT	4 + 16 (2)	--
77	MPTW	TENSION	RESIDUAL, USAGE	15 + 5 (1)	19.95
78 - 1	"	"	" "	14 + 5 (1)	8.16
79	"	"	" "	16 + 4 (1)	9.63
76 SRTW (T)	RTW	TENSION	STATIC, LARGE SCALE JOINT	7	15.47
76 SRTW (C)	"	COMPRESSION	STATIC, "	3 (4)	--

NOTES :

(1) Number of Specimens Survived Fatigue Test + Number of Specimens Failed During Fatigue Test, α Was Determined Based on Residual Strength Distribution of Survived Specimens Only.

(2) Not Enough Specimens Survived for Weibull Analysis.

(3) Test Series 10A Specimens Were Tested Under Compression Dominated Spectrum, Part of the Survived Specimens Were Tested for Tension Residual Strength and the Others for Compression Residual Strength.

(4) Not Enough Specimens Tested for Weibull Analysis.

The specimen geometry tested in Reference A.2 was a double lap joint configuration with titanium bonded to graphite epoxy. The composite material used in the reference was Narmco T300/5208 graphite/epoxy laminate, 20 plies thick, with $(0/45/0/-45/0_2/-45/0/45/0)_2$ layup. The adhesive material was Reliabond 398 system. Static tests were conducted under five different temperatures and three different loading rates at ambient humidity. Ten specimens were tested at each combination of temperature and loading rate. Constant amplitude fatigue tests were conducted at room temperature and humidity for seven load levels. Residual strengths were obtained for specimens that survived the fatigue tests. A total of 15 static and 6 residual strength data sets were included in the scatter analysis.

The overall distribution of the Weibull shape parameter, α, is shown in Figure A.1. The actual values of α range from 6.75 to 24.39. Figure A.1 shows that the combined data (all data) have a modal α value of approximately 10. The mean α from all data is computed to be 12.2 This trend is similar to the α distribution of the laminate and bolted joint data (Reference 1), i. e., the modal α value is lower than the mean α. Figure A.1 also shows the distributions of α from data in Reference A.1 (Northrop Data) and Reference A.2 (UD Data). It is seen from the figure that these two distributions have a similar shape and location. The overall mean for the Northrop data is 12.3 and for the UD data the mean is 11.8. This suggests that the two data sets may be pooled to form a single data base for reliability analysis of bonded joints.

Figure A.2 shows a comparison of the Weibull shape parameter distribution for static strength and residual strength data. The figure shows that scatter in static strength is lower than the residual strength data scatter. The mean α for the static strength data is 13.7 and that of the residual strength data is 11.7. However, the difference in α is not significant when statistically tested. This trend justifies the combined use of static strength and residual strength data.

The overall bonded joint static and residual strength α distribution is compared with that of unnotched and open or loaded hole composite laminate data in Figure A.3. It is seen that the bonded joint scatter is significantly higher (lower α) than that of laminates and open or loaded hole

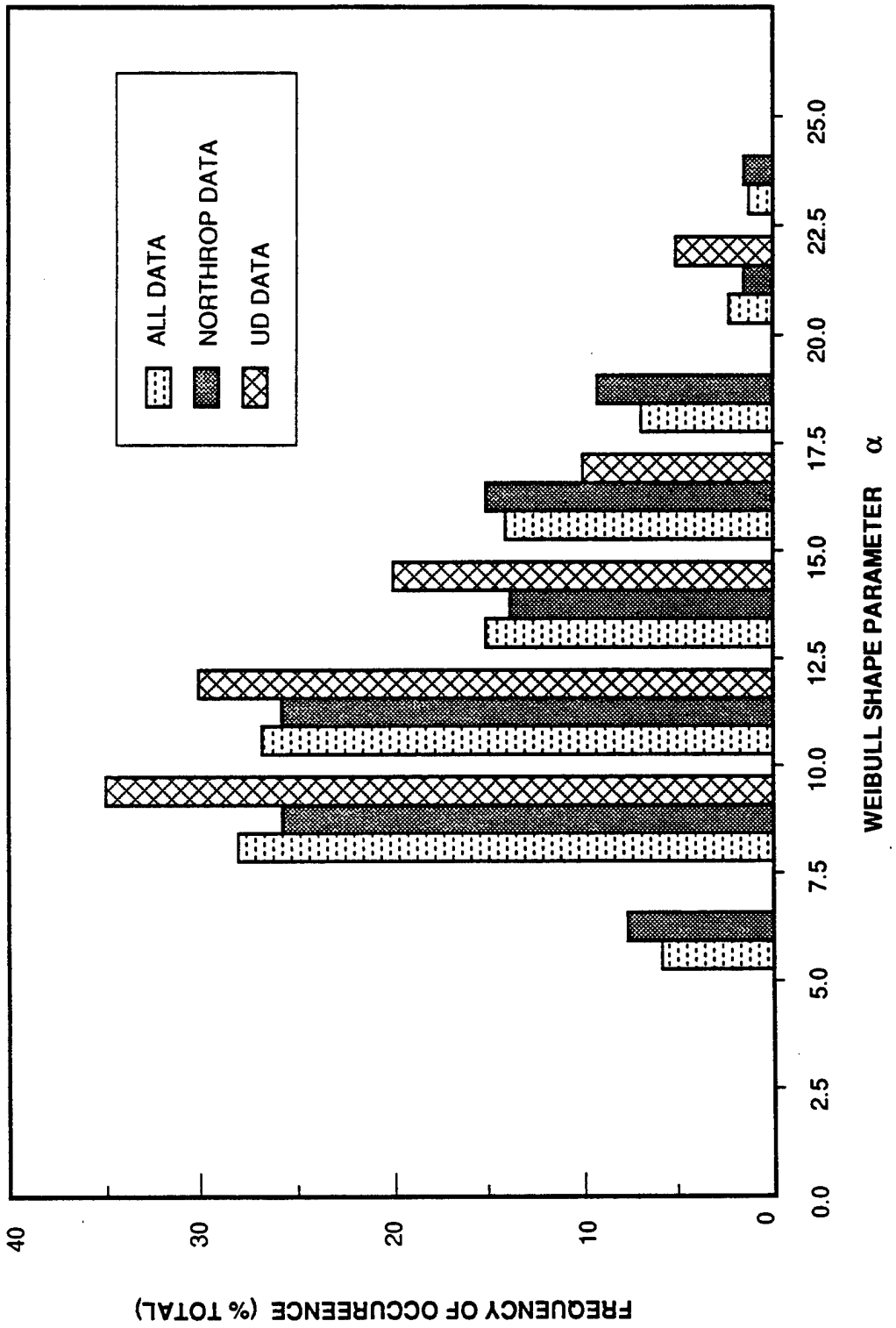

Figure A.1. Overall Distribution of Weibull Shape Parameters for Bonded Joint Strength.

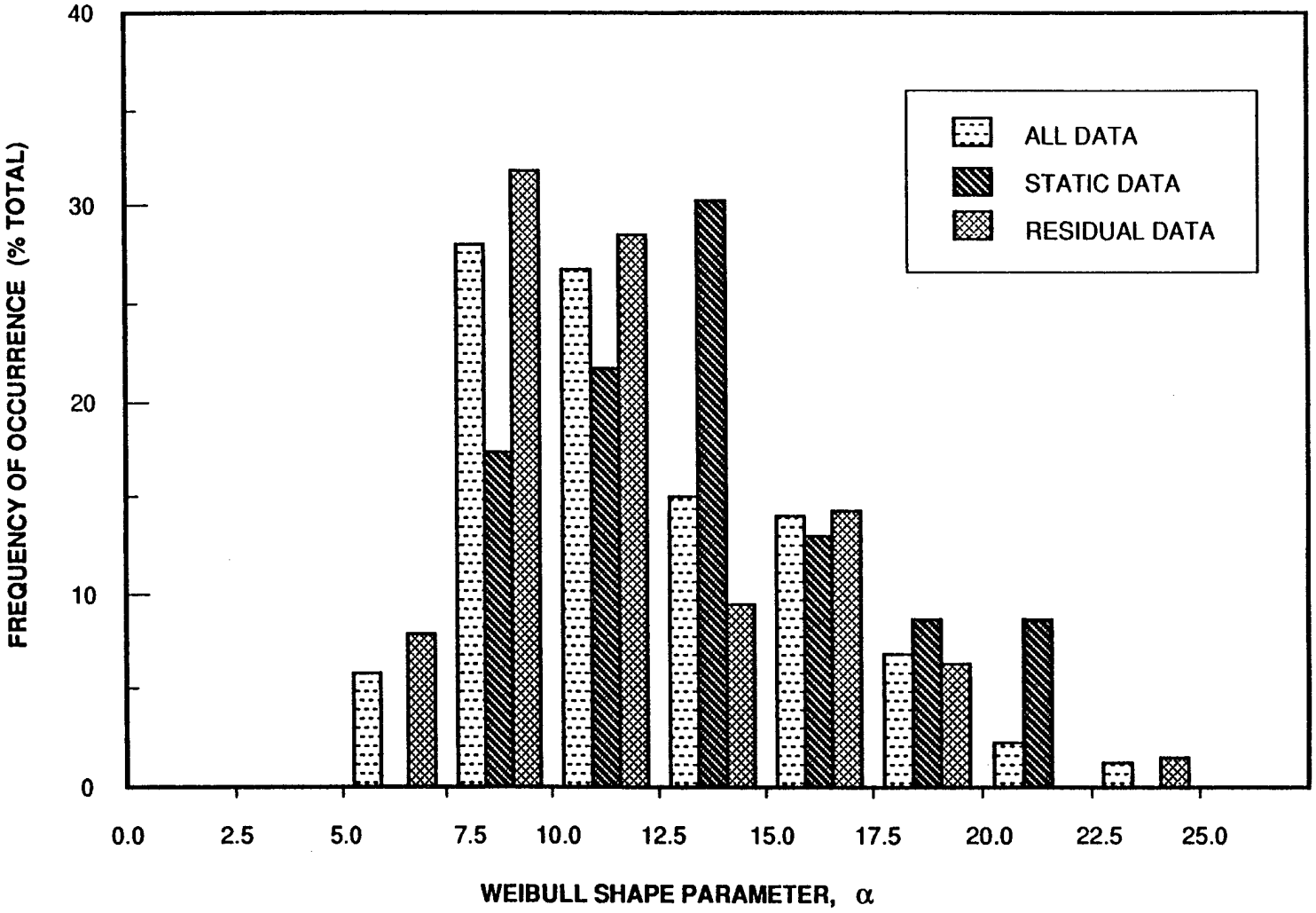

Figure A.2. Comparison of Weibull Shape Parameter Distribution for Static Strength and Residual Strength Data.

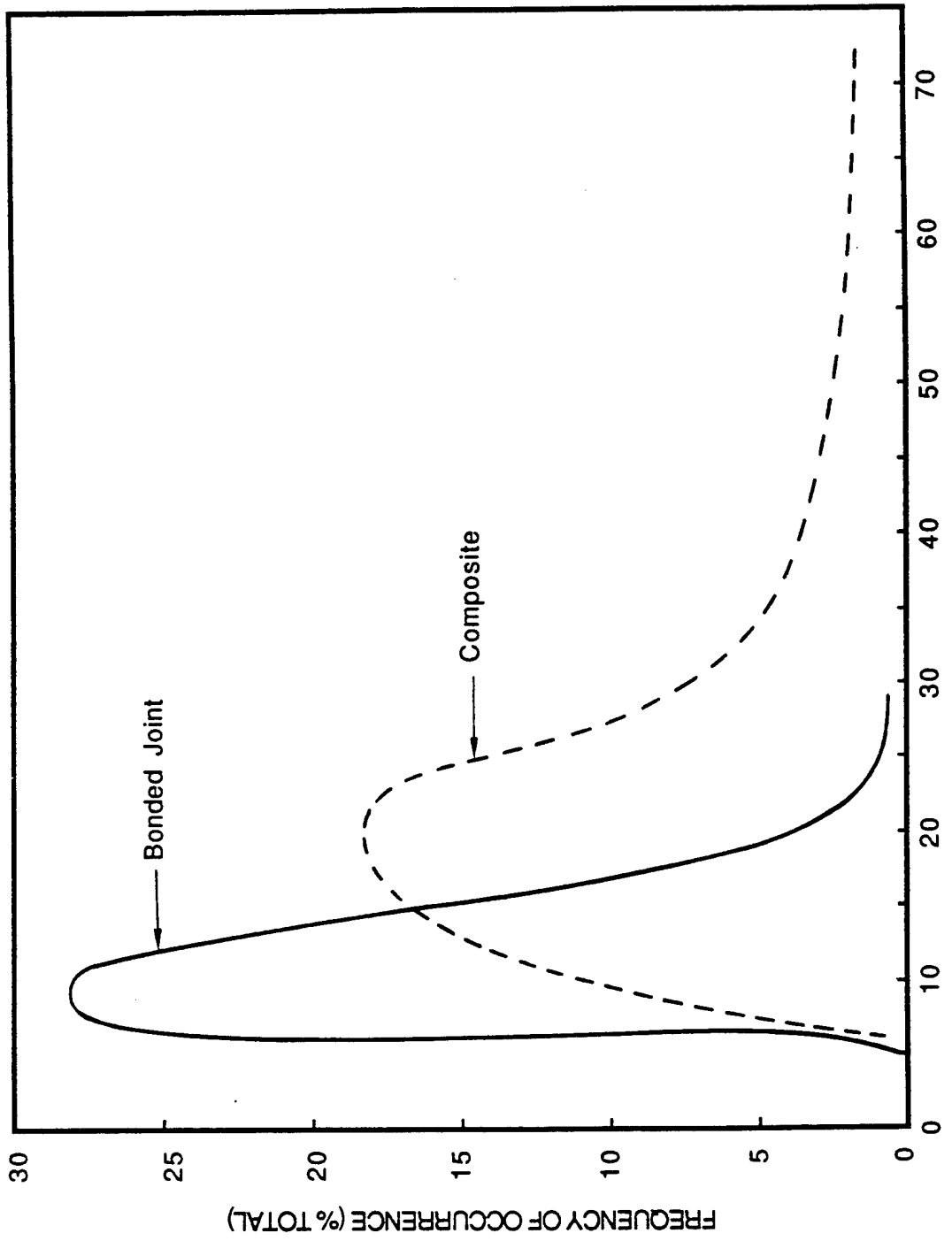

Figure A.3. Comparison of Bonded Joint Strength Scatter with Unnotched Composite Laminate and Bolted Composite Joint Strength Scatter.

composite data. In Reference 1, a modal α value of 20 was recommended for laminates and bolted joints. This value is reduced to 9.0 for bonded joints. The higher scatter in bonded joints significantly influences the determination of design allowables and structural reliability from the test data.

The influences of different test variables on the mean Weibull shape parameter are shown in Figures A.4 through A.8. Figure A.4 shows the influence of test environment on static strength Weibull shape parameter. The figure shows that the LTW (-65°F with approximately 1 percent moisture) compression data exhibit significantly higher scatter (lower α). However, since only one data set (20 tests) was available for each static test environmental condition, no statistical significance check was conducted. Figure A.5 shows the influence of test environment on the scatter of combined static and residual strength data. The figure shows that the mean α's for all test environments range from 11 to 15. Statistical checks were conducted to determine the significance of this difference. The results showed that the differences between the mean α's are not significant.

Figure A.6 shows the influence of joint configuration on the strength (static and residual) data scatter. Static and residual strength data for three joint configurations are included. These are: (a) the three-step joint used in Reference A.1 (standard);(b) the six-step joint also used in Reference A.1 (large); and (c) the double lap joint used in Reference A.2 (UD data). The values of α range from 12 to 14. Statistical check again shows no significant difference in the mean α's.

The influence of test temperature on the static strength data scatter for the Reference A.2 data (UD) is shown in Figure A.7. The figure shows that the 250°F static strength has significantly higher value of α (mean α = 17.25). The values of α for specimens tested at other temperatures range from 10.47 to 12.18 and they are not significantly different. Figure A.8 shows the influence of loading rate on the scatter of static strength data (UD data). It can be seen from the figure that the mean values of α for the three loading rate are not significantly different.

A.2 Fatigue Data Analysis

A total of 34 data sets from Reference A.1 and 8 data sets from Reference A.2 were found suitable for statistical analysis. The Weibull shape

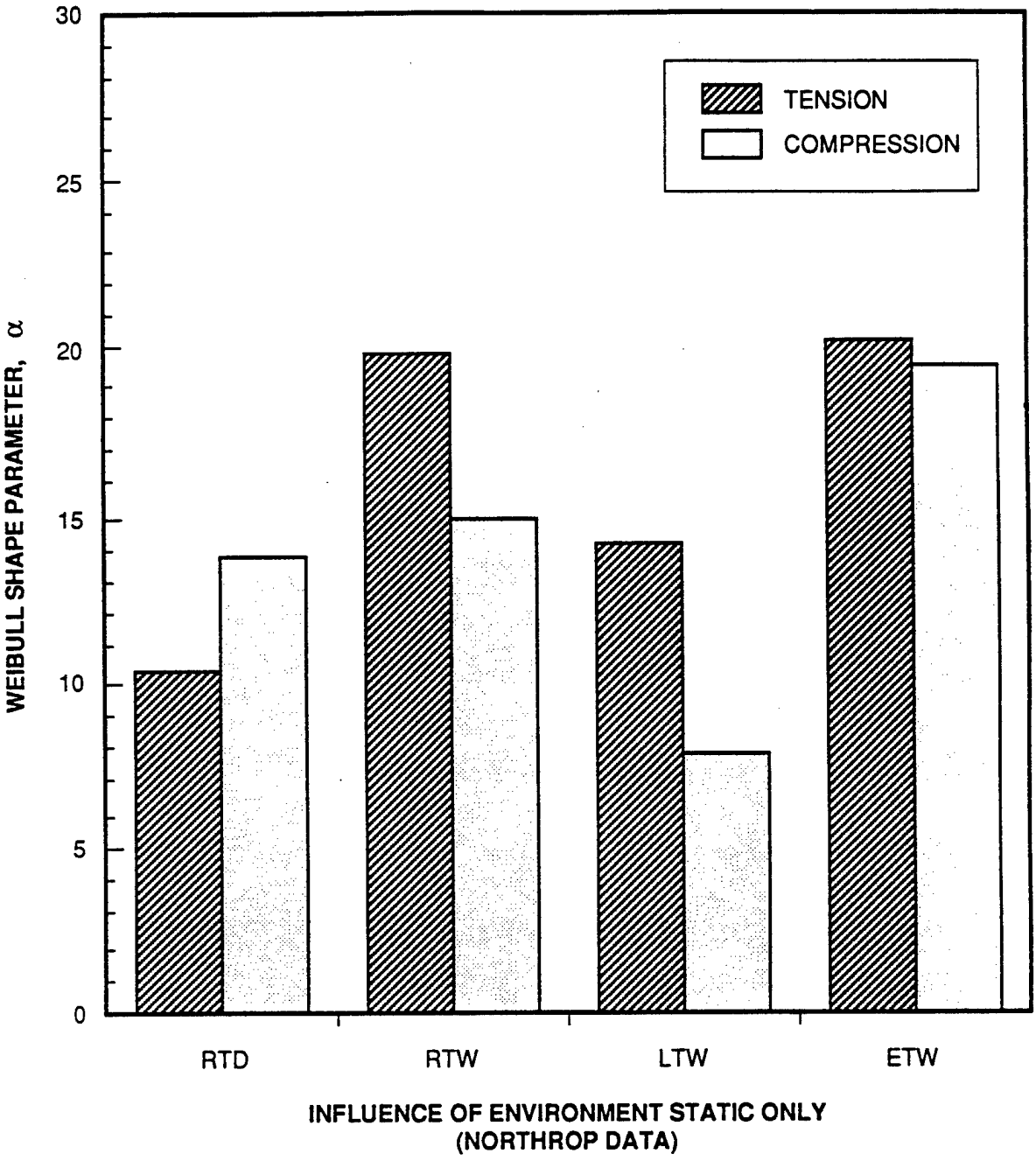

Figure A.4. Influence of Test Environment on Static Strength Scatter (Northrop Data Ref. A.1).

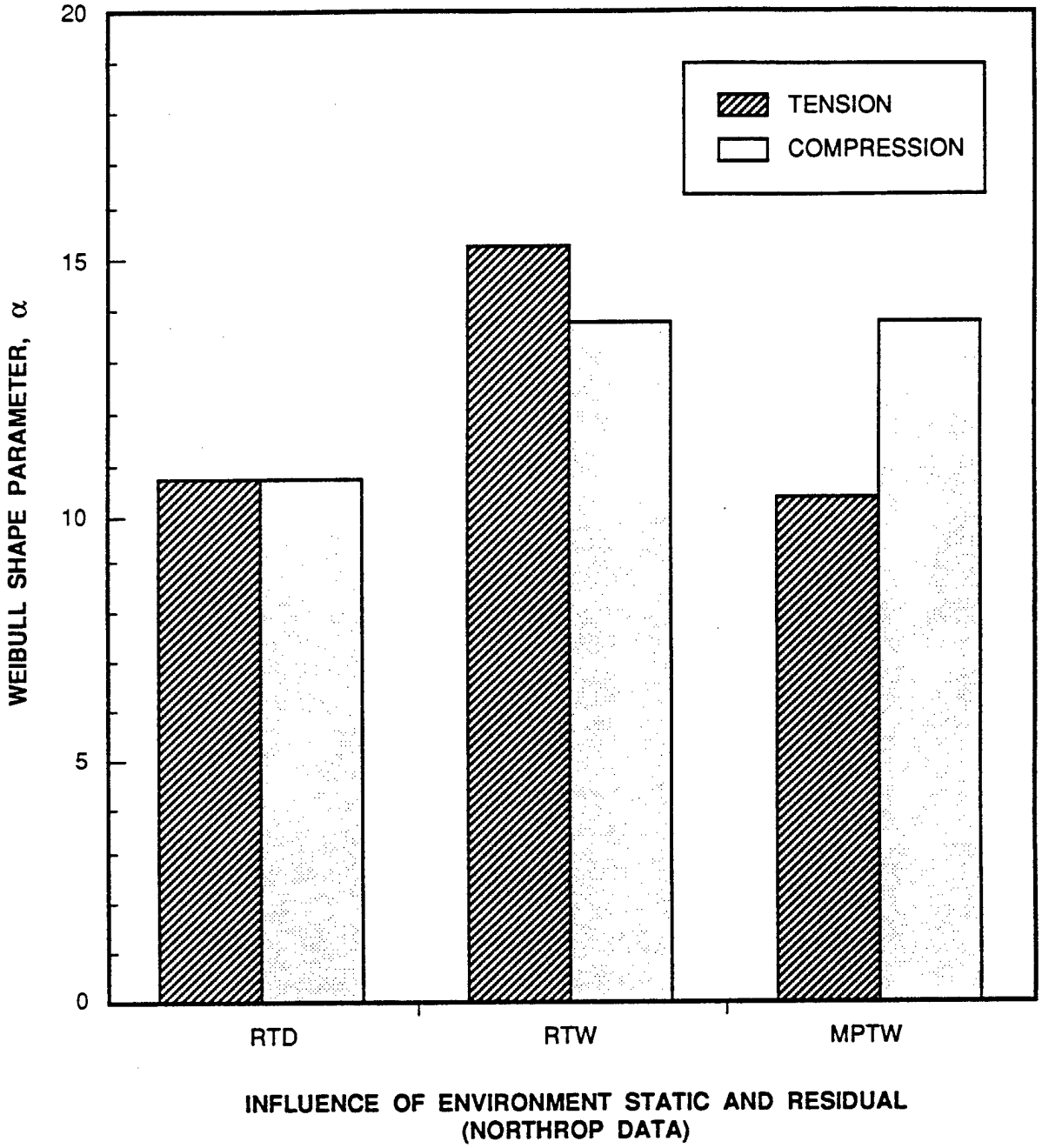

Figure A.5. Influence of Test Environment on Combined Static and Residual Strength Scatter (Northrop Data Ref. A.1).

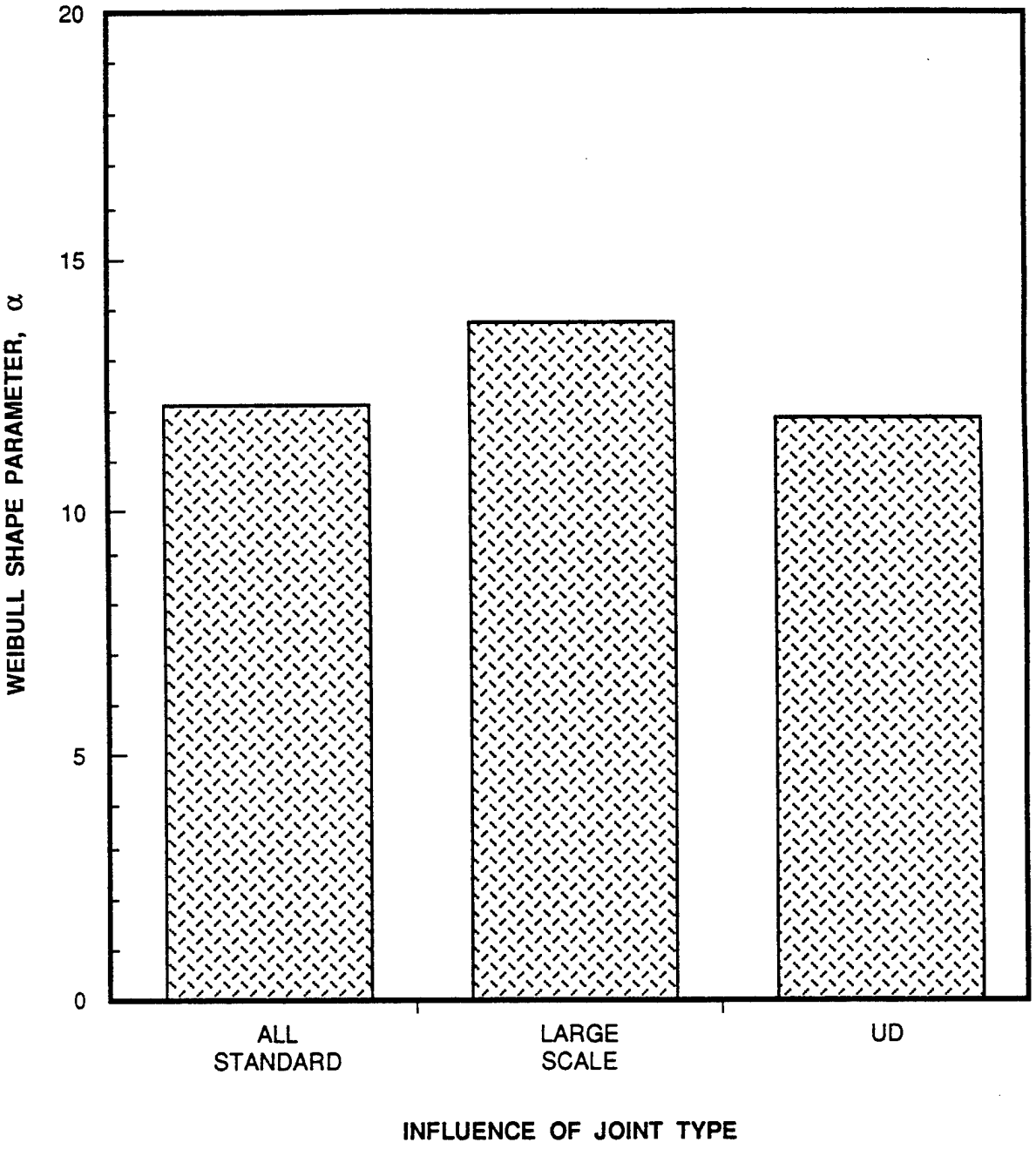

Figure A.6. Influence of Joint Configuration on Strength Scatter.

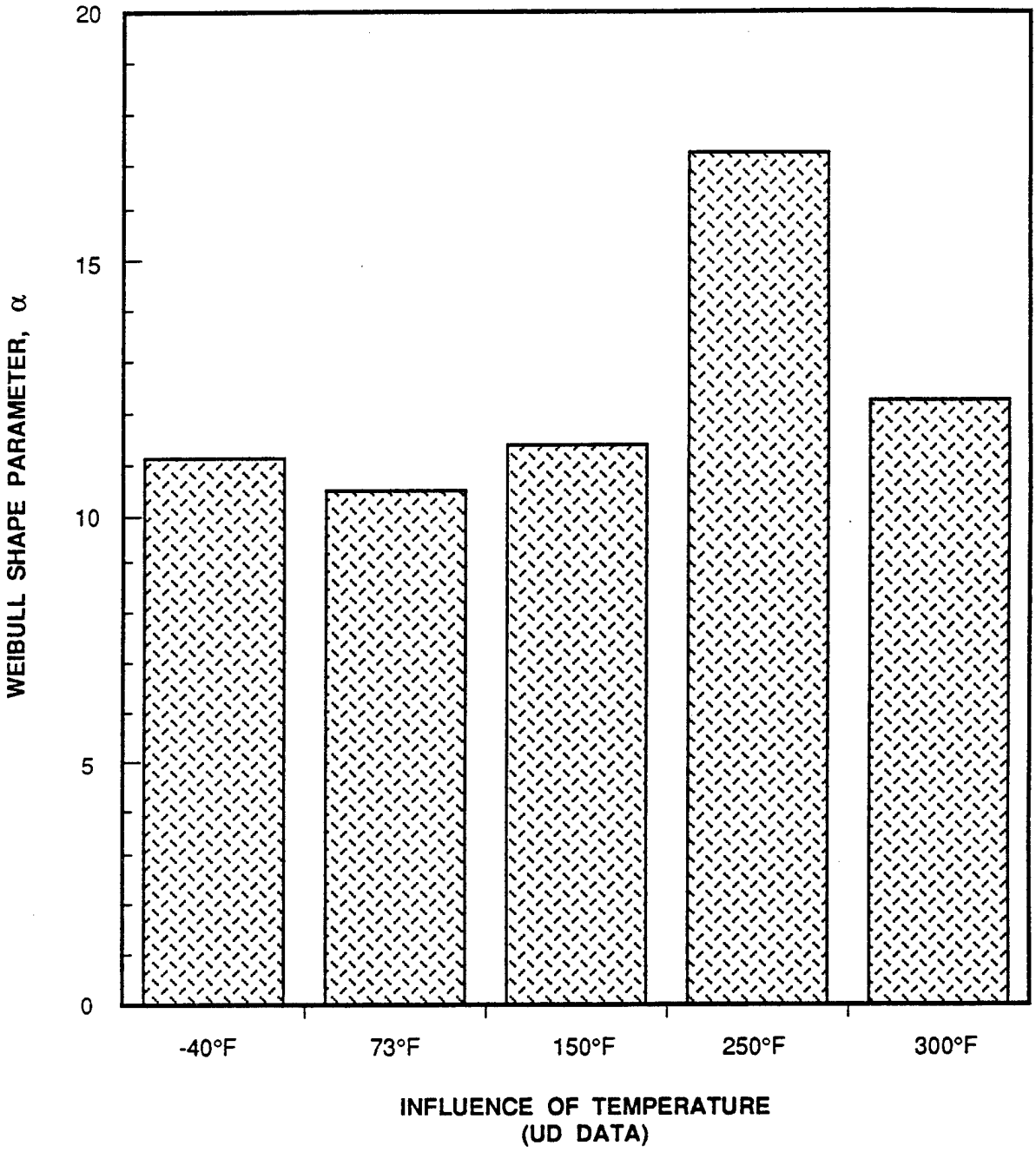

Figure A.7. Influence of Test Temperature on Static Strength Scatter (UD Data Ref. A.2).

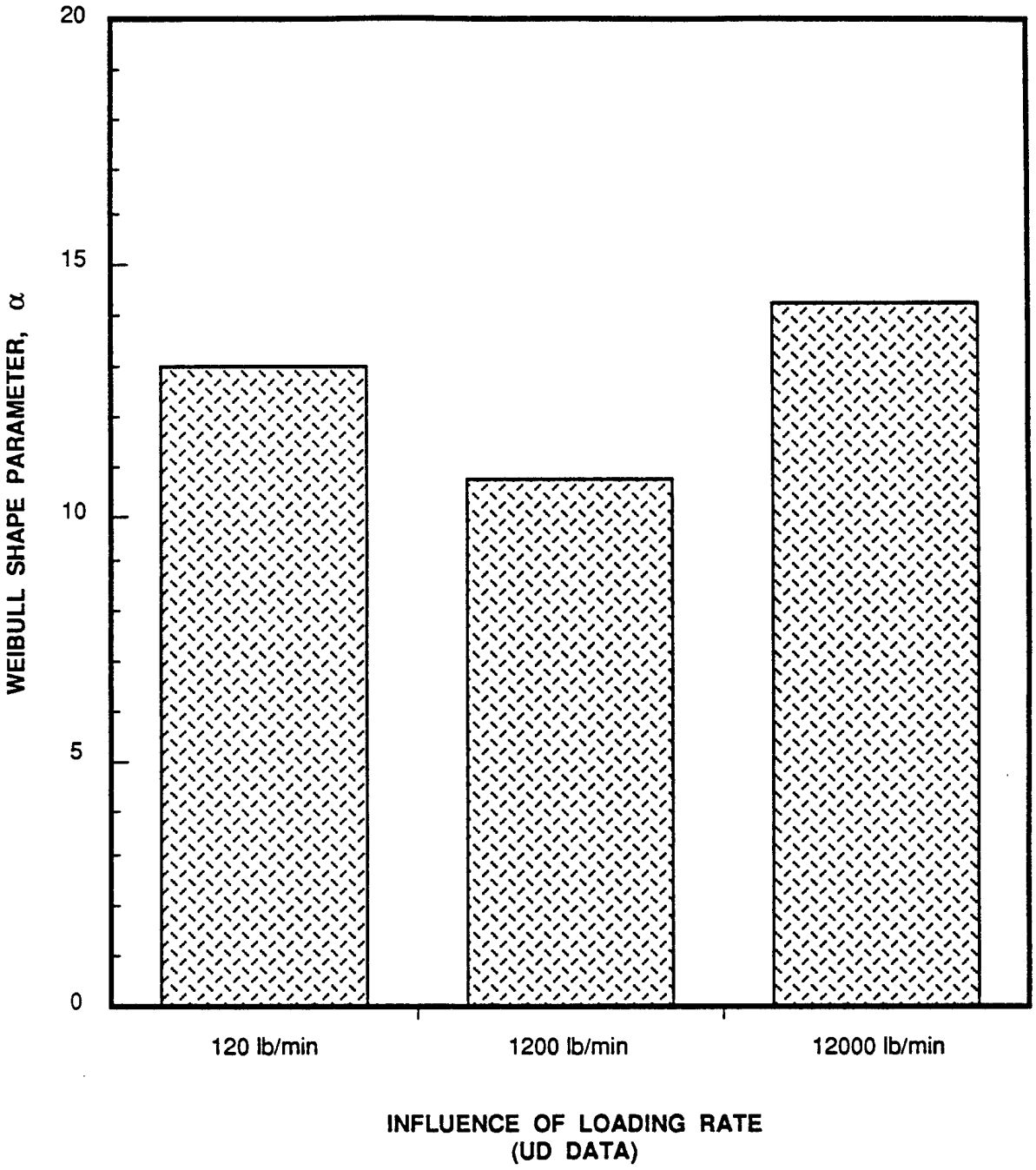

Figure A.8. Influence of Loading Rate on Static Strength Scatter (UD Data Ref. A.2).

parameter for each data set was determined individually and these values form the overall distribution shown in Figure A.9. The mean value of all α's is 1.76. The modal value of the distribution is 1.25. This distribution is very similar to that for laminates and bolted joints (Reference 1) in which the mean α is 2.17 and modal α is 1.25. The distributions of α's from fatigue life data of References A.1 and A.2 are shown in Figures A.10 and A.11, respectively. Figure A.10 shows that the Northrop data scatter distribution is similar to that for the overall data and that for laminates and bolted joints. The mean α for this group of data is 1.87 and the modal value is 1.25. The UD fatigue life data scatter distribution is shown in Figure A.11. The mean α for this group of data is 1.33. However, the distribution was constructed with only eight data sets. Therefore, a modal value could not be determined from the figure. Despite the limited number of data sets for the UD data, the two groups of data have a similar range of α's. These data are combined to form the overall distribution for future applications.

The overall distribution of fatigue life Weibull shape parameter for bonded joints is compared with that for composites and bolted joints in Figure A.12. The figure shows that the two distributions are similar both in shape and location. They both have a modal α value of 1.25.

The influence of test environment on the fatigue life scatter is shown in Figure A.13. The figure shows that the scatter in compression fatigue life is higher than in tension fatigue life data. Also, the test environment has a stronger influence on the tension fatigue life. However, the modal α value of 1.25 is a conservative estimate of the overall fatigue life scatter.

In conclusion, the bonded joint static and residual strength data have higher scatter than the strength data for commonly used composite laminates and bolted joints. The fatigue life scatter is similar for bonded joints laminates and bolted joints. Table A.2 summarizes the key scatter parameters obtained from the above scatter analysis, and shows a comparison with the scatter parameters for laminates and bolted joints. The table also includes the B-basis knockdown factor based on a sample size of 15. As can be seen from the table, using the modal α, the B-basis knockdown factor is 0.789 for bonded joints as compared to 0.901 for laminates and bolted joints.

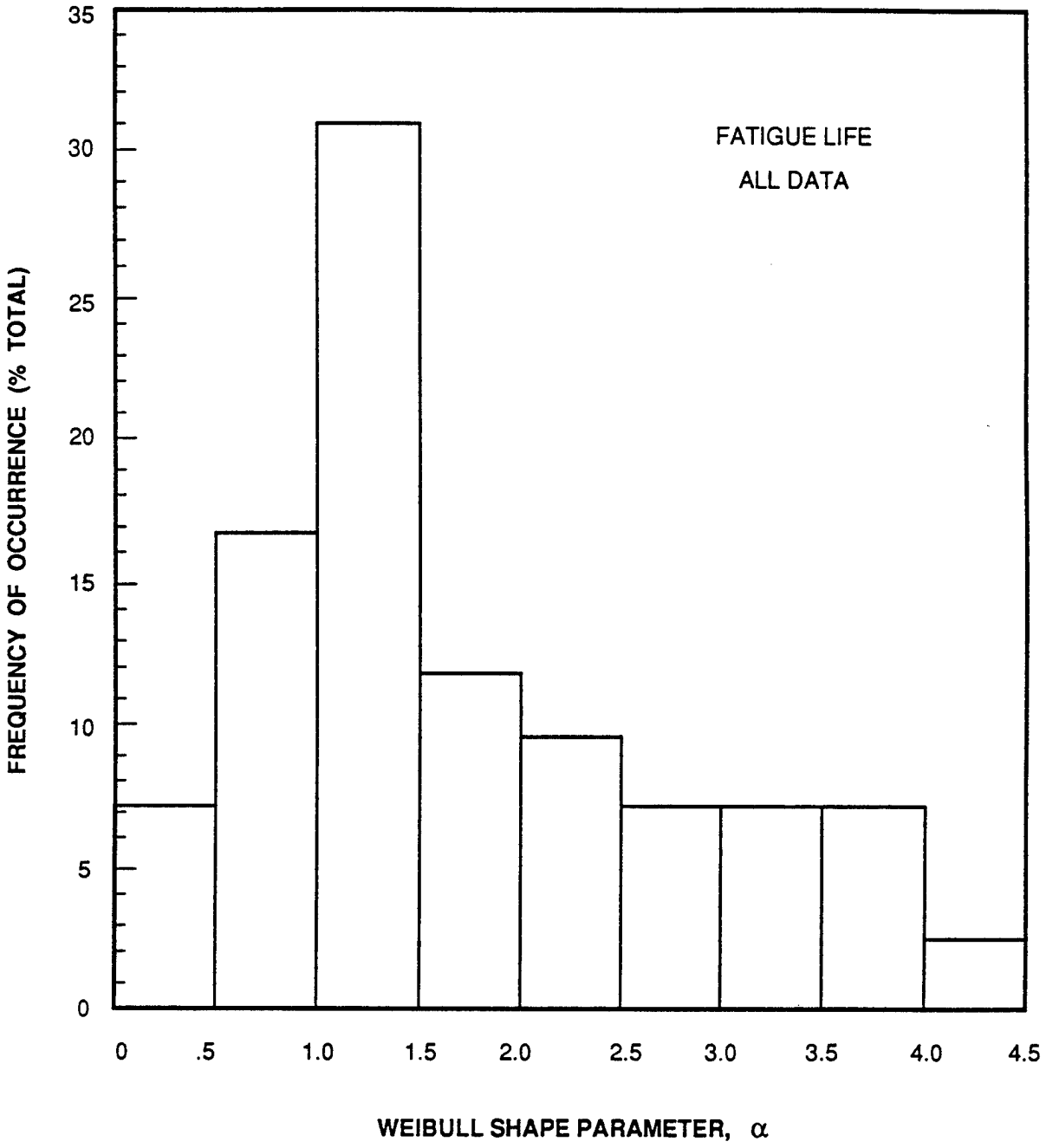

Figure A.9. Overall Distribution of Weibull Shape Parameter for Bonded Joint Fatigue Life.

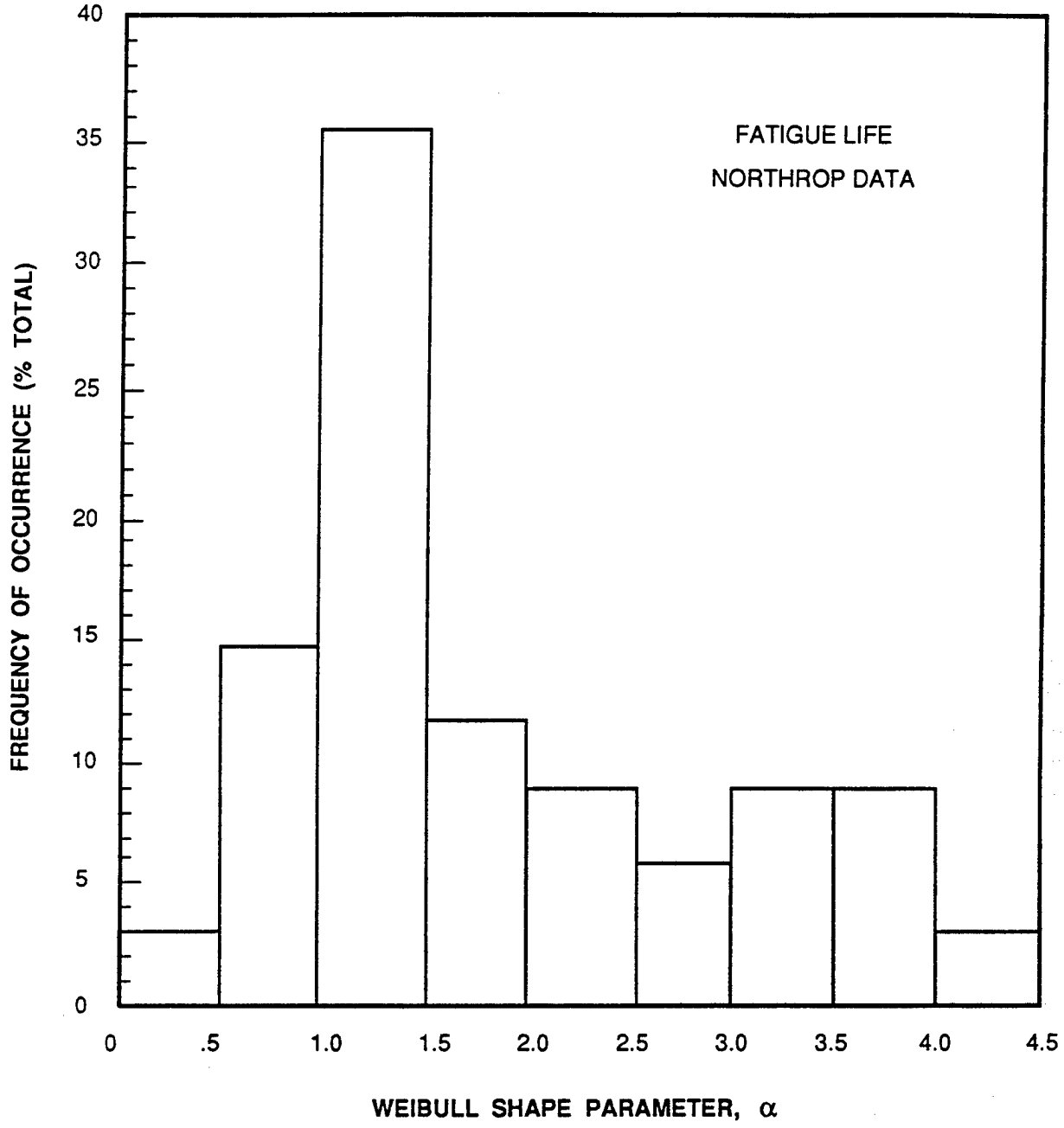

Figure A.10. Fatigule Life Data Scatter Distribution (Northrop Data).

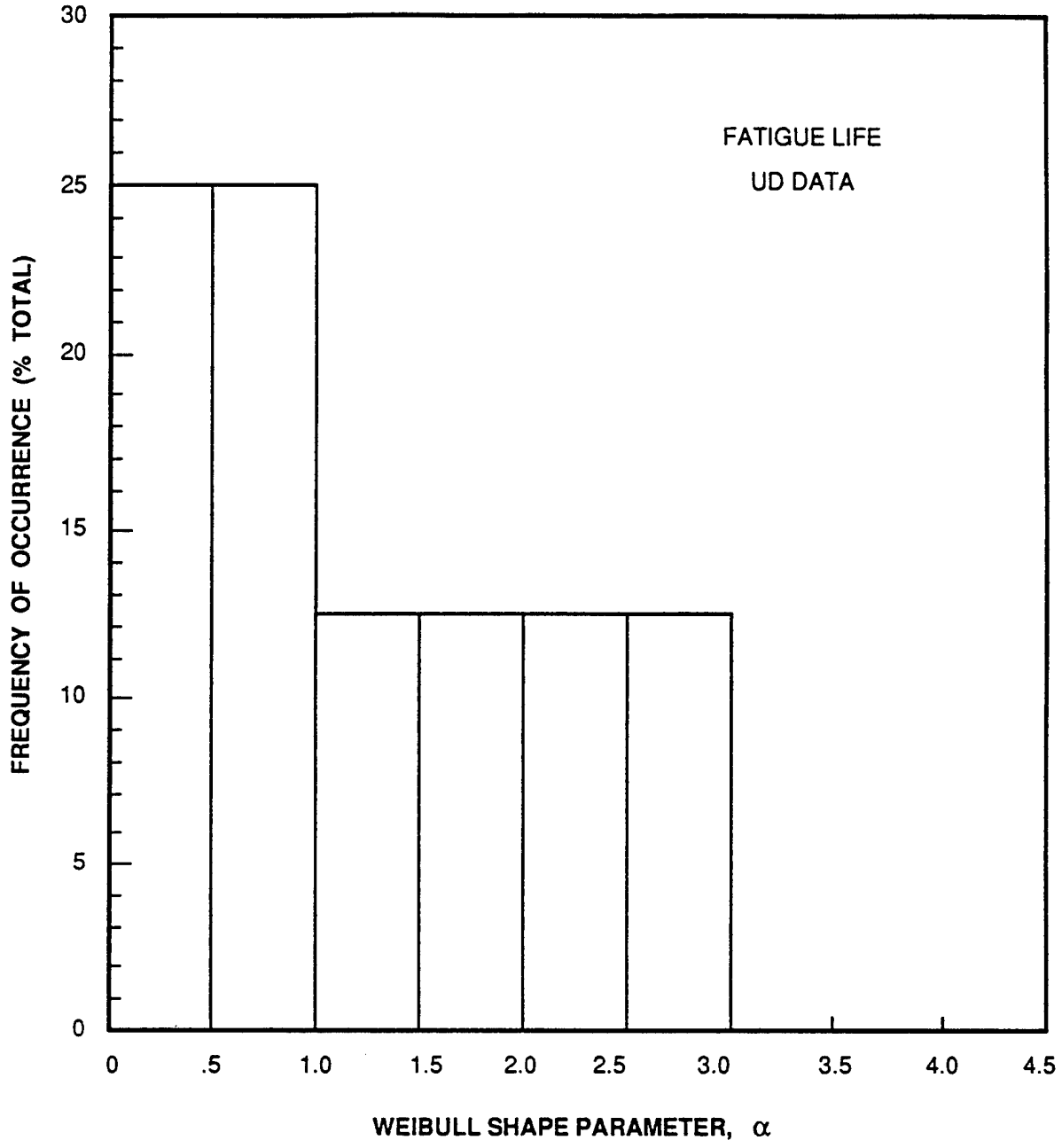

Figure A.11. Fatigue Life Data Scatter Distribution (UD Data).

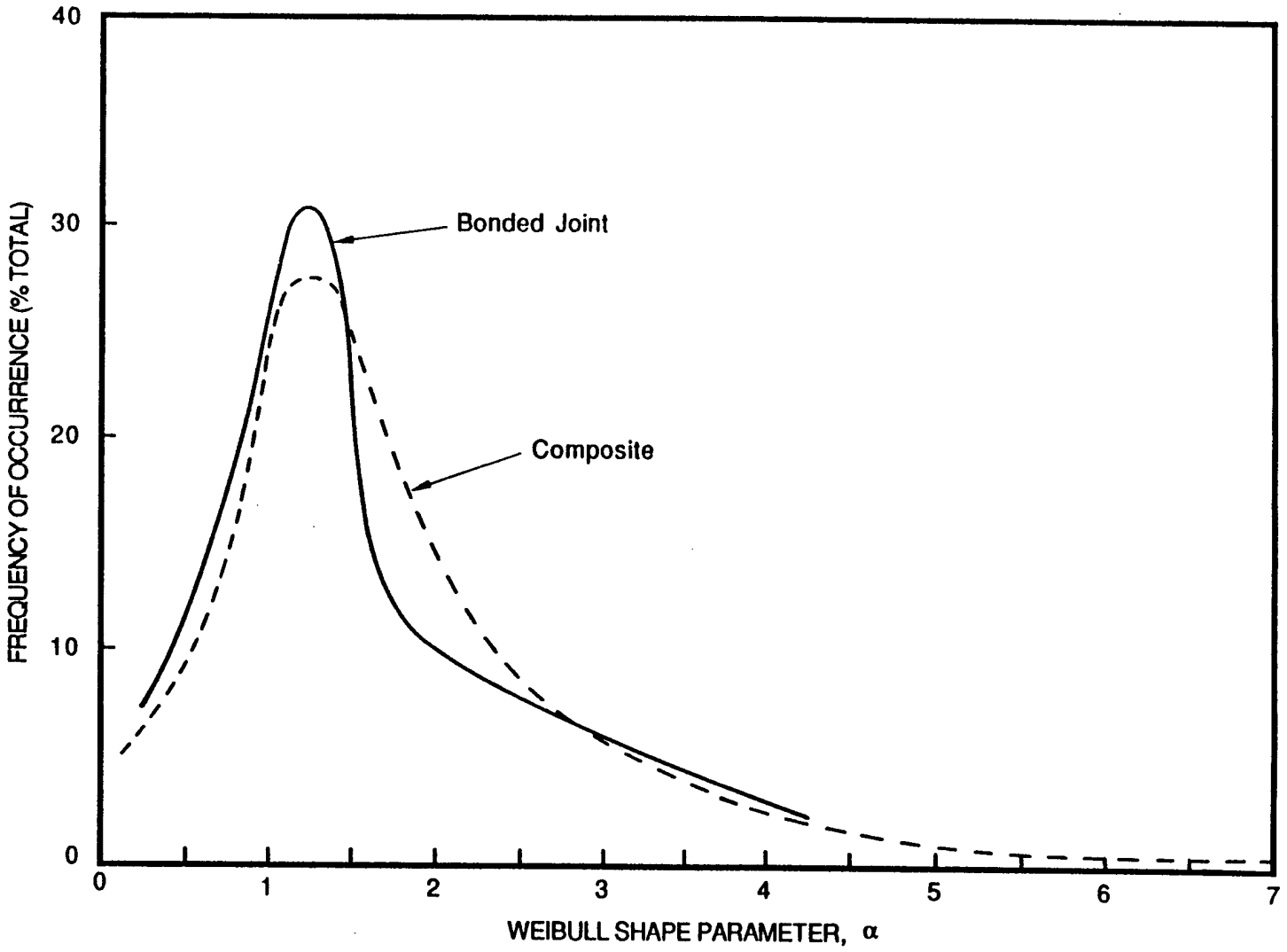

Figure A.12. Comparison of Bonded Joint Life Scatter and Laminate and Bolted Joint Scatter.

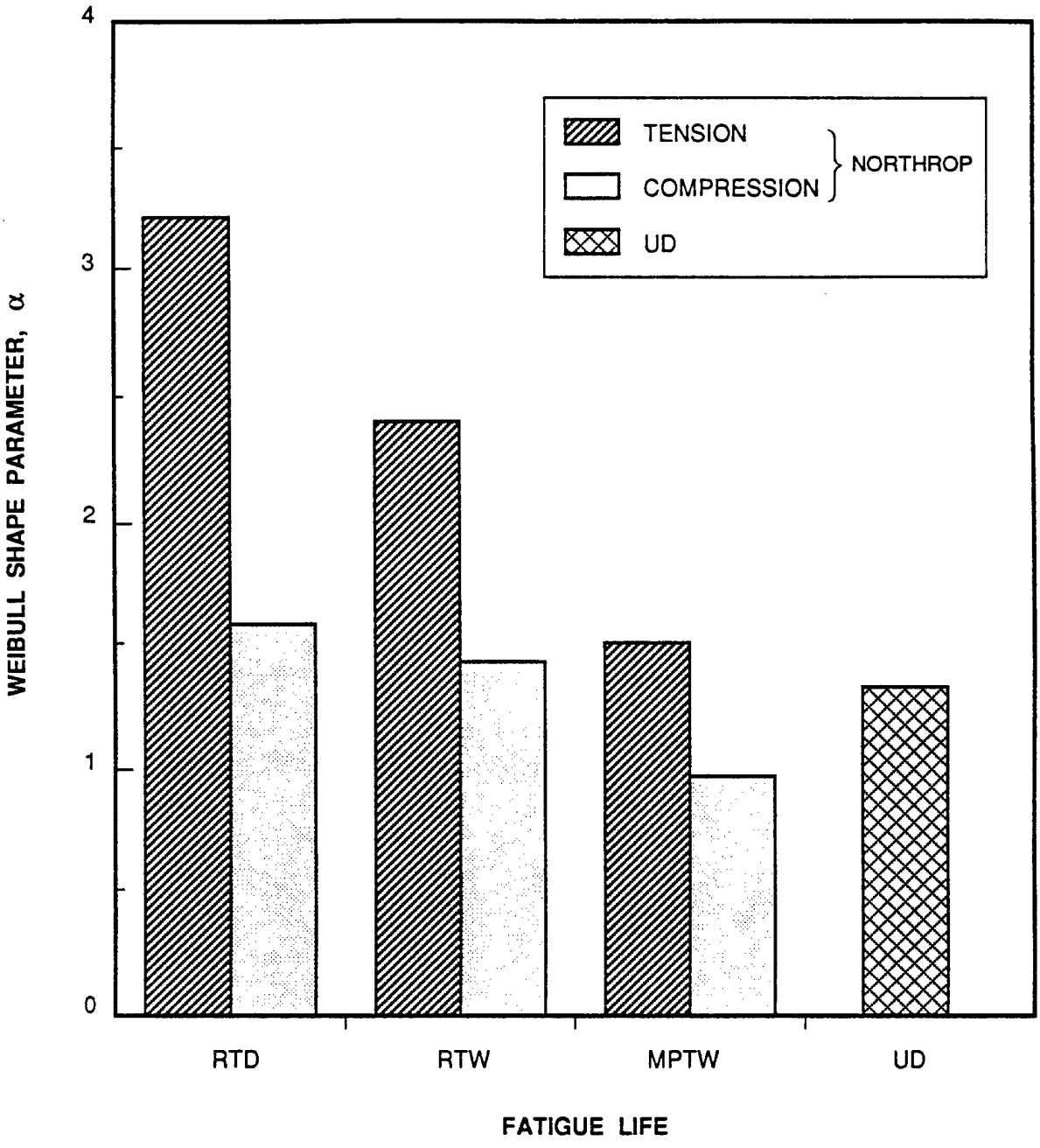

Figure A.13. Influence of Test Environment on the Fatigue Life Scatter of Bonded Joints.

TABLE A.2. COMPARISON OF KEY SCATTER PARAMETERS FOR BONDED JOINTS, LAMINATES AND BOLTED JOINTS.

	STATIC		FATIGUE	
	BONDED JOINTS	LAMINATES AND BOLTED JOINTS	BONDED JOINTS	LAMINATES AND BOLTED JOINTS
MEAN α	12.2	23.2	1.76	2.17
B-BASIS KNOCKDOWN	0.841	0.914	0.252	0.336
MODAL α	9.0	20.0	1.25	1.25
B-BASIS KNOCKDOWN	0.789	0.901	0.131	0.131

APPENDIX B

COMPUTER PROGRAMS

Three computer programs developed during the course of this research effort are documented in this Appendix. These programs are 'PISTRE1', 'PISTRE2' and 'DABSR'. All programs are written in FORTRAN language and are operational on IBM compatible personal computers. The theoretical backgrounds of these programs were presented in Sections 3 and 4 of this report. The program listings, input and output descriptions and sample examples are given in the following paragraphs.

B.1 PROGRAM 'PISTRE1'

Program PISTRE1 (Post-Impact STructural REliability) computes the initial (local) and final (structural) failure strain of a composite structure damaged by low-velocity impact of specified energy. It also computes the damage tolerance design allowables and margins of safety at design ultimate load (DUL), based on four different damage tolerance design requirements. The structural reliability for initial failure (IF) and final failure (FF) at dul, maximum service load (MSL = DUL/1.25) and design limit load (DLL = DUL/1.5) are also computed.

The required input to PISTRE1 are:

1. A 72-character problem title (TITLE).
2. Percents of 0-, 45-, 90-degree plies of the skin laminate (ZERO, Z45, Z90).
3. Thickness of the skin in inch (T).
4. Fracture toughness of the skin material in-lb/in**2 (GIC).
5. Impact energy in ft-lb (E).
6. Impactor diameter in inch (D).
7. Lamina properties and ultimate strain (EL, ET, GLT, PNU, EULT).
   EL is the longitudinal Young's modulus in MSI,
   ET is the transverse Young's modulus in MSI,
   GLT is the in-plane shear modulus in MSI,
   PNU or NULT is the in-plane Poisson's ratio,
   EULT is the failure strain of the undamaged laminate in micro-in/in.
8. Number of spars and spar stiffness (AE) in 10**6 lb. (NSP, AE).
9. Spar spacing of the impacted bay and edge width of the adjacent bays in inch (B2, A1, A2).
10. Effective energy coefficient (AK).
11. Impact event code (ID).
12. Strain at design ultimate load (DUL)

B.1.1 'PISTRE1' LISTING

```
C*****************************************************************
C  PROGRAM 'PISTRE1' (Post-Impact STructural REliability, version 1)   *
C  WAS DEVELOPED BY NORTHROP AIRCRAFT DIVISION UNDER NADC/FAA          *
C  CONTRACT NO. N62269-87-C-0259, 'ADVANCED CERTIFICATION METHODOLOGY  *
C  FOR COMPOSITE STRUCTURES'                                           *
C  THE PROGRAM COMPUTES THE COMPRESSIVE RESIDUAL STRENGTH FOR AN IMPACT*
C  DAMAGED COMPOSITE STRUCTURE. IT ALSO DETERMINES THE A- AND B-BASIS  *
C  DESIGN ALLOWABLES BASED ON FOUR DIFFERENT DAMAGE TOLERANCE DESIGN   *
C  REQUIREMENTS. THE STRUCTURAL RELIABILITIES AT DUL, MSL AND DLL      *
C  ARE DETERMINED BASED ON TYPICAL SCATTER OF POST-IMPACT STRENGTHS    *
C  OF COMPOSITES.                                                      *
C  THE REQUIRED INPUTS TO THE PROGRAM ARE: LAMINA PROPERTIES, LAMINATE *
C  LAYUP, STRUCTURAL CONFIGURATION, IMPACT ENERGY AND STRAIN AT DUL    *
C*****************************************************************

      DIMENSION TITLE(18)
      DOUBLEPRECISION T,E
      CHARACTER*3 ARE
      WRITE(*,306)
  306 FORMAT(2X,'PLEASE ENTER PROBLEM TITLE')
  307 FORMAT(18A4)
      READ(*,307) TITLE
      WRITE(*,2)
    2 FORMAT(2X,'PLEASE INPUT % OF (0,45,90)-DEG. PLIES')
      READ(*,*) ZERO,Z45,Z90
      C2 = 3.707
      WRITE(*,3)
    3 FORMAT(2X,'PLEASE INPUT SKIN THICKNESS')
      READ(*,*) T
      WRITE(*,4)
    4 FORMAT(2X,'PLEASE INPUT TOUGHNESS--GIC')
      READ(*,*) GIC
      C4 = 1.0
      A4 = 0.07486/GIC+0.01448
      GC = GIC
      IF(GIC.GT.5.554) GC=5.554
      B4 = (-0.00981*GC+0.10897)*GC+0.43449
      WRITE(*,5)
    5 FORMAT(2X,'PLEASE INPUT IMPACT ENERGY')
      READ(*,*) E
      WRITE(*,6)
    6 FORMAT(2X,'PLEASE INPUT IMPACTOR DIAMETER ')
      READ(*,*) D
      WRITE(*,302)
  302 FORMAT(2X,'PLEASE INPUT SKIN EL,ET,GLT AND NULT IN MSI'
     A/2X,'AND ULTIMATE STRAIN IN MICRO-IN/IN')
      READ(*,*) EL,ET,GLT,PNU,EULT
      WRITE(*,303)
  303 FORMAT(2X,'PLEASE INPUT NUMBER OF SPARS AND SPAR AE IN 10**6')
      READ(*,*) NSP,AE
```

```
      SN = NSP
      WRITE(*,304)
  304 FORMAT(2X,'PLEASE INPUT SPAR SPACING AND EDGE WIDTH A1,A2')
      READ(*,*) B2,A1,A2
      B = B2/2.
      B1 = 6.54319
      ALPHA = 0.71257
      A0 = 1.31616
      WRITE(*,11)
   11 FORMAT(2X,'PLEASE INPUT EFFECTIVE ENERGY COEFFICIENT, AK')
      READ(*,*) AK
      WRITE(*,12)
   12 FORMAT(2X,'PLEASE INPUT IMPACT EVENT CODE, ID',
     A/2X,'ID = 1  SINGLE MID-BAY IMPACT',
     B/2X,'ID = 2  TWO BAYS, MID-BAY IMPACTS',
     C/2X,'ID = 3  SINGLE NEAR SPAR IMPACT')
      READ(*,*) ID
      WRITE(*,310)
  310 FORMAT(2X,'PLEASE INPUT DUL STRAIN')
      READ(*,*) DUL
      W = A1+A2+2.0*B2
      WF = 2.*(A1+B)
      WR = 1.0-D/WF
      WE = (2.0+WR**3.0)/WR-1.0
      WRITE(*,308) TITLE
  308 FORMAT(//2X,18A4)
      CALL LAME(ZERO,Z45,Z90,EL,ET,GLT,PNU,ESK)
      WRITE(*,7) D,GIC,ZERO,Z45,Z90
    7 FORMAT(2X,'IMPACTOR DIAMETER   D = ',F7.3
     A      /2X,'FRACTURE TOUGNESS GIC = ',F7.3,
     B      /2X,'% (0/45/90)-DEG PLIES =( ',F5.0,'/',F5.0,'/',F5.0,')'/)
      IF(ID.EQ.1.OR.ID.GT.3) WRITE(*,13)
      IF(ID.EQ.2) WRITE(*,14)
      IF(ID.EQ.3) WRITE(*,15)
   13 FORMAT(2X,'SINGLE MID-BAY IMPACT')
   14 FORMAT(2X,'TWO BAYS MID-BAY IMPACTS')
   15 FORMAT(2X,'SINGLE NEAR SPAR IMPACT')
      PE = ESK/EL
      C1 = 0.54671*(PE**0.52647)
  101 WRITE(*,16) T,ESK
   16 FORMAT(2X,'SKIN THICKNESS = ',F12.4,' INCH',
     A/2X,'SKIN MODULUS = ',F9.4,' MSI'/)
      C3 = 0.499/(T**0.5056)
      TE = T*ESK
      SAE = TE*W+SN*AE
      IF(ID.EQ.2.OR.ID.EQ.3) GOTO 250
      IF(A1.LT.B) GOTO 151
      CON1 = TE*(A1-B+ALPHA*B*(1.+7.*B1/24.))
      GOTO 152
  151 CON1 = ALPHA*TE*(A1+B1*B*(1.-(B/(A1+B))**3.)/3.)
  152 CON2 = TE*B*(1.+ALPHA*(1.+7.*B1/24.))
```

```
      CON3 = A2*TE
      CON4 = SN*AE
      AI = AMIN1(A0,A1)
      FAC = CON1+CON2+CON3+CON4
      CONST = 1.+B1*B*(1.-(B/(B+AI))**3.)/(3.*AI)
      ELIM = EULT/(CONST*ALPHA)
      PFL = ELIM*FAC
      GOTO 100
  250 CON4 = SN*AE
      IF(A1.LT.B2) GOTO 251
      CON1 = TE*(A1-B2+ALPHA*B2*(1.+7.*B1/24.))
      GOTO 252
  251 CON1 = ALPHA*TE*(A1+B1*B2*(1.-(B2/(A1+B2))**3.)/3.)
  252 IF(A2.LT.B2) GOTO 253
      CON2 = TE*(A2-B2+ALPHA*B2*(1.+7.*B1/24.))
      GOTO 254
  253 CON2 = TE*ALPHA*(A2+B1*B2*(1.-(B2/(A2+B2))**3.)/3.)
  254 FAC = CON1+CON2+CON4
      AI = AMIN1(A0,A1,A2)
      CONST = 1.+B1*B2*(1.-(B2/(B2+AI))**3.)/(3.*AI)
      ELIM = EULT/(CONST*ALPHA)
      PFL = ELIM*FAC
  100 C5 = A4*(AK*E)**B4
      CTOT = C1*C2*C3*C4*C5*WE
      RESN = 1.0/(1.0+CTOT)
      RES = RESN*EULT
      PIF = SAE*RES
      ESP0 = PIF/FAC
      ESPA = ESP0*CONST*ALPHA
      ARE = 'YES'
      IF(ESPA.GE.EULT) ARE='NO '
      PFF = PIF
      IF(ESPA.LT.EULT) PFF=PFL
      EFF = PFF/SAE
      WRITE(*,9) E,RES,EFF,DUL
    9 FORMAT(2X,'ENERGY = ',F7.2,
     A/5X,'INITIAL FAILURE STRAIN = ',F12.0,
     B/5X,'FINAL FAILURE STRAIN =   ',F12.0,
     C/5X,'STRAIN AT DUL        =   ',F12.0)
      ALP = 12.0
      ALI = 1.0/12.0
      ALL = -ALOG(0.99)
      ALL = ALL**ALI
      BLL = -ALOG(0.90)
      BLL = BLL**ALI
C ASSUME STRENGTH ALPHA=12.0 AND SAMPLE SIZE N=15
      FACTR = 1.01116
      BIF = FACTR*RES
      ALLIF = BIF*ALL
      BLLIF = BIF*BLL
      BFF = FACTR*EFF
      ALLFF = BFF*ALL
```

```
      BLLFF = BFF*BLL
      ALLDIF = 1.50*ALLIF
      ALLDFF = 1.25*ALLFF
      ALLDUL = ALLDIF
      BLLDIF = 1.50*BLLIF
      BLLDFF = 1.25*BLLFF
      BLLDUL = BLLDIF
      IF(ALLDFF.LT.ALLDIF) ALLDUL = ALLDFF
      IF(BLLDFF.LT.BLLDIF) BLLDUL = BLLDFF
      AMS = ALLFF/DUL-1.0
      BMS = BLLFF/DUL-1.0
      WRITE(*,31)
      WRITE(*,10) BLLFF,BMS,ALLFF,AMS
      AMS = ALLDFF/DUL-1.0
      BMS = BLLDFF/DUL-1.0
      WRITE(*,32)
      WRITE(*,10) BLLDFF,BMS,ALLDFF,AMS
      AMS = ALLDUL/DUL-1.0
      BMS = BLLDUL/DUL-1.0
      WRITE(*,33)
      WRITE(*,10) BLLDUL,BMS,ALLDUL,AMS
      AMS = ALLIF/DUL-1.0
      BMS = BLLIF/DUL-1.0
      WRITE(*,34)
      WRITE(*,10) BLLIF,BMS,ALLIF,AMS
   10 FORMAT(5X,'B-BASIS ALLOWABLE STRAIN = ',F12.0,2X,'M.S. = ',F7.2
     A      /5X,'A-BASIS ALLOWABLE STRAIN = ',F12.0,2X,'M.S. = ',F7.2)
   31 FORMAT(2X,'FOR DAMAGE TOLERANCE DESIGN REQUIREMENT NO. 1',
     A      /2X,'NO CATASTROPHIC STRUCTURAL FAILURE AT DUL')
   32 FORMAT(2X,'FOR DAMAGE TOLERANCE DESIGN REQUIREMANT NO. 2',
     A      /2X,'NO CATASTROPHIC STRUCTURAL FAILURE AT MSL=1.2DLL')
   33 FORMAT(2X,'FOR DAMAGE TOLERANCE DESIGN REQUIREMANT NO. 3',
     A      /2X,'NO INITIAL FAILURE AT DLL AND NO CATASTROPHIC '
     B      /2X,'STRUCTURAL FAILURE AT MSL')
   34 FORMAT(2X,'FOR DAMAGE TOLERANCE DESIGN REQUIREMANT NO. 4',
     A      /2X,'NO INITIAL/LOCAL FAILURE AT DLL')
      PDULI = DUL/BIF
      PDULI = -PDULI**ALP
      PDULI = EXP(PDULI)
      PDULF = DUL/BFF
      PDULF = -PDULF**ALP
      PDULF = EXP(PDULF)
      PDLLI = DUL/(1.5*BIF)
      PDLLI = -PDLLI**ALP
      PDLLI = EXP(PDLLI)
      PDLLF = DUL/(1.5*BFF)
      PDLLF = -PDLLF**ALP
      PDLLF = EXP(PDLLF)
      PMSLI = DUL/(1.25*BIF)
      PMSLI = -PMSLI**ALP
      PMSLI = EXP(PMSLI)
      PMSLF = DUL/(1.25*BFF)
```

```
      PMSLF = -PMSLF**ALP
      PMSLF = EXP(PMSLF)
      WRITE(*,312) PDULI,PDULF,PMSLI,PMSLF,PDLLI,PDLLF
  312 FORMAT(2X,'RELIABILITY AT DUL: IF = ',F12.5,2X,'FF = ',F12.5,
     +      /2X,'RELIABILITY AT MSL: IF = ',F12.5,2X,'FF = ',F12.5,
     +      /2X,'RELIABILITY AT DLL: IF = ',F12.5,2X,'FF = ',F12.5)
  110 STOP
      END
      SUBROUTINE LAME(ZERO,Z45,Z90,EL,ET,GLT,PNU,EX)
      PI = 3.141592654
      PI2 = PI*PI
      P2 = PNU*PNU
      QT = EL/(EL-P2*ET)
      Q11B = 0.0
      Q22B = 0.0
      Q12B = 0.0
      Q66B = 0.0
      Q11 = EL*QT
      Q22 = ET*QT
      Q12 = PNU*Q22
      Q66 = GLT
      QT1 = Q11+Q22
      QT2 = 4.*Q66
      QT3 = 2.*Q12
      U1 = (3.*QT1+QT3+QT2)/8.
      U2 = (Q11-Q22)/2.
      U3 = (QT1-QT3-QT2)/8.
      U4 = (QT1+3.*QT3-QT2)/8.
      U5 = (QT1-QT3+QT2)/8.
      U61 = (Q11-Q22+2.*Q66)/8.
      U62 = (Q12-Q22+2.*Q66)/8.
      TT = 100.
      K = 0
      TI = ZERO
      TH = 0.0
  100 K = K+1
      TH2 = 2.*TH
      TH4 = 4.*TH
      CO2 = COS(TH2)
      CO4 = COS(TH4)
      CS = 2.*SIN(TH2)+SIN(TH4)
      SC = 2.*SIN(TH2)-SIN(TH4)
      Q1 = U1+U2*CO2+U3*CO4
      Q2 = U1-U2*CO2+U3*CO4
      Q3 = U4-U3*CO4
      Q6 = U5-U3*CO4
      Q11B = Q11B+Q1*TI
      Q22B = Q22B+Q2*TI
      Q12B = Q12B+Q3*TI
      Q66B = Q66B+Q6*TI
      IF(K.EQ.3) GOTO 101
      IF(K.EQ.2) GOTO 102
```

```
      TH = 45.*PI/180.
      TI = Z45
      GOTO 100
  102 TH = 90.*PI/180.
      TI = Z90
      GOTO 100
  101 CONTINUE
      Q11B = Q11B/TT
      Q22B = Q22B/TT
      Q12B = Q12B/TT
      Q66B = Q66B/TT
      QB = Q11B*Q22B-Q12B*Q12B
      EX = QB/Q22B
      RETURN
      END
```

B.1.2 'PISTRE1' SMAPLE INPUT

```
 PLEASE ENTER PROBLEM TITLE
SAMPLE EXAMPLE FOR PROGRAM PISTRE1
 PLEASE INPUT % OF (0,45,90)-DEG. PLIES
40.0, 50.0, 10.0
 PLEASE INPUT SKIN THICKNESS
0.25
 PLEASE INPUT TOUGHNESS--GIC
0.75
 PLEASE INPUT IMPACT ENERGY
80.0
 PLEASE INPUT IMPACTOR DIAMETER
1.0
 PLEASE INPUT SKIN EL,ET,GLT AND NULT IN MSI
 AND ULTIMATE STRAIN IN MICRO-IN/IN
18.7, 1.9, 0.8, 0.3, 11000.0
 PLEASE INPUT NUMBER OF SPARS AND SPAR AE IN 10**6
3, 6.0
 PLEASE INPUT SPAR SPACING AND EDGE WIDTH A1,A2
7.0, 3.5, 3.5
 PLEASE INPUT EFFECTIVE ENERGY COEFFICIENT, AK
1.0
 PLEASE INPUT IMPACT EVENT CODE, ID
 ID = 1  SINGLE MID-BAY IMPACT
 ID = 2  TWO BAYS, MID-BAY IMPACTS
 ID = 3  SINGLE NEAR SPAR IMPACT
1
 PLEASE INPUT DUL STRAIN
3000.0
```

B.1.3 'PISTRE1' SAMPLE OUTPUT

```
 SAMPLE EXAMPLE FOR PROGRAM PISTRE1
 IMPACTOR DIAMETER   D =    1.000
 FRACTURE TOUGNESS GIC =     .750
 % (0/45/90)-DEG PLIES =(    40./  50./  10.)

 SINGLE MID-BAY IMPACT
 SKIN THICKNESS =         .2500 INCH
 SKIN MODULUS =     9.6900 MSI

 ENERGY =    80.00
    INITIAL FAILURE STRAIN =          2673.
    FINAL FAILURE STRAIN =            3435.
    STRAIN AT DUL        =            3000.
 FOR DAMAGE TOLERANCE DESIGN REQUIREMENT NO. 1
 NO CATASTROPHIC STRUCTURAL FAILURE AT DUL
    B-BASIS ALLOWABLE STRAIN =          2880.  M.S. =     -.04
    A-BASIS ALLOWABLE STRAIN =          2367.  M.S. =     -.21
 FOR DAMAGE TOLERANCE DESIGN REQUIREMANT NO. 2
 NO CATASTROPHIC STRUCTURAL FAILURE AT MSL=1.2DLL
    B-BASIS ALLOWABLE STRAIN =          3599.  M.S. =      .20
    A-BASIS ALLOWABLE STRAIN =          2959.  M.S. =     -.01
 FOR DAMAGE TOLERANCE DESIGN REQUIREMANT NO. 3
 NO INITIAL FAILURE AT DLL AND NO CATASTROPHIC
 STRUCTURAL FAILURE AT MSL
    B-BASIS ALLOWABLE STRAIN =          3361.  M.S. =      .12
    A-BASIS ALLOWABLE STRAIN =          2764.  M.S. =     -.08
 FOR DAMAGE TOLERANCE DESIGN REQUIREMANT NO. 4
 NO INITIAL/LOCAL FAILURE AT DLL
    B-BASIS ALLOWABLE STRAIN =          2241.  M.S. =     -.25
    A-BASIS ALLOWABLE STRAIN =          1842.  M.S. =     -.39
 RELIABILITY AT DUL: IF =        .03050   FF =         .84175
 RELIABILITY AT MSL: IF =        .78676   FF =         .98823
 RELIABILITY AT DLL: IF =        .97346   FF =         .99867
Stop - Program terminated.
```

B.2 PROGRAM 'PISTRE2'

Program PISTRE2 (Post-Impact STructural REliability) computes the reliability of a composite structure exposed to a low-velocity impact threat. The impact threat is described by a probabilistic distribution using a Weibull model. The structural reliability, at a 95% confidence level, is computed by numerical integration. In addition, the A- and B-basis design allowables and margins of safety are also determined for four different damage tolerance design requirements.

The required input to PISTRE2 are:

1. A 72-character problem title (INAME).
2. Impact threat distribution parameters:
   Modal impact energy in ft-lb (XM),
   Impact energy with remote probabity of occurrence in ft-lb (XP),
   Probability associated with XP (P).
3. Skin properties and impact parameters:
   Percents of 0-, 45-, 90-degree plies of the skin laminate (ZERO, Z45, Z90),
   Skin thickness and impactor diameter in inch (T,D),
   Lamina properties and ultimate strain (EL, ET, GLT, PNU,EULT),
   EL is the longitudinal Young's modulus in MSI,
   ET is the transeverse Young's modulus in MSI,
   GLT is the in-plane shear modulus in MSI,
   PNU or NULT is the in-plane Poisson's ratio,
   EULT is the failure strain of the undamaged laminate in micro-in/in,
   Fracture toughness of the skin material in in-lb/in**2 and effective energy coefficient (GIC, AK),
   Post-impact Strength scatter parameters (ALIP, GAM)
   ALIP is the Weibull shape parameter and GAM is the value of the Gamma function (enter 0.0, 0.0 for default values of ALIP=12 and GAM=0.95831).
4. Number of spars and spar stiffness (AE) in 10**6 lb. (NSP, AE).
5. Spar spacing of the impacted bay and edge width of the adjacent bays in inch (B2, A1, A2).
6. Impact event code (ID).
7. Post-impact structural strength scatter parameters (ALIS, GAMS)
   ALIS is the Weibull shape parameter and GAMS is the value of the Gamma function (enter 0.0, 0.0 for default values of ALIS=15 and GAMS=0.96568).
8. Strain at design ultimate load in micro-in/in (DUL).

B.2.1 'PISTRE2' LISTING

```
C*****************************************************************
C  PROGRAM 'PISTRE2' (Post-Impact STructural REliability, version 2)   *
C  WAS DEVELOPED BY NORTHROP AIRCRAFT DIVISION UNDER NADC/FAA          *
C  CONTRACT NO. N62269-87-C-0259, 'ADVANCED CERTIFICATION METHODOLOGY  *
C  FOR COMPOSITE STRUCTURES'.                                          *
C  THE PROGRAM COMPUTES THE STRUCTURAL RELIABILITY OF COMPOSITE        *
C  STRUCTURES EXPOSED TO LOW-VELOCITY IMPACT THREATS. THE IMPACT THREAT*
C  IS DESCRIBED BY A PROBABILISTIC DISTRIBUTION USING A WEIBULL MODEL. *
C  THE STRUCTURAL RELIABILITY, AT 95% CONFIDENCE, IS COMPUTED BY       *
C  NUMERICAL INTEGRATION. IN ADDITION, THE A- AND B-BASIS DESIGN       *
C  ALLOWABLES AND MARGINS OF SAFETY AT DUL ARE DETERMINED FOR FOUR     *
C  DIFFERENT DAMAGE TOLERANCE DESIGN REQUIREMENTS.                     *
C  THE REQUIRED INPUTS TO THE PROGRAM ARE: IMPACT THREAT DESCRIPTIONS, *
C  LAMINA PROPERTIES, LAMINATE LAYUP, STRUCTURAL CONFIGURATION, STRAIN *
C  AT DUL, POST-IMPACT STRENGTH SCATTERS.                              *
C*****************************************************************

      IMPLICIT REAL*8(A-H,O-Z)
      DIMENSION INAME(18)
      WRITE(*,18)
      READ(*,19) INAME
   18 FORMAT(2X,'PLEASE ENTER PROBLEM TITLE')
   19 FORMAT(18A4)
      WRITE(*,1)
    1 FORMAT(2X,'PLEASE ENTER IMPACT THREAT DISTRIBUTION PARAMETERS:')
      WRITE(*,2)
    2 FORMAT(5X,'MODAL ENERGY')
      READ(*,*) XM
      WRITE(*,3)
    3 FORMAT(5X,'ENERGY LEVEL WITH LOW PROBABILITY--XP')
      READ(*,*) XP
      WRITE(*,4)
    4 FORMAT(5X,'PROBABILITY AT ENERGY LEVEL XP')
      READ(*,*) P
      WRITE(*,5)
    5 FORMAT(2X,'PLEASE ENTER IMPACT PARAMETERS:')
      WRITE(*,6)
    6 FORMAT(5X,'LAMINATE LAYUP IN % OF (0/45/90)-DEG PLIES')
      READ(*,*) ZERO,Z45,Z90
      WRITE(*,7)
    7 FORMAT(5X,'LAMINATE THICKNESS AND IMPACTOR DIAMETER')
      READ(*,*) T,D
      WRITE(*,8)
    8 FORMAT(5X,'LAMINA EL,ET,GLT IN MSI AND NULT',
     A/5X,'AND ULTIMATE STRAIN IN MICRO-IN/IN')
      READ(*,*)EL,ET,GLT,PNU,EULT
      WRITE(*,9)
    9 FORMAT(5X,'MATERIAL GIC AND SUPPORT COEFF.--AK')
      READ(*,*) GIC,AK
      WRITE(*,10)
   10 FORMAT(5X,'POST-IMPACT STRENGTH ALPHA AND GAMMA',
```

```
     A       /5X,'ENTER 0.0,0.0 FOR DEFAULT VALUES')
      READ(*,*) ALIP,GAM
      IF(ALIP.EQ.0.0) ALIP = 12.0D0
      IF(GAM.EQ.0.0) GAM = 0.95831D0
      WRITE(*,303)
  303 FORMAT(2X,'PLEASE ENTER NUMBER OF SPARS AND SPAR AE IN 10**6')
      READ(*,*) NSP,AE
      SN = NSP
      WRITE(*,304)
  304 FORMAT(2X,'PLEASE ENTER SPAR SPACING AND EDGE DISTANCE A1, A2')
      READ(*,*) B2,A1,A2
      B = B2/2.0D0
      B1 = 6.54319D0
      AREST = 0.71257D0
      W = A1+A2+2.0D0*B2
      WF = 2.0D0*(A1+B)
      WR = 1.0D0-D/WF
      A0 = 1.31616D0
      WRITE(*,306)
  306 FORMAT(2X,'PLEASE ENTER IMPACT EVENT CODE, ID',
     A/4X,'ID = 1  FOR SINGLE MID-BAY IMPACT',
     B/4X,'ID = 2  FOR MID-BAY IMPACTS ON TWO ADJACENT BAYS',
     C/4X,'ID = 3  FOR SINGLE NEAR SPAR IMPACT')
      READ(*,*) ID
      WRITE(*,307)
  307 FORMAT(2X,'PLEASE ENTER POST-IMPACT STRENGTH ALPHA AND GAMMA',
     A/2X,'FOR BUILT-UP STRUCTURE, ENTER 0., 0. FOR DEFAULT VALUES')
      READ(*,*) ALIS,GAMS
      IF(ALIS.EQ.0.0) ALIS = 15.0D0
      IF(GAMS.EQ.0.0) GAMS = 0.96568D0
      WRITE(*,20)
   20 FORMAT(2X,'PLEASE ENTER DUL STRAIN')
      READ(*,*) DUL
      CHI = 1.4591D0
      TEST = 1.0D-6
      AL1 = 2.0D0
      AA = -DLOG(P)
      XR = XM/XP
      XRL = DLOG(XR)
  101 RAT = (AL1-1.0D0)/(AL1*AA)
      RA = DLOG(RAT)
      AL2 = RA/XRL
      ERR = AL2/AL1-1.0D0
      ERR = DABS(ERR)
      IF(ERR.LT.TEST)GOTO 100
      AL1 = (AL1+AL2)/2.0D0
      IF(AL1.LE.1.0D0) GOTO 110
      GOTO 101
  110 AL0 = 2.0D0
      DA = 1.0D-1
      DRR = 1.0D0
  113 F = (AL0-1.0D0)/(AL0*AA)
```

```
      FR = F**(1.0D0/AL0)
      R = FR/XR
      DR = R-1.0D0
      ADR = DABS(DR)
      IF(ADR.LT.TEST) GOTO 112
      ADR = DR/DRR
      IF(ADR.LT.0.0D0) DA=DA/2.0D0
      DRR = DR
      IF(DR.GT.0.0D0) GOTO 114
      AL0 = AL0+DA
      GOTO 113
  114 AL0 = AL0-DA
      AL01 = ABS(AL0-1.0D0)
      IF(AL01.LT.TEST) GOTO 115
      GOTO 116
  115 DA = DA/2.0D0
      AL0 = AL0+DA
  116 GOTO 113
  112 AL = AL0
      GOTO 111
  100 AL = (AL1+AL2)/2.0D0
  111 BB = AA**(1.0D0/AL)
      BET = XP/BB
      WRITE(*,36) INAME
   36 FORMAT(//2X,18A4,/)
      WRITE(*,12) AL,BET,XM,XP,P
   12 FORMAT(2X,'IMPACT THREAT DISTRIBUTION WEIBULL PARAMETERS:'
     A/5X,'ALPHA = ',F9.4
     B/5X,'BETA  = ',F9.4
     C/5X,'MODAL IMPACT ENERGY XM = ',F5.1
     D/5X,'AT ENERGY XP =',F7.1
     E/5X,'THE PROBABILITY OF OCCURRENCE P =',F12.6)
      CALL LAME(ZERO,Z45,Z90,EL,ET,GLT,PNU,ESK)
      WRITE(*,15) ZERO,Z45,Z90,ESK,EULT
      WRITE(*,16) T,D
      WRITE(*,17) GIC,AK,ALIP
   15 FORMAT(5X,'LAMINATE LAYUP:  (',F3.0,'/',F3.0,'/',F3.0,')'
     A/5X,'MODULUS ESK = ',F9.3
     B/5X,'ULTIMATE STRAIN EULT = ',F10.0)
   16 FORMAT(5X,'THICKNESS T = ',F10.3
     B/5X,'IMPACTOR DIAMETER D = ',F10.2)
   17 FORMAT(5X,'FRACTURE TOUGHNESS GIC = ',F10.3
     A/5X,'SUPPORT COEFFICIENT AK = ',F10.2
     B/5X,'POST-IMPACT STRENGTH ALPHA = ',F10.3)
      PE = ESK/EL
      C1 = 5.4671D-1*(PE**5.2647D-1)
      C2 = 3.707D0
      C3 = 4.99D-1/(T**5.056D-1)
      C4 = 1.0D0
      GC = GIC
      IF(GIC.GT.5.554D0) GC=5.554D0
      A4 = 7.486D-2/GIC+1.448D-2
```

```
      B4 = (-9.81D-3*GC+1.0897D-1)*GC+4.3339D-1
      WE = (2.0D0+WR**3.0D0)/WR-1.0D0
      TOT = C1*C2*C3*C4*WE
C      WRITE(*,*) TOT
      TE = T*ESK
      SAE = TE*W+SN*AE
      IF(ID.EQ.2.OR.ID.EQ.3) GOTO 350
      IF(A1.LT.B) GOTO 351
      CON1 = TE*(A1-B+AREST*B*(1.0D0+7.0D0*B1/24.0D0))
      GOTO 352
  351 CON1 = AREST*TE*(A1+B1*B*(1.0D0-(B/(A1+B))**3.0D0)/3.0D0)
  352 CON2 = TE*B*(1.0D0+AREST*(1.0D0+7.0D0*B1/24.0D0))
      CON3 = A2*TE
      CON4 = SN*AE
      AI = DMIN1(A0,A1)
      FAC = CON1+CON2+CON3+CON4
C      WRITE(*,*) FAC
      CONST = 1.0D0+B1*B*(1.0D0-(B/(B+AI))**3.0D0)/(3.0D0*AI)
      ELIM = EULT/(CONST*AREST)
      PFL = ELIM*FAC
      GOTO 360
  350 CON4 = SN*AE
      IF(A1.LT.B2) GOTO 353
      CON1 = TE*(A1-B2+AREST*B2*(1.0D0+7.0D0*B1/24.0D0))
      GOTO 354
  353 CON1 = AREST*TE*(A1+B1*B2*(1.0D0-(B2/(A1+B2))**3.0D0)/3.0D0)
  354 IF(A2.LT.B2) GOTO 355
      CON2 = TE*(A2-B2+AREST*B2*(1.0D0-7.0D0*B1/24.0D0))
      GOTO 356
  355 CON2 = TE*AREST*(A2+B1*B2*(1.0D0-(B2/(A2+B2))**3.0D0)/3.0D0)
  356 FAC = CON1+CON2+CON4
      AI = DMIN1(A0,A1,A2)
      CONST = 1.0D0+B1*B2*(1.0D0-(B2/(B2+AI))**3.0D0)/(3.0D0*AI)
      ELIM = EULT/(CONST*AREST)
      PFL = ELIM*FAC
  360 EFF = PFL/SAE
      WRITE(*,361) EFF
  361 FORMAT(2X,'FINAL STRUCTURAL FAILURE STRAIN GT ',F8.0)
      DMS = DUL/1.25D0
      DLL = DUL/1.50D0
      WRITE(*,362) DUL
  362 FORMAT(2X,'STRAIN AT DUL = ',F12.0)
      BETSC = EFF/GAMS
      BETSL = BETSC/(CHI**(1.0D0/ALIS))
      ES = 0.15D0*EULT
      DES = 1.0D+2
      IDS = ES/DES
      ES = IDS*DES
      MDLL = DLL/DES
      IF(ES.LE.DLL) ES = (MDLL-2)*DES
      EMAX = 0.8D0*EULT
      AVAL = 0.99D0
```

```
      BVAL = 0.90D0
      IKMA = 0
      IKMB = 0
      IKSA = 0
      IKSB = 0
      IDUL = 0
      IMSL = 0
      IDLL = 0
      WRITE(*,14)
   14 FORMAT(/8X,'STRAIN',4X,'REL.(COUPON)',4X,'REL.(STRUCTURE)'
     A/8X,'----------------------------------------',/)
      DEN = 2.0D0
      DEN2 = 1.0D0
  105 SUM = 0.0D0
      SUML = 0.0D0
      SUS = 0.0D0
      SUSL = 0.0D0
      PMS =  DEXP(-(ES/BETSC)**ALIS)
      PMLS = DEXP(-(ES/BETSL)**ALIS)
      EN = 1.0D0
      EN1 = EN-DEN2
      PEN1 = DEXP(-(EN1/BET)**AL)
  103 EN2 = EN+DEN2
      PEN2 = DEXP(-(EN2/BET)**AL)
      EEF = AK*EN
      C5 = A4*(EEF**B4)
      CTOT = C5*TOT
      RES = 1.0D0/(1.0D0+CTOT)
      ESM = RES*EULT
      BETS = ESM/GAM
      BETL = BETS/(CHI**(1.0D0/ALIP))
      PM = DEXP(-(ES/BETS)**ALIP)
      PML = DEXP(-(ES/BETL)**ALIP)
      DELTP = PM*(PEN1-PEN2)
      DELTL = PML*(PEN1-PEN2)
      DELS = DELTP
      IF(EFF.GT.ESM) DELS=PMS*(PEN1-PEN2)
      DELSL = DELTL
      IF(EFF.GT.ESM) DELSL=PMLS*(PEN1-PEN2)
      SUM = SUM+DELTP
      SUML = SUML+DELTL
      SUS = SUS+DELS
      SUSL = SUSL+DELSL
      IF(DELS.LT.TEST.AND.DELSL.LT.TEST) GOTO 102
      EN = EN+DEN
      PEN1 = PEN2
      GOTO 103
  102 WRITE(*,13) ES,SUML,SUSL
   13 FORMAT(5X,F10.0,5X,F9.6,10X,F9.6)
      IF(SUML.GE.AVAL) ECA = ES
      IF(SUML.GE.AVAL) PECA = SUML
      IF(SUSL.GE.AVAL) ESA = ES
```

```
      IF(SUSL.GE.AVAL) PESA = SUSL
      IF(SUML.GE.BVAL) ECB = ES
      IF(SUML.GE.BVAL) PECB = SUML
      IF(SUSL.GE.BVAL) ESB = ES
      IF(SUSL.GE.BVAL) PESB = SUSL
      IF(SUML.LT.AVAL) IKMA = IKMA+1
      IF(SUSL.LT.AVAL) IKSA = IKSA+1
      IF(SUML.LT.BVAL) IKMB = IKMB+1
      IF(SUSL.LT.BVAL) IKSB = IKSB+1
      IF(IKMA.EQ.1) ECA1 = ES
      IF(IKMA.EQ.1) PECA1 = SUML
      IF(IKSA.EQ.1) ESA1 = ES
      IF(IKSA.EQ.1) PESA1 = SUSL
      IF(IKMB.EQ.1) ECB1 = ES
      IF(IKMB.EQ.1) PECB1 = SUML
      IF(IKSB.EQ.1) ESB1 = ES
      IF(IKSB.EQ.1) PESB1 = SUSL
      IF(ES.LT.DLL) GOTO 51
      IDLL = IDLL+1
      IF(ES.LT.DMS) GOTO 52
      IMSL = IMSL+1
      IF(ES.LT.DUL) GOTO 53
      IDUL = IDUL+1
      GOTO 50
   51 PDLLI = SUML
      PDLLF = SUSL
      DLL1 = ES
      GOTO 50
   52 PMSLI = SUML
      PMSLF = SUSL
      DMS1 = ES
      GOTO 50
   53 PDULI = SUML
      PDULF = SUSL
      DUL1 = ES
   50 IF(IDLL.EQ.1) GOTO 61
      IF(IMSL.EQ.1) GOTO 62
      IF(IDUL.EQ.1) GOTO 63
      GOTO 60
   61 PDLLI1 = SUML
      PDLLF1 = SUSL
      DLL2 = ES
      GOTO 60
   62 PMSLI1 = SUML
      PMSLF1 = SUSL
      DMS2 = ES
      GOTO 60
   63 PDULI1 = SUML
      PDULF1 = SUSL
      DUL2 = ES
   60 CONTINUE
      IF(ES.GT.EMAX) GOTO 104
```

```
      ES = ES+DES
      GOTO 105
  104 CONTINUE
      ALLIF = ECA+DES*(AVAL-PECA)/(PECA1-PECA)
      ALLFF = ESA+DES*(AVAL-PESA)/(PESA1-PESA)
      BLLIF = ECB+DES*(BVAL-PECB)/(PECB1-PECB)
      BLLFF = ESB+DES*(BVAL-PESB)/(PESB1-PESB)
      ALLDIF = 1.50D0*ALLIF
      ALLDFF = 1.25D0*ALLFF
      ALLDUL = ALLDIF
      BLLDIF = 1.50D0*BLLIF
      BLLDFF = 1.25D0*BLLFF
      BLLDUL = BLLDIF
      IF(ALLDFF.LT.ALLDIF) ALLDUL = ALLDFF
      IF(BLLDFF.LT.BLLDIF) BLLDUL = BLLDFF
      AMS = ALLFF/DUL-1.0D0
      BMS = BLLFF/DUL-1.0D0
      WRITE(*,31)
      WRITE(*,30) BLLFF,BMS,ALLFF,AMS
      AMS = ALLDFF/DUL-1.0D0
      BMS = BLLDFF/DUL-1.0D0
      WRITE(*,32)
      WRITE(*,30) BLLDFF,BMS,ALLDFF,AMS
      AMS = ALLDUL/DUL-1.0D0
      BMS = BLLDUL/DUL-1.0D0
      WRITE(*,33)
      WRITE(*,30) BLLDUL,BMS,ALLDUL,AMS
      AMS = ALLIF/DUL-1.0D0
      BMS = BLLIF/DUL-1.0D0
      WRITE(*,34)
      WRITE(*,30) BLLIF,BMS,ALLIF,AMS
   30 FORMAT(5X,'B-BASIS ALLOWABLE STRAIN = ',F12.0,2X,'M.S. = ',F7.2
     A        /5X,'A-BASIS ALLOWABLE STRAIN = ',F12.0,2X,'M.S. = ',F7.2)
   31 FORMAT(//2X,'FOR DAMAGE TOLERANCE DESIGN REQUIREMENT NO. 1',
     A       /2X,'NO CATASTROPHIC STRUCTURAL FAILURE AT DUL')
   32 FORMAT(/2X,'FOR DAMAGE TOLERANCE DESIGN REQUIREMENT NO. 2',
     A       /2X,'NO CATASTROPHIC STRUCTURAL FAILURE AT MSL=1.2DLL')
   33 FORMAT(/2X,'FOR DAMAGE TOLERANCE DESIGN REQUIREMENT NO. 3',
     A       /2X,'NO INITIAL FAILURE AT DLL AND NO CATASTROPHIC '
     B       /2X,'STRUCTURAL FAILURE AT MSL')
   34 FORMAT(/2X,'FOR DAMAGE TOLERANCE DESIGN REQUIREMENT NO. 4',
     A       /2X,'NO INITIAL/LOCAL FAILURE AT DLL')
      RDLLI = PDLLI+(PDLLI1-PDLLI)*(DLL-DLL1)/DES
      RDLLF = PDLLF+(PDLLF1-PDLLF)*(DLL-DLL1)/DES
      RMSLI = PMSLI+(PMSLI1-PMSLI)*(DMS-DMS1)/DES
      RMSLF = PMSLF+(PMSLF1-PMSLF)*(DMS-DMS1)/DES
      RDULI = PDULI+(PDULI1-PDULI)*(DUL-DUL1)/DES
      RDULF = PDULF+(PDULF1-PDULF)*(DUL-DUL1)/DES
      WRITE(*,35) RDULI,RDULF,RMSLI,RMSLF,RDLLI,RDLLF
   35 FORMAT(/2X,'RELIABILITY AT DUL:  IF = ',F12.5,2X,'FF = ',F12.5,
     A       /2X,'RELIABILITY AT MSL:  IF = ',F12.5,2X,'FF = ',F12.5,
     B       /2X,'RELIABILITY AT DLL:  IF = ',F12.5,2X,'FF = ',F12.5)
```

```
      STOP
      END
      SUBROUTINE LAME(ZERO,Z45,Z90,EL,ET,GLT,PNU,EX)
      IMPLICIT REAL*8(A-H,O-Z)
      PI = 4.0D0*DATAN(1.0D0)
      PI2 = PI*PI
      P2 = PNU*PNU
      QT = EL/(EL-P2*ET)
      Q11B = 0.0D0
      Q22B = 0.0D0
      Q12B = 0.0D0
      Q66B = 0.0D0
      Q11 = EL*QT
      Q22 = ET*QT
      Q12 = PNU*Q22
      Q66 = GLT
      QT1 = Q11+Q22
      QT2 = 4.0D0*Q66
      QT3 = 2.0D0*Q12
      U1 = (3.0D0*QT1+QT3+QT2)/8.0D0
      U2 = (Q11-Q22)/2.0D0
      U3 = (QT1-QT3-QT2)/8.0D0
      U4 = (QT1+3.0D0*QT3-QT2)/8.0D0
      U5 = (QT1-QT3+QT2)/8.0D0
      U61 = (Q11-Q22+2.*Q66)/8.0D0
      U62 = (Q12-Q22+2.*Q66)/8.0D0
      TT = 100.0D0
      K = 0
      TI = ZERO
      TH = 0.0D0
  100 K = K+1
      TH2 = 2.0D0*TH
      TH4 = 4.0D0*TH
      CO2 = DCOS(TH2)
      CO4 = DCOS(TH4)
      CS = 2.0D0*DSIN(TH2)+DSIN(TH4)
      SC = 2.0D0*DSIN(TH2)-DSIN(TH4)
      Q1 = U1+U2*CO2+U3*CO4
      Q2 = U1-U2*CO2+U3*CO4
      Q3 = U4-U3*CO4
      Q6 = U5-U3*CO4
      Q11B = Q11B+Q1*TI
      Q22B = Q22B+Q2*TI
      Q12B = Q12B+Q3*TI
      Q66B = Q66B+Q6*TI
      IF(K.EQ.3) GOTO 101
      IF(K.EQ.2) GOTO 102
      TH = 45.0D0*PI/180.0D0
      TI = Z45
      GOTO 100
  102 TH = 90.0D0*PI/180.0D0
      TI = Z90
```

```
      GOTO 100
  101 CONTINUE
      Q11B = Q11B/TT
      Q22B = Q22B/TT
      Q12B = Q12B/TT
      Q66B = Q66B/TT
      QB = Q11B*Q22B-Q12B*Q12B
      EX = QB/Q22B
      RETURN
      END
```

B.2.2 'PISTRE2' SAMPLE INPUT

```
 PLEASE ENTER PROBLEM TITLE
F/A-18A UPPER INBOARD WING SKIN, MEDIUM THREAT, REGION 1
 PLEASE ENTER IMPACT THREAT DISTRIBUTION PARAMETERS:
    MODAL ENERGY
6.0
    ENERGY LEVEL WITH LOW PROBABILITY--XP
100.0
    PROBABILITY AT ENERGY LEVEL XP
0.01
 PLEASE ENTER IMPACT PARAMETERS:
    LAMINATE LAYUP IN % OF (0/45/90)-DEG PLIES
47.0, 47.0, 6.0
    LAMINATE THICKNESS AND IMPACTOR DIAMETER
0.3586, 1.0
    LAMINA EL,ET,GLT IN MSI AND NULT
    AND ULTIMATE STRAIN IN MICRO-IN/IN
18.7, 1.9, 0.8, 0.3, 11000.0
    MATERIAL GIC AND SUPPORT COEFF.--AK
0.75, 1.0
    POST-IMPACT STRENGTH ALPHA AND GAMMA
    ENTER 0.0,0.0 FOR DEFAULT VALUES
12.0, 0.95831
 PLEASE ENTER NUMBER OF SPARS AND SPAR AE IN 10**6
3, 8.12
 PLEASE ENTER SPAR SPACING AND EDGE DISTANCE A1, A2
4.5, 0.5, 20.0
 PLEASE ENTER IMPACT EVENT CODE, ID
   ID = 1  FOR SINGLE MID-BAY IMPACT
   ID = 2  FOR MID-BAY IMPACTS ON TWO ADJACENT BAYS
   ID = 3  FOR SINGLE NEAR SPAR IMPACT
1
 PLEASE ENTER POST-IMPACT STRENGTH ALPHA AND GAMMA
 FOR BUILT-UP STRUCTURE, ENTER 0., 0. FOR DEFAULT VALUES
15.0, 0.96568
 PLEASE ENTER DUL STRAIN
2700.0
```

B.2.3 'PISTRE2' SAMPLE OUTPUT

```
F/A-18A UPPER INBOARD WING SKIN, MEDIUM THREAT, REGION 1

IMPACT THREAT DISTRIBUTION WEIBULL PARAMETERS:
   ALPHA =    1.1919
   BETA  =   27.7685
   MODAL IMPACT ENERGY XM =   6.0
   AT ENERGY XP =  100.0
   THE PROBABILITY OF OCCURRENCE P =     .010000
   LAMINATE LAYUP:  (47./47./ 6.)
   MODULUS ESK =    10.679
   ULTIMATE STRAIN EULT =     11000.
   THICKNESS T =       .359
   IMPACTOR DIAMETER D =       1.00
   FRACTURE TOUGHNESS GIC =       .750
   SUPPORT COEFFICIENT AK =      1.00
   POST-IMPACT STRENGTH ALPHA =     12.000
FINAL STRUCTURAL FAILURE STRAIN GT    2787.
STRAIN AT DUL =        2700.
```

STRAIN	REL.(COUPON)	REL.(STRUCTURE)
1600.	.999864	.999940
1700.	.999727	.999881
1800.	.999468	.999767
1900.	.999001	.999552
2000.	.998194	.999159
2100.	.996860	.998463
2200.	.994755	.997263
2300.	.991580	.995248
2400.	.986996	.991964
2500.	.980650	.986788
2600.	.972210	.978963
2700.	.961393	.967766
2800.	.947991	.952843
2900.	.931892	.934584
3000.	.913086	.913994
3100.	.891659	.891781
3200.	.867785	.867777
3300.	.841709	.841707
3400.	.813728	.813728
3500.	.784168	.784168
3600.	.753373	.753373
3700.	.721685	.721685
3800.	.689434	.689434
3900.	.656925	.656925
4000.	.624439	.624439
4100.	.592223	.592223
4200.	.560490	.560490
4300.	.529423	.529423

4400.	.499171	.499171
4500.	.469853	.469853
4600.	.441562	.441562
4700.	.414366	.414366
4800.	.388312	.388312
4900.	.363429	.363429
5000.	.339730	.339730
5100.	.317213	.317213
5200.	.295868	.295868
5300.	.275675	.275675
5400.	.256605	.256605
5500.	.238628	.238628
5600.	.221705	.221705
5700.	.205797	.205797
5800.	.190862	.190862
5900.	.176858	.176858
6000.	.163739	.163739
6100.	.151464	.151464
6200.	.139989	.139989
6300.	.129272	.129272
6400.	.119271	.119271
6500.	.109946	.109946
6600.	.101259	.101259
6700.	.093172	.093172
6800.	.085651	.085651
6900.	.078659	.078659
7000.	.072166	.072166
7100.	.066140	.066140
7200.	.060552	.060552
7300.	.055375	.055375
7400.	.050579	.050579
7500.	.046137	.046137
7600.	.042027	.042027
7700.	.038229	.038229
7800.	.034730	.034730
7900.	.031515	.031515
8000.	.028556	.028556
8100.	.025816	.025816
8200.	.023246	.023246
8300.	.020800	.020800
8400.	.018438	.018438
8500.	.016142	.016142
8600.	.013911	.013911
8700.	.011766	.011766
8800.	.009736	.009736
8900.	.007858	.007858

```
 FOR DAMAGE TOLERANCE DESIGN REQUIREMENT NO. 1
 NO CATASTROPHIC STRUCTURAL FAILURE AT DUL
    B-BASIS ALLOWABLE STRAIN =          3063.   M.S. =      .13
    A-BASIS ALLOWABLE STRAIN =          2438.   M.S. =     -.10

 FOR DAMAGE TOLERANCE DESIGN REQUIREMENT NO. 2
 NO CATASTROPHIC STRUCTURAL FAILURE AT MSL=1.2DLL
    B-BASIS ALLOWABLE STRAIN =          3829.   M.S. =      .42
    A-BASIS ALLOWABLE STRAIN =          3047.   M.S. =      .13

 FOR DAMAGE TOLERANCE DESIGN REQUIREMENT NO. 3
 NO INITIAL FAILURE AT DLL AND NO CATASTROPHIC
 STRUCTURAL FAILURE AT MSL
    B-BASIS ALLOWABLE STRAIN =          3829.   M.S. =      .42
    A-BASIS ALLOWABLE STRAIN =          3047.   M.S. =      .13

 FOR DAMAGE TOLERANCE DESIGN REQUIREMENT NO. 4
 NO INITIAL/LOCAL FAILURE AT DLL
    B-BASIS ALLOWABLE STRAIN =          3061.   M.S. =      .13
    A-BASIS ALLOWABLE STRAIN =          2334.   M.S. =     -.14

 RELIABILITY AT DUL:  IF =        .96139   FF =        .96777
 RELIABILITY AT MSL:  IF =        .99560   FF =        .99774
 RELIABILITY AT DLL:  IF =        .99947   FF =        .99977
Stop - Program terminated.
```

B.3 PROGRAM 'DABSR'

Program DABSR (Damage Area Based Structural Reliability) computes the structural reliability with a low-velocity impact damage. The damage is characterized by measured C-scan damage area. The progrom also computes the reliability at DUL, MSL and DLL for structure with a 2-inch diameter circular, or equivalent area, C-scan damage. The B- and A-basis critical damage areas at DUL, MSL and DLL are also given. Finally, the program computes the B- and A-basis design allowables for the 2.0-inch damage area design requirement.

The required input to DABSR are:

1. A 72-character problem title (INAME).
2. Compression strain at DUL in micro-in/in (ESP).
3. Material and impact parameters:
   Laminate layup in percent of 0-, 45-, and 90-degree plies (ZER0, Z45, Z90),
   Laminate thickness in inch (T),
   Lamina properties (EL, ET, GLT, PNU, EULT) (see PISTRE1),
   Material toughness in in-lb/in**2 (GIC),
   Post impact strength scatter parameter (ALPHA).
4. Number of spars and spar stiffness(AE) in 10**6 lb. (NSP, AE).
5. Spar spacing of the impacted bay and edge width of the adjacent bays in inch (B2, A1, A2).
6. Impact event code (ID).

B.3.1 'DABSR' LISTING

```
C*********************************************************************
C  PROGRAM 'DABSR'  (Damage Area Based Structural Reliability) WAS     *
C  DEVELOPED BY NORTHROP AIRCRAFT DIVISION UNDER NADC/FAA CONTRACT     *
C  NO. N62269-87-C-0259, 'ADVANCED CERTIFICATION METHODOLOGY FOR       *
C  COMPOSITE STRUCTURES'.                                              *
C  THE PROGRAM COMPUTES THE RELIABILITY OF COMPOSITE STRUCTURE WITH    *
C  LOW-VELOCITY IMPACT DAMAGE. THE DAMAGE IS CHARACTERIZED BY MEASURED *
C  C-SCAN AREA. THE RELIABILITY IS COMPUTED AT A GIVEN APPLIED         *
C  COMPRESSION STRAIN FOR DIFFERENT C-SCAN DAMAGE AREA. IN ADDITION,   *
C  CRITICAL DAMAGE AREA AT DUL, MSL AND DLL ARE COMPUTED AND THE DESIGN*
C  ALLOWABLES FOR A 2-INCH DIAMETER CIRCULAR DAMAGE ARE DETERMINED     *
C  THE REQUIRED INPUT TO THE PROGRAM ARE: STRAIN AT DUL, LAMINATE LAYUP*
C  LAMINATE PROPERTIES, AND STRUCTURAL CONFIGURATIONA.                 *
C*********************************************************************

      DIMENSION INAME(18)
      COMMON/GMA/BG(101),Y(101)
      COMMON/CHI/CHL(15)
      OPEN(5,FILE='PSI.DAT')
      READ(5,*) (BG(I),I=1,101)
      READ(5,*) (Y(I),I=1,101)
      READ(5,*) (CHL(I),I=1,15)
      PI = 4.0*ATAN(1.0)
      WRITE(*,18)
      READ(*,19) INAME
   18 FORMAT(2X,'PLEASE ENTER PROBLEM TITLE')
   19 FORMAT(18A4)
      WRITE(*,1)
    1 FORMAT(2X,'PLEASE ENTER COMPRESSION STRAIN AT DUL')
      READ(*,*) ESP
      WRITE(*,5)
    5 FORMAT(2X,'PLEASE ENTER IMPACT PARAMETERS:')
      WRITE(*,6)
    6 FORMAT(5X,'LAMINATE LAYUP IN % OF (0/45/90)-DEG PLIES')
      READ(*,*) ZERO,Z45,Z90
      WRITE(*,7)
    7 FORMAT(5X,'LAMINATE THICKNESS ')
      READ(*,*) T
      WRITE(*,8)
    8 FORMAT(5X,'LAMINA EL,ET,GLT IN MSI AND NULT',
     A/5X,'AND ULTIMATE STRAIN IN MICRO-IN/IN')
      READ(*,*)EL,ET,GLT,PNU,EULT
      WRITE(*,9)
    9 FORMAT(5X,'MATERIAL GIC ')
      READ(*,*) GIC
      WRITE(*,10)
   10 FORMAT(5X,'POST-IMPACT STRENGTH ALPHA ')
      READ(*,*) ALPHA
      N = 20
      WRITE(*,303)
```

```
303 FORMAT(2X,'PLEASE ENTER NUMBER OF SPARS AND SPAR AE IN 10**6')
    READ(*,*) NSP,AE
    SN = NSP
    WRITE(*,304)
304 FORMAT(2X,'PLEASE ENTER SPAR SPACING AND EDGE DISTANCE A1, A2')
    READ(*,*) B2,A1,A2
    B = B2/2.0
    ALIM = PI*B*B
    B1 = 6.54319
    AREST = 0.71257
    W = A1+A2+2.0*B2
    WF = 2.0*(A1+B)
    WR = 1.0
    A0 = 1.31616
    WRITE(*,306)
306 FORMAT(2X,'PLEASE ENTER IMPACT EVENT CODE, ID',
   A/4X,'ID = 1  FOR SINGLE MID-BAY IMPACT',
   B/4X,'ID = 2  FOR MID-BAY IMPACTS ON TWO ADJACENT BAYS',
   C/4X,'ID = 3  FOR SINGLE NEAR SPAR IMPACT')
    READ(*,*) ID
    CALL LAME(ZERO,Z45,Z90,EL,ET,GLT,PNU,ESK)
    WRITE(*,20) INAME
 20 FORMAT(//2X,18A4/)
    WRITE(*,15) ZERO,Z45,Z90,ESK,EULT
    WRITE(*,16) T
    WRITE(*,17) GIC,ALPHA
 15 FORMAT(5X,'LAMINATE LAYUP:  (',F3.0,'/',F3.0,'/',F3.0,')'
   A/5X,'MODULUS ESK = ',F9.3
   B/5X,'ULTIMATE STRAIN EULT = ',F10.0)
 16 FORMAT(5X,'THICKNESS T = ',F10.3)
 17 FORMAT(5X,'FRACTURE TOUGHNESS GIC = ',F10.3
   B/5X,'POST-IMPACT STRENGTH ALPHA = ',F10.3)
    PE = ESK/EL
    AM1 = 0.78937
    AM2 = 0.35139
    AM3 = -0.17517
    C1 = 0.54671*(PE**0.52647)
    C2 = 3.707
    C3 = 0.499/(T**0.5056)
    C4 = GIC**AM3
    TOT = C1*C2*C3*C4*AM1
    TE = T*ESK
    SAE = TE*W+SN*AE
    IF(ID.EQ.2.OR.ID.EQ.3) GOTO 350
    IF(A1.LT.B) GOTO 351
    CON1 = TE*(A1-B+AREST*B*(1.0+7.0*B1/24.0))
    GOTO 352
351 CON1 = AREST*TE*(A1+B1*B*(1.0-(B/(A1+B))**3.0)/3.0)
352 CON2 = TE*B*(1.0+AREST*(1.0+7.0*B1/24.0))
    CON3 = A2*TE
    CON4 = SN*AE
    AI = AMIN1(A0,A1)
```

```
      FAC = CON1+CON2+CON3+CON4
      CONST = 1.0+B1*B*(1.0-(B/(B+AI))**3.0)/(3.0*AI)
      ELIM = EULT/(CONST*AREST)
      PFL = ELIM*FAC
      GOTO 360
  350 CON4 = SN*AE
      IF(A1.LT.B2) GOTO 353
      CON1 = TE*(A1-B2+AREST*B2*(1.0+7.0*B1/24.0))
      GOTO 354
  353 CON1 = AREST*TE*(A1+B1*B2*(1.0-(B2/(A1+B2))**3.0)/3.0)
  354 IF(A2.LT.B2) GOTO 355
      CON2 = TE*(A2-B2+AREST*B2*(1.0-7.0*B1/24.0))
      GOTO 356
  355 CON2 = TE*AREST*(A2+B1*B2*(1.0-(B2/(A2+B2))**3.0)/3.0)
  356 FAC = CON1+CON2+CON4
      AI = AMIN1(A0,A1,A2)
      CONST = 1.0+B1*B2*(1.0-(B2/(B2+AI))**3.0)/(3.0*AI)
      ELIM = EULT/(CONST*AREST)
      PFL = ELIM*FAC
  360 EFF = PFL/SAE
      WRITE(*,361) EFF
      WRITE(*,362) ALIM
  361 FORMAT(2X,'FINAL STRUCTURAL FAILURE STRAIN GT ',F8.0)
  362 FORMAT(2X,'MAXIMUM WITHIN BAY DAMAGE AREA = ',F8.2)
      ALI = 1.0/ALPHA
      CHSQ = CHIS(N)
      ARM = 1.0+ALI
      GAM = GAMMA1(ARM)
      AC1 = 1.0/(GAM*(CHSQ**ALI))
      ARG = (ESP/(EFF*AC1))**ALPHA
      RELS = EXP(-ARG)
      WRITE(*,14)
   14 FORMAT(/8X,'DAM. AREA',4X,'REL.(COUPON)',4X,'REL.(STRUCTURE)'
     A/8X,'-----------------------------------------',/)
      AA = 0.0
      DA = 0.5
  105 BE = 1.0+TOT*(AA**AM2)
      EIF = EULT/BE
C      WRITE(*,*) EIF
      BET = AC1*EIF
      ARG = (ESP/BET)**ALPHA
C      WRITE(*,*) ARG
      RELL = EXP(-ARG)
      REFF = RELL
      IF(EFF.GE.EIF) REFF=RELS
      WRITE(*,13) AA,RELL,REFF
   13 FORMAT(7X,F10.2,7X,F9.6,10X,F9.6)
      AA = AA+DA
      IF(AA.GT.ALIM) GOTO 99
      IF(RELL.LT.0.0005) GOTO 99
      GOTO 105
   99 CONTINUE
```

```
C  TWO-INCH DIAMETER CIRCULAR DAMAGE
      AA = PI
      BE = 1.0+TOT*(AA**AM2)
      EIF = EULT/BE
      BET = AC1*EIF
      ARG = (ESP/BET)**ALPHA
      RELL = EXP(-ARG)
      REFF = RELL
      IF(EFF.GE.EIF) REFF = RELS
      DMSL = ESP/1.25
      ARG = (DMSL/(EFF*AC1))**ALPHA
      REMSL = EXP(-ARG)
      ARG = (DMSL/BET)**ALPHA
      REMSLI = EXP(-ARG)
      REMSLF = REMSLI
      IF(EFF.GE.EIF) REMSLF = REMSL
      DLL = ESP/1.50
      ARG = (DLL/(EFF*AC1))**ALPHA
      REDLL = EXP(-ARG)
      ARG = (DLL/BET)**ALPHA
      REDLLI = EXP(-ARG)
      REDLLF = REDLLI
      IF(EFF.GE.EIF) REDLLF = REDLL
      WRITE(*,21) RELL,REFF,REMSLI,REMSLF,REDLLI,REDLLF
   21 FORMAT(//2X,'STRUCTURAL RELIABILITY FOR 2.0-INCH DIA. DAMAGE',
     A       /5X,'AT DUL:  IF = ',F12.5,2X,'FF = ',F12.5,
     B       /5X,'AT MSL:  IF = ',F12.5,2X,'FF = ',F12.5,
     C       /5X,'AT DLL:  IF = ',F12.5,2X,'FF = ',F12.5)
      AVAL = (-ALOG(0.99))**ALI
      BVAL = (-ALOG(0.90))**ALI
      AESP = AVAL*EFF*AC1
      BESP = BVAL*EFF*AC1
      AM2I = 1.0/AM2
      AFACT = (EULT*AVAL*AC1/ESP-1.0)/TOT
      ACDUL = AFACT**AM2I
      IF(ACDUL.GE.ALIM) ACDUL = ALIM
      AFACT = (EULT*AVAL*AC1/DMSL-1.0)/TOT
      ACMSL = AFACT**AM2I
      IF(ACMSL.GE.ALIM) ACMSL = ALIM
      AFACT = (EULT*AVAL*AC1/DLL-1.0)/TOT
      ACDLL = AFACT**AM2I
      IF(ACDLL.GE.ALIM) ACDLL = ALIM
      BFACT = (EULT*BVAL*AC1/ESP-1.0)/TOT
      BCDUL = BFACT**AM2I
      IF(BCDUL.GE.ALIM) BCDUL = ALIM
      BFACT = (EULT*BVAL*AC1/DMSL-1.0)/TOT
      BCMSL = BFACT**AM2I
      IF(BCMSL.GE.ALIM) BCMSL = ALIM
      BFACT = (EULT*BVAL*AC1/DLL-1.0)/TOT
      BCDLL = BFACT**AM2I
      IF(BCDLL.GE.ALIM) BCDLL = ALIM
      ACDULF = ACDUL
```

```
      IF(ESP.LT.AESP) ACDULF = ALIM
      ACMSLF = ACMSL
      IF(DMSL.LT.AESP) ACMSLF = ALIM
      ACDLLF = ACDLL
      IF(DLL.LT.AESP) ACDLLF = ALIM
      BCDULF = BCDUL
      IF(ESP.LT.BESP) BCDULF = ALIM
      BCMSLF = BCMSL
      IF(DMSL.LT.BESP) BCMSLF = ALIM
      BCDLLF = BCDLL
      IF(DLL.LT.BESP) BCDLLF = ALIM
      WRITE(*,22)BCDUL,ACDUL,BCDULF,ACDULF,BCMSL,ACMSL,BCMSLF,ACMSLF,
     +BCDLL,ACDLL,BCDLLF,ACDLLF
   22 FORMAT(/2X,'CRITICAL DAMAGE AREA:',
     A/18X,'INITIAL FAILURE',10X,'FINAL FAILURE',
     B/14X,'B-BASIS',6X,'A-BASIS',6X,'B-BASIS',6X,'A-BASIS',
     C/2X,'AT DUL',4(3X,F10.2),/2X,'AT MSL',4(3X,F10.2),
     D/2X,'AT DLL',4(3X,F10.2))
      AESPI = BET*AVAL
      BESPI = BET*BVAL
      AESPF = AESPI
      IF(AESP.GT.AESPI) AESPF = AESP
      BESPF = BESPI
      IF(BESP.GT.BESPI) BESPF = BESP
      BMSI = BESPI/ESP-1.0
      BMSF = BESPF/ESP-1.0
      AMSI = AESPI/ESP-1.0
      AMSF = AESPF/ESP-1.0
      WRITE(*,23) BESPI,BMSI,BESPF,BMSF,AESPI,AMSI,AESPF,AMSF
   23 FORMAT(/2X,'2.0-INCH DIAMETER CIRCULAR DAMAGE TOLERANCE DESIGN REQ
     +UIREMENT:',
     A       /3X,'B-BASIS: INITIAL FAILURE ALLOWABLE = ',F10.0,2X,
     +'M.S. = ',F7.2,
     B       /12X,'FINAL FAILURE   ALLOWABLE = ',F10.0,2X,'M.S. = ',F7.2,
     C       /3X,'A-BASIS: INITIAL FAILURE ALLOWABLE = ',F10.0,2X,
     +'M.S. = ',F7.2,
     D       /12X,'FINAL FAILURE   ALLOWABLE = ',F10.0,2X,'M.S. = ',F7.2)
      STOP
      END
      SUBROUTINE LAME(ZERO,Z45,Z90,EL,ET,GLT,PNU,EX)
      PI = 4.0*ATAN(1.0)
      PI2 = PI*PI
      P2 = PNU*PNU
      QT = EL/(EL-P2*ET)
      Q11B = 0.00
      Q22B = 0.00
      Q12B = 0.00
      Q66B = 0.00
      Q11 = EL*QT
      Q22 = ET*QT
      Q12 = PNU*Q22
      Q66 = GLT
```

```
      QT1 = Q11+Q22
      QT2 = 4.00*Q66
      QT3 = 2.00*Q12
      U1 = (3.00*QT1+QT3+QT2)/8.00
      U2 = (Q11-Q22)/2.00
      U3 = (QT1-QT3-QT2)/8.00
      U4 = (QT1+3.00*QT3-QT2)/8.00
      U5 = (QT1-QT3+QT2)/8.00
      U61 = (Q11-Q22+2.*Q66)/8.00
      U62 = (Q12-Q22+2.*Q66)/8.00
      TT = 100.00
      K = 0
      TI = ZERO
      TH = 0.00
  100 K = K+1
      TH2 = 2.00*TH
      TH4 = 4.00*TH
      CO2 = COS(TH2)
      CO4 = COS(TH4)
      CS = 2.00*SIN(TH2)+SIN(TH4)
      SC = 2.00*SIN(TH2)-SIN(TH4)
      Q1 = U1+U2*CO2+U3*CO4
      Q2 = U1-U2*CO2+U3*CO4
      Q3 = U4-U3*CO4
      Q6 = U5-U3*CO4
      Q11B = Q11B+Q1*TI
      Q22B = Q22B+Q2*TI
      Q12B = Q12B+Q3*TI
      Q66B = Q66B+Q6*TI
      IF(K.EQ.3) GOTO 101
      IF(K.EQ.2) GOTO 102
      TH = 45.00*PI/180.00
      TI = Z45
      GOTO 100
  102 TH = 90.00*PI/180.00
      TI = Z90
      GOTO 100
  101 CONTINUE
      Q11B = Q11B/TT
      Q22B = Q22B/TT
      Q12B = Q12B/TT
      Q66B = Q66B/TT
      QB = Q11B*Q22B-Q12B*Q12B
      EX = QB/Q22B
      RETURN
      END
      FUNCTION CHIS(N)
      COMMON/CHI/CHL(15)
      AN = N
      BN = 2.0*AN
      IF(N.GE.15) GOTO 50
      CHIS = CHL(N)
```

```
      RETURN
   50 BE = 1.0/(9.0*AN)
      CL = 1.0-BE+1.645*SQRT(BE)
      CHIS = CL*CL*CL
      RETURN
      END
      FUNCTION GAMMA1(X)
      COMMON/GMA/B(101),Y(101)
      ARG = X
      A = 1.0
      IF(ARG.LT.1.0) GOTO 10
      IF(ARG.EQ.1.0) GOTO 110
      IF(ARG.EQ.2.0) GOTO 110
      IF(ARG.GT.2.0) GOTO 20
      GOTO 30
   10 A = A/ARG
      ARG = ARG+1.0
      IF(ARG.LT.1.0) GOTO 10
      IF(ARG.EQ.1.0) GOTO 110
      GOTO 30
   20 ARG = ARG-1.0
      IF(ARG.EQ.2.0) GOTO 110
      IF(ARG.GT.2.0) GOTO 20
   30 DO 40 I=1,101
      IF(B(I).GT.ARG) GOTO 50
   40 CONTINUE
   50 SLOP = (Y(I)-Y(I-1))/(B(I)-B(I-1))
      F = Y(I-1)+(ARG-B(I-1))*SLOP
      GOTO 60
  110 F = 1.0
   60 GAMMA1 = F*A
      RETURN
      END

DATA FILE 'PSI.DAT' FOR FILE #5
1.0,  1.01, 1.02, 1.03, 1.04, 1.05, 1.06, 1.07, 1.08, 1.09, 1.1,  1.11,
1.12, 1.13, 1.14, 1.15, 1.16, 1.17, 1.18, 1.19, 1.2,  1.21, 1.22, 1.23,
1.24, 1.25, 1.26, 1.27, 1.28, 1.29, 1.3,  1.31, 1.32, 1.33, 1.34, 1.35,
1.36, 1.37, 1.38, 1.39, 1.4,  1.41, 1.42, 1.43, 1.44, 1.45, 1.46, 1.47,
1.48, 1.49, 1.5,  1.51, 1.52, 1.53, 1.54, 1.55, 1.56, 1.57, 1.58, 1.59,
1.6,  1.61, 1.62, 1.63, 1.64, 1.65, 1.66, 1.67, 1.68, 1.69, 1.7,  1.71,
1.72, 1.73, 1.74, 1.75, 1.76, 1.77, 1.78, 1.79, 1.8,  1.81, 1.82, 1.83,
1.84, 1.85, 1.86, 1.87, 1.88, 1.89, 1.9,  1.91, 1.92, 1.93, 1.94, 1.95,
1.96, 1.97, 1.98, 1.99, 2.,
1.,     .99433, .98884, .98355, .97844, .9735,  .96874, .96415, .95973,
 .95546, .95135, .94739, .94359, .93993, .93642, .93304, .9298,  .9267,
 .92373, .92088, .91817, .91558, .91311, .91075, .90852, .9064,  .9044,
 .9025,  .90072, .89904, .89747, .896,   .89464, .89338, .89222, .89115,
 .89018, .88931, .88854, .88785, .88726, .88676, .88636, .88604, .8858,
 .88565, .8856,  .88563, .88575, .88595, .88623, .88659, .88704, .88757,
 .88818, .88887, .88964, .89049, .89142, .89243, .89352, .89468, .89592,
 .89724, .89864, .90012, .90167, .9033,  .905,   .90678, .90864, .91057,
```

```
 .91258, .91466, .91683, .91906, .92137, .92376, .92623, .92877, .93138,
 .93408, .93685, .93969, .94261, .94561, .94869, .95184, .95507, .95838,
 .96177, .96523, .96878, .9724,  .9761,  .97988, .98374, .98768, .99171,
 .99581, 1.,
2.9955, 2.372,  2.09867, 1.93838, 1.8307,  1.75217, 1.69179, 1.6435,
1.60383, 1.5705, 1.542,  1.51729, 1.49558, 1.47632, 1.4591
```

B.3.2 'DABSR' SAMPLE INPUT

```
 PLEASE ENTER PROBLEM TITLE
DAMAGE AREA BASED RELIABILITY, F/A-18A INBOARD WING REGION 1
 PLEASE ENTER COMPRESSION STRAIN AT DUL
2750.0
 PLEASE ENTER IMPACT PARAMETERS:
    LAMINATE LAYUP IN % OF (0/45/90)-DEG PLIES
47.0, 47.0, 6.0
    LAMINATE THICKNESS
0.3586
    LAMINA EL,ET,GLT IN MSI AND NULT
    AND ULTIMATE STRAIN IN MICRO-IN/IN
18.7, 1.9, 0.8, 0.3, 11000.0
    MATERIAL GIC
0.75
    POST-IMPACT STRENGTH ALPHA
8.5
 PLEASE ENTER NUMBER OF SPARS AND SPAR AE IN 10**6
3, 8.0
 PLEASE ENTER SPAR SPACING AND EDGE DISTANCE A1, A2
4.5, 0.5, 21.5
 PLEASE ENTER IMPACT EVENT CODE, ID
   ID = 1  FOR SINGLE MID-BAY IMPACT
   ID = 2  FOR MID-BAY IMPACTS ON TWO ADJACENT BAYS
   ID = 3  FOR SINGLE NEAR SPAR IMPACT
1
```

B.3.3 'DABSR' SAMPLE OUTPUT

DAMAGE AREA BASED RELIABILITY, F/A-18A INBOARD WING REGION 1

LAMINATE LAYUP: (47./47./ 6.)
MODULUS ESK = 10.679
ULTIMATE STRAIN EULT = 11000.
THICKNESS T = .359
FRACTURE TOUGHNESS GIC = .750
POST-IMPACT STRENGTH ALPHA = 8.500
FINAL STRUCTURAL FAILURE STRAIN GT 2789.
MAXIMUM WITHIN BAY DAMAGE AREA = 15.90

DAM. AREA	REL.(COUPON)	REL.(STRUCTURE)
.00	.999993	.999993
.50	.998923	.998923
1.00	.997083	.997083
1.50	.994465	.994465
2.00	.991059	.991059
2.50	.986850	.986850
3.00	.981821	.981821
3.50	.975960	.975960
4.00	.969256	.969256
4.50	.961701	.961701
5.00	.953291	.953291
5.50	.944025	.944025
6.00	.933906	.933906
6.50	.922940	.922940
7.00	.911138	.911138
7.50	.898512	.898512
8.00	.885081	.885081
8.50	.870865	.870865
9.00	.855889	.855889
9.50	.840182	.840182
10.00	.823774	.823774
10.50	.806700	.806700
11.00	.788998	.788998
11.50	.770709	.770709
12.00	.751875	.751875
12.50	.732542	.732542
13.00	.712758	.712758
13.50	.692573	.692573
14.00	.672036	.672036
14.50	.651202	.651202
15.00	.630123	.630123
15.50	.608854	.608854

STRUCTURAL RELIABILITY FOR 2.0-INCH DIA. DAMAGE
AT DUL: IF = .98025 FF = .98025

```
   AT MSL:  IF =       .99701  FF =       .99701
   AT DLL:  IF =       .99936  FF =       .99936

 CRITICAL DAMAGE AREA:
                  INITIAL FAILURE          FINAL FAILURE
              B-BASIS      A-BASIS      B-BASIS      A-BASIS
 AT DUL         7.44         2.14         7.44         2.14
 AT MSL        15.90         5.94        15.90         5.94
 AT DLL        15.90        12.58        15.90        12.58

 2.0-INCH DIAMETER CIRCULAR DAMAGE TOLERANCE DESIGN REQUIREMENT:
  B-BASIS: INITIAL FAILURE ALLOWABLE =      3345.  M.S. =     .22
           FINAL FAILURE   ALLOWABLE =      3345.  M.S. =     .22
  A-BASIS: INITIAL FAILURE ALLOWABLE =      2537.  M.S. =    -.08
           FINAL FAILURE   ALLOWABLE =      2537.  M.S. =    -.08
Stop - Program terminated.
```

REFERENCES

1. Whitehead, R.S., Kan, H.P., Cordero, R., and Saether, E.S., "Certification Testing Methodology for Composite Structures," Volumes I and II, Report No. NADC-87042-60, October 1986.

2. Sanger, K. B., "Certification Testing Methodology for Composite Structures," Report No. NADC-86132-60, January 1986.

3. Labor, J.D., "Service/Maintainability of Advanced Composite Structures," Report No. AFFDL-TR-78-155, November 1978.

4. Labor, J.D., "Design Criteria Guidelines for the Service/Maintainability of Advanced Composite Structures," Report No. AFFDL-TR-78-156, November 1978.

5. Butler, B.M., "Wing Fuselage Critical Component, Preliminary Design (Northrop)," Report No. AFFDL-TR-78-174, March 1979.

6. Fiscus, I.B., and Watson, D.C., "Study of Impact Damage to B-1B Weapon Bay Doors," Report No. AFWAL-TR-84-4153, December 1984.

7. Wood, H.A., and Bon, T.J., "Advanced Composites Supportability Working Group Findings and Recommendations," Report No. ASD(ENF)-TR-83-5017, January 1984.

8. "US Navy Survey of Damage and Defects in Advanced Composite Components in Service," Report No. TTCP/HTP-3, September 1985.

9. Stone, R.H., "Repair Techniques for Graphite/Epoxy Structures," NASA Report No. CF 159056, January 1983.

10. Cook, T.N., Adami, M.G., DiGenova, R.R., and Maass, D.P., "Advanced Structures Maintenance Concepts," Report No. USAAVRADCOM-TR-80-D-16, June 1980.

11. Ramkumar, R.L., "Composite Impact Damage Susceptibility," Report No. NADC-79068-60, January 1981.

12. Horton, R.E., Whitehead, R.S., et al, "Damage Tolerance of Composites," Volumes I, II, and III, Report No. AFWAL-TR-87-3030, July 1988.

13. ACEE Composites Project Office (Compiler), "Standard Tests for Toughened Resin Composite Revised Edition," NASA RP-1092, July 1983.

14. Dominguez, J., "F/A-18 Wing Skin Impact Test," Naval Air Development Center, December 1987.

15. Dobyns, A. L., "The Analysis of Simply Supported Orthotropic Plates Subject to Static and Dynamic Loads," presented at the 21st AIAA/ASME/ASCE/AHS SDM Conference, Seattle, Washington, May 1980.

16. Yang, S. H., and Sun, C. T., "Indentation Law for Composite Laminates," Composite Materials: Testing and Design, ATSM STP 787, I. M. Daniel, ed., pp. 425-440, 1982.

17. Sun, C. T. and Chen, J. K., "On the Impact of Initially Stressed Composite Laminates," Journal of Composite Materials, Volume 19, pp. 490-504, November 1985.

18. Tan, T. M., and Sun, C. T., "Use of Statical Indentation Laws in the Impact Analysis of Laminated Composite Plates," Journal of Applied Mechanics, Tran. ASME, Volume 52, pp. 6-12, March 1985.

19. Ramkumar, R.L., "Composite Impact Damage Susceptibility," Report No. NADC-79068-60, January 1981.

20. Chen, P.C., and Ramkumar, R.L., "Static and Dynamic Analysis of Clamped Orthotropic Plates Using Lagrangian Multiplier Technique" AIAA Journal, Volume. 25, No. 2, pp. 316-323, February 1987.

21. Shivakumar, K. N., Elber, W., and Illg, W., "Predictions of Low-Velocity Impact Damage in Thin Circular Laminates," AIAA Journal, Volume 23, No. 3, pp. 442-449, March 1985.

22. Ramkumar, R. L., and Chen, P. C., "An Analysis of Laminated Plates Subjected to Low Velocity, Transverse Normal Impact," Northrop Corporation Report NOR 80-175, November 1980.

23. Greszczuk, L. B., "Damage in Composite Materials Due to Low Velocity Impact," Impact Dynamics, John Wiley and Sons, New York, 1982.

24. Kelkar, A., Elber, W. and Raju, I. S., "Large Deflection Behavior of Circular Quasi-Isotropic Laminates Under Point Loading," AIAA Journal, Volume 25, No. 1, pp. 99-106, January 1987.

25. Cairns, D.C., "Impact and Post-Impact Response of Graphite/Epoxy and Kevlar/Epoxy Structures," TELAC Report 87-15, Ph.D. Thesis, Massachusetts Institute of Technology, August 1987.

26. Whitehead, R.S., Ritchie, G.L., and Mullineaux, J.L., "Durability of Composites," presented at the 9th Mechanics of Composites Review, Dayton, Ohio, October 1983.

A.1 Jeans, L.L., Grimes, G.C., and Kan, H.P., "Fatigue Spectrum Sensitivity Study for Advanced Composite Materials," Report No. AFWAL-TR-80-3130, December 1980.

A.2 Berens, A.P., Johnson, P.E., and West, B.S., "Experimental Evaluation of Reliability Assessment Model for Adhesively Bonded Joints," Report No. AFML-TR-74-120, June 1974.